1987

Separation and determination of trace metal ions using organic chelating reagents

Margo Doris Palmieri
Iowa State University

INFORMATION TO USERS

The most advanced technology has been used to photograph and reproduce this manuscript from the microfilm master. UMI films the original text directly from the copy submitted. Thus, some dissertation copies are in typewriter face, while others may be from a computer printer.

In the unlikely event that the author did not send UMI a complete manuscript and there are missing pages, these will be noted. Also, if unauthorized copyrighted material had to be removed, a note will indicate the deletion.

Oversize materials (e.g., maps, drawings, charts) are reproduced by sectioning the original, beginning at the upper left-hand corner and continuing from left to right in equal sections with small overlaps. Each oversize page is available as one exposure on a standard 35 mm slide or as a 17″ × 23″ black and white photographic print for an additional charge.

Photographs included in the original manuscript have been reproduced xerographically in this copy. 35 mm slides or 6″ × 9″ black and white photographic prints are available for any photographs or illustrations appearing in this copy for an additional charge. Contact UMI directly to order.

Accessing the World's Information since 1938

300 North Zeeb Road, Ann Arbor, MI 48106-1346 USA

Order Number 8805122

Separation and determination of trace metal ions using organic chelating reagents

Palmieri, Margo Doris, Ph.D.

Iowa State University, 1987

U·M·I
300 N. Zeeb Rd.
Ann Arbor, MI 48106

PLEASE NOTE:

In all cases this material has been filmed in the best possible way from the available copy. Problems encountered with this document have been identified here with a check mark __✓__.

1. Glossy photographs or pages _____
2. Colored illustrations, paper or print _____
3. Photographs with dark background _____
4. Illustrations are poor copy _____
5. Pages with black marks, not original copy __✓__
6. Print shows through as there is text on both sides of page _____
7. Indistinct, broken or small print on several pages __✓__
8. Print exceeds margin requirements _____
9. Tightly bound copy with print lost in spine _____
10. Computer printout pages with indistinct print _____
11. Page(s) _____ lacking when material received, and not available from school or author.
12. Page(s) _____ seem to be missing in numbering only as text follows.
13. Two pages numbered _____. Text follows.
14. Curling and wrinkled pages _____
15. Dissertation contains pages with print at a slant, filmed as received _____
16. Other _____

_____

_____

Separation and determination of trace metal ions using organic chelating reagents

by

Margo Doris Palmieri

A Dissertation Submitted to the
Graduate Faculty in Partial Fulfillment of the
Requirements for the Degree of
DOCTOR OF PHILOSOPHY

Department: Chemistry
Major: Analytical Chemistry

Approved:

Signature was redacted for privacy.

In Charge of Major Work

Signature was redacted for privacy.

For the Major Department

Signature was redacted for privacy.

For the Graduate College

Iowa State University
Ames, Iowa

1987

TABLE OF CONTENTS

GENERAL INTRODUCTION

Trace metal ion analysis has been a major focus of analytical chemists. Metal impurities in samples have been determined using a variety methods. An important part of many metal ion analyses involves the formation of metal complexes with organic chelating reagents. Organic chelating reagents are used in the separation and determination of metal ions in a sample containing potential interferents. Organic metal complexes have been formed for gravimetric, extraction, spectrophotometric, and various types of chromatographic analyses.

The purpose of this work was to study the metal ion complex formation and separation with organic chelating reagents. Four different organic reagents are investigated for their complexing ability with metal ions. The first two sections emphasize the formation of uranium(VI) complexes. The complexing agent N,N-dihexylacetamide (DHA) is fairly selective for uranium, and extraction characteristics of the DHA-uranium(VI) complex in a nitric acid solution are shown. Trace metal ions are also determined in uranium solutions by inductively coupled plasma- mass spectrometry (ICP-MS) after the uranium is removed by DHA extraction. In section II, a new hydrazone, 2,6-diacetylpyridine bis(furoylhydrazone) (H_2dapf), is synthesized, characterized, and its chelating capabilities with several metal ions are presented. H_2dapf forms a relatively strong complex with uranium(VI), and the metal complex can be determined colorimetrically.

The final two sections describe high performance liquid chromatographic (HPLC) separations of metal complexes of two different types of chelating reagents. The first complexing agent, 1,3-dimethyl-4-acetyl-2-pyrazolin-5-one (DMAP), forms water-soluble chelates with a

large number of metal ions. The DMAP separation conditions are investigated, and a method for selectively determining uranium(VI) by HPLC of its DMAP metal complex is developed. The second complexing agent, N-methylfurohydroxamic acid (NMFHA), reacts preferentially with metal ions having a high valence state to form water-soluble complexes. Zirconium(IV), hafnium(IV), and other metal NMFHA complexes are separated by reverse phase HPLC, and analytical conditions and applications of the HPLC separation are presented.

SECTION I. SEPARATION OF TRACE METALS FROM URANIUM BY SOLVENT EXTRACTION WITH DETECTION USING INDUCTIVELY COUPLED PLASMA-MASS SPECTROMETRY

INTRODUCTION

In the past forty years the world has entered the nuclear age. Nuclear fission reactors have been developed and are used to supply electrical energy, nuclear weapons, and radiochemicals. Central to nuclear power is the use of uranium as the source of nuclear reactor material. Uranium in the form of ^{235}U is used directly as fuel in conventional reactors; ^{238}U is the precurser for plutonium in breeder reactors (1).

Because of the critical role of uranium in the nuclear industry, the purity of the ore used is of primary importance. The fissionability of the uranium fuel is governed by the level of contaminants present in uranium. Those elements which contain a high neutron cross section capture for neutrons will remove neutrons released in the fission process. These neutrons control the rate of the fission reaction and are used to produce plutonium from uranium in the breeder reactors. Some contaminants may be useful in controlling the rate of the fission process, but large concentrations of contaminants may undesirably inhibit fission reactions. In addition, knowledge of contaminants in uranium is useful when disposing of spent reactor fuel and in separating radiochemicals for use in medicine and radiochemistry.

This chapter focuses on the separation and determination of trace elements in uranium using solvent extraction with N,N-dihexylacetamide (DHA) and detection with inductively coupled plasma-mass spectometry (ICP-MS). DHA preferentially extracts uranium in nitric acid solutions and the extaction of uranium in nitric acid using DHA will be investigated. Recoveries of trace impurities of transition metals and

trivalent lanthanide ions will be determined in spiked uranium solutions and in unspiked uranium salts. Experiments describing possible extensions of this project will also be described.

LITERATURE REVIEW

Extensive study has been carried out in the determination of trace elements in uranium. Trace impurities have been quantified using a variety of wet chemical and instrumental procedures, but problems surrounding the analysis have arisen which stem from many causes (2). First of all, the large excess of uranium relative to other elements poses detection problems. The uranium signal can swamp out signals being emitted by the impurities. The low levels of impurities can be difficult to determine by noninstrumental means. The chemistry of uranium may also be similar to that of other elements, producing identification and separation problems. Finally, the radioactivity of the uranium can affect a chemical analysis procedure and cause safety problems for the chemist.

Most uranium analyses have been carried out using spectroscopic techniques. Direct spectrographic analysis has been done since the mid 1940s but interference caused by the uranium present in the sample has severely limited the use of this procedure. Uranium has numerous spectral lines which overlap with the spectral lines emitted by other elements and cause high backgrounds. Because of the high background noise, the trace analyte signal was almost impossible to detect. Some work has been done using direct excitation of certain impurities in uranium. Scribner and Mullin (3) and Franklin and Woodman (4) have determined calcium directly in uranium. A method for determining silicon in uranium was developed by Birks (5), and Schoenfeld (6) determined some rare earths in uranium. Special instumentation has been designed by Harrison and Kent (7) and Walsh (8) which allow some other impurities in

uranium to be directly detected.

Because of the spectral problems associated with uranium, most analytical methods for determining trace impurities have included a separation procedure before spectroscopic analysis. Three means of separations are performed: carrier distillation, thermal evaporation, and chemical separation. These three procedures utilize different physical and chemical properties in order to achieve a separation.

Carrier distillation has seen the most use in uranium analysis and was first reported in the literature by Scribner and Mullin in 1946 (3). In carrier distillation the uranium is converted to a form, typically U_3O_8, which has low volatility. A volatile carrier material is added, the sample is placed in a direct current arc, and a partial distillation occurs. The impurities are volatilized with the carrier materials, collected, and analyzed using spectrographic techniques. The most popular carrier material is gallium oxide and in the initial paper, Scribner and Mullin determined thirty three impurities. Pepper lists other papers where carrier distillation is used to determine trace impurities in uranium (2).

Carrier distillation has certain advantages which makes it a popular method (2). Because of reduced sample manipulation, there is less contamination, and separations are achieved fairly quickly. A large variety of elements can be separated using this procedure. Some impurities can be determined to the sub part per million level. For most elements, however, determination of trace elements is at the part per million level or higher depending upon the volatility of the element and its spectral characteristics. Elements which form refractory oxides or are not effectively carried over in the distillation have higher

detection limits and can not be determined at low levels.

The second separation procedure involves thermal evaporation which was pioneered by Zaidel in the 1940s and 1950s and developed by researchers in the Soviet Union and Poland (2). In thermal evaporation, impurities are thermally distilled using a temperature below the evaporation temperature of U_3O_8. Impurities are condensed on a receiver electrode, and are then excited using an arc or spark and are analyzed spectrographically. Thermal evaporation is more sensitive than carrier distillation and can be used as a preconcentration procedure for many impurities. However, refractory elements are again difficult to evaporate reproducibly, and many different evaporation conditions are required in order to analyze many different elements. Equipment can be expensive and the method is laborious to carry out.

The third major separation method involves chemical separation of the trace impurities from uranium. Chemical separation methods are preferred to carrier distillation and thermal evaporation when high sensitivity is required: variation of sample sizes causes changes in detection limits, incorporation of internal standards is easily carried out, and in spark sources, reproducible excitation is achieved. In addition, chemical separation methods can be varied to achieve single element or group separations. The major limitation to chemical separation involves the extensive sample handling required which can introduce impurities into the sample. Chemical separations are carried out using one of the following separation schemes: column separations by ion exchange, precipitation, and solvent extraction. Each method has been used to separate impurities from uranium before spectral analysis.

The chemical separation method which has received the most attention

has been solvent extraction. Extractions are quickly and easily carried out, and selectivity for various elements can be achieved by varying extraction conditions. Solvent extraction reagents are chosen to achieve one of two types of separation: extraction of the trace elements from uranium and extraction of the uranium from the solution. Extraction of trace elements is specific for certain elements, but the number of elements extracted tends to be limited. Extraction of the uranium allows a large number of impurities to be determined because only the uranium is removed. Table 1 describes some papers using extraction as the separation method for determining trace elements in uranium.

Most of the extraction procedures described use extraction to remove the uranium from the sample before analysis in order to be able to analyze large numbers of impurities. Many of the uranium extractants used belong to the oxonium class of reagents. Coordination occurs through the polar oxygen on the ligand. Typically, phosphorous based extraction reagents are used to effect a separation because they are relatively cheap and, using certain extraction conditions, are fairly specific for uranium. The most commonly used phosphorous-based complexing agents are tributylphosphate (TBP), tri n-octyl phosphine oxide (TOPO), tri-(2-ethylhexyl)phosphate (TEHP). Complexation of these phosphorous based reagents occurs through the oxygen bound to phosphorous. Some of the phosphorous-based extractants have the disadvantage of not being stable over long periods of exposure to radiation, are not very safe to work with, and degradation products interfere with the reaction.

One class of uranium extractants which has not been widely used is the N,N-dialkyl substituted alkyl amides. Amides have the structure

Table 1: Solvent extraction of impurities in uranium before analysis

Extractant	Species Extracted	Impurities Detected	Method of Analysis	Reference Number
Tributyl phosphate	Uranium	Cd,Cr,Mo,Ti,V	Spectrography	9
		Rare Earth Ions	Spectrography	10-13
		Al,Ag,Cd,Co,Cr,Cu,Fe,Ga, In,Mn,Mo,Ni,Pb,Sn,Ti,V	Spectrography	14
		Al,As,B,Ba,Cd,Co,Cr,Cu,Fe, Li,Mg,Mn,Mo,Ni,Pb,Rh,Se,Sr, Ti,V,Zn	ICP-AES[a]	15
		Al,Ca,Cd,Cr,Cu,Fe,K,Mg,Na, Ni,Pb,Zn	Atomic Absorption	16
		Al,Fe,Ni	Atomic Absorption	17
		Cd,Co,Cu,Ni,Zn	Polarography	18
		Cd,Co,Cu,Fe,Mn,Ni,Pb,Zn	Polarography	19
		Zr	Photometry	20
		Th	Photometry	21
Diethylether	uranium	Ce,Eu,Gd,Nd,Sn	Spectrography	22
		Rare Earth Ions	Spectrography	23,24
		Co,Cr,Fe,Zn	Spectrography	25

Table 1: Continued

Extractant	Species Extracted	Impurities Detected	Method of Analysis	Reference Number
Cupferron	impurities	Mo,Nb,Sn,Ta,Ti,W,V,Zr	Spectrography	26
		Zr,Hf	Spectrography	27
		Ga,Hf,Mo,Nb,Ta,W,V,Zr	Spectrography	28,29
Tri-(2-ethylhexyl) phosphate	uranium	Al,Ba,Ca,Cd,Co,Cr,Cu,Fe,Mg, Mn,Mo,Nb,Ni,Sr,Ti,V,W,Zn,Zr	ICP-AES	30
		Al,B,Ba,Bw,Bi,Ca,Cd,Co,Cu, Dy,Eu,Fe,Gd,Li,Mg,Mn,Mo,Na, Nb,Ni,Pb,Ru,Sb,Si,Sm,Sn,Ta, Sr,Ti,V,W,	ICP-AES	31
		Al,B,Cd,Cr,Cu,Fe,Mg,Mn,Mo,Ni	ICP-AES	32
		Na,Pb,Si,Sn,V,Zn,Zr	ICP-AES	33
Tri-n-octylamine	uranium	Dy,Eu,Gd,Sm,Th	ICP-AES	34
		Pb,Zn	Spectrography	35
Tri-isooctylamine	uranium	Rare Earth Ions	Spectrography	36
		As,Bi,Be,Ca,Cr,Co,Fe,Ga, In,Mg,Mn,Pb,Sn,V,Zn,Zr	Spectrography	37
Molybdate	impurities	P,Si	Photometry	38,39

Table 1: Continued

Extractant	Species Extracted	Impurities Detected	Method of Analysis	Reference Number
Benzoylphenyl-hydroxamic acid	impurities	Mo,Nb,Ta,Ti,W,Zr	Spectrography	40
	impurities	Nb,Ta,Ti	Spectrography	41
monomethyl-thionine	impurities	BF_4	Photometry	42
n-amylacetate	impurities	Fe,Mo,Sb	Atomic Absorption	43
Tri-octylphos-phine oxide	uranium	Al,B,Cd,Co,Cu,Fe,Mn,Ni, Si,V	ICP-AES	44
Dibutoxytetra-ethylene	impurities	Ce,Dy,Er,Gd,Sm	Spectrography	45
Dithizone	impurities	Cd,Co,Cu,Ni,Pb,Zn	Polarography	46

[a]ICP-AES = Inductively Coupled Plasma - Atomic Emission Spectroscopy.

$RC(=O)NR_2$ and also belong to the oxonium class of reagents. The nitrogen withdraws electrons to give a resonance effect as shown in Equation (1).

$$R\text{-}\overset{\overset{O}{\|}}{C}\text{-}N\text{-}R_2 \rightleftharpoons R\text{-}\overset{\overset{O^-}{|}}{C}\text{=}N\text{-}R_2 \qquad (1)$$

The inductive effect of the nitrogen is responsible for the increased complex formation of the amides relative to ketones. Drago et al. (47) and Bright et al. (48) have determined that complexation of amides with metal ions takes place through the polar carbonyl oxygen. Siddall (49) and Gasparini and Grossi (50) have noted that these compounds are easy to synthesize, extract as well as TBP, are as resistant to radiolytic degradation, and the degradation products do not interfere with the extraction.

Feder (51) first demonstrated that uranium could be extracted using amides and found that N,N-dibutylacetamide was comparable to TBP in uranium extraction power. Siddall (52) expanded the initial work of Feder to several amides and saw marked differences in the extraction power of amides depending upon the amide used. Substitution at the α-carbon caused a slight decrease in the uranium extraction efficiency but large changes in the extraction efficiency of other elements. Lengthening and branching amine substituents also decreased uranium extraction. These changes in extraction efficiency based upon amide structure were attributed to steric hindrance around the metal ion when the amide forms the complex. Siddall also reported that the amide formed a two to one complex with uranium. Other studies were carried out on amides and reflect data similar to that reported by Siddall (53-56).

The acetamide used in this study, N,N-dihexylacetamide (DHA) displays the favorable characteristics found in the other amides. DHA was first

tested as an extraction reagent by Fritz and Orf (57) using a sodium nitrate aqueous phase. It was found to extract uranium to a large extent without extracting many other elements from the aqueous phase. Of the other ions tested, only iron(III) and thorium(IV) were extracted to a large extent. In addition DHA is easy and inexpensive to synthesize and is a stable molecule.

Most of the methods for determining impurities in uranium use spectroscopic detection, which is sensitive for most elements. In addition, many elements can be determined simultaneously which decreases sample analysis time. In recent years spectrography has been displaced by inductively coupled plasma atomic emission spectroscopy (ICP-AES) as the method of detection for multiple trace elements. ICP-AES is a fast multi-elemental analysis method with reproducible signals and high sensitivity. ICP-AES does suffer from the same uranium spectral line interference problems which has plagued spectrography, and some separation procedure is required before analysis (58). In the past five years ICP-AES has been used in conjunction with solvent extraction to determine trace elements in uranium (12, 30-34, 44).

Inductively coupled plasma-mass spectrometry (ICP-MS) is a new technique for multielemental analysis of solutions (59-61). Now that commercial instrumentation is available, ICP-MS is being evaluated for its ability to solve tough analytical problems. Both ICP-MS and ICP-AES are capable of multielemental analysis, but in the present application ICP-MS has two main advantages over its sister technique. Spectral interferences from U are not a problem in ICP-MS in that U^{+2} (m/e = 117, 117.5 and 119) is the only uranium species observed in the m/z range corresponding to analyte elements. A second advantage of ICP-MS is the

very low detection limits (10-100 ng L^{-1}), which are an order of magnitude better than ICP-AES for most elements (62).

EXPERIMENTAL

Reagents and Standards

N,N-dihexylacetamide was synthesized using the method outlined by Fritz and Orf (57) using acetic anhydride and dihexylamine from Aldrich. Reagent grade or better chemicals were used in the DHA synthesis and in making up the stock solutions. Reagent grade uranyl nitrate was obtained from Mallinkrodt and Fisher.

Multielement standards were prepared by combining and diluting single element reference stock solutions. The rare earths were obtained as oxides (Ames Laboratory), and were dried, weighed, and dissolved in dilute nitric acid (in deionized water). The purity of these standards was verified by ICP-MS by scanning the entire mass spectrum of a 1000 mg L^{-1} solution. No impurities were found in the concentrated standards above a 10 µg L^{-1} level. Other stock solutions came from Fisher Scientific. The 1% (v/v) HNO_3 used to dilute all samples and standards was made from the reagent grade acid (Fisher Scientific), except for the experiments where the low mass blanks became substantial at the 10 µg L^{-1} level. For those experiments, sub-boiling distilled nitric acid, made in an all quartz apparatus, was required. Deionized water came from either a Milli-Q water purifier (Millipore Corporation) or from a Nanopure II system (Barnstead). The digital pipets (Rainin) used in dilution and in the addition of the internal standard were calibrated gravimetrically and found to be within the manufacturer's specifications for precision and accuracy (better than 2% at all the volumes used). All glassware used was soaked in 6 M hydrochloric acid for at least 24 hours between extraction experiments, then were rinsed with the

deionized water and air-dried. The extraction, evaporation, and dilution steps were carried out in a convection hood to prevent contamination of samples.

Solvent Extraction: Determination of Distribution Coefficient

In the determination of the distribution coefficients, 500 mg L^{-1} solutions were prepared in nitric acid solutions of varying molarity and were extracted with an equal volume of DHA in toluene. The mixture was placed on a Burrel Wrist Action shaker and equilibrated for one hour. The aqueous phase was removed, diluted, and analyzed for metal ion content. Atomic absorption spectrometry was used to determine the concentration of Cs(I), Ag(I), Sr(II), Ba(II), and Cr(III). The metals Cu(II), Hg(II), Ni(II), Zn(II), Mn(II), Co(II), Pb(II), and Cd(II) were determined colorimetrically at a pH of 9.2 with 4-(Pyridylazo)resorcinol (Aldrich Chemical) (63). Uranium(VI) was determined using the method developed by Fritz and Johnson-Richard (64). The ASTM method was followed in the determination of iron(III) (65). The remaining metals were determineded using the methods outlined by Phillips (66).

Equipment

Two ICP-MS instruments were used in the analysis of the uranium samples. The work was originally started on the Ames Laboratory instrument as described by Olivares and Houk (67). The Sciex ICP-MS was used for the majority of the experiments because it was more reliable and had better detection limits than the Ames Laboratory instrument. The analytical characteristics of this particular device have recently been described in detail (68). The mass analyzer was operated in a "peak hopping" mode and also has been described elsewhere (69).

Analysis of a Uranium Sample

For the separation and determination of trace metals in a uranium matrix, a 119,000 mg L^{-1} (0.5 M) solution of U in 2 M HNO_3 was made up from uranyl nitrate salt. Various trace metals were added to the uranium solution so that their final concentration was 100 or 10 µg L^{-1} (0.84 or 0.084 µg per g of U). An aliquot of the spiked uranium solution was then extracted with an equal volume of 2 M DHA in toluene. When using the Sciex instrument three extractions were performed and when using the Ames Laboratory instrument two extractions were carried out. An aliquot of the aqueous phase was taken, evaporated almost to dryness, dissolved in 1% HNO_3, spiked with the internal standard, and analyzed by ICP-MS. Lutetium was the internal standard for the rare earths while rubidium and holmium were used as internal standards for other metals.

The standards used were not run through the extractions with the samples. Instead, a single blank was carried through the procedure along with 3-4 samples. This insured that trace impurities in the 0.5 M U, which might be substantial at the 10 µg L^{-1} level, would be detected. Standards contained either 10 or 100 µg L^{-1} of the internal standard, and were matrix matched to contain the same amount of uranium as the samples (approximately three ppm uranium). Calibration curves were prepared using 2, 5, 10, and 30 µg L^{-1} standards (or ten times higher for the high blank metals). During the analysis, the 10 µg L^{-1} standard was reintroduced after each sample to verify that the calibration curve had not shifted. If there had been a small drift, these data could be used to normalize subsequent sample concentrations.

The reported detection limits were calculated as the analyte

concentration necessary to yield a net (blank subtracted) signal equal to three times the standard deviation of the blank count rate.

Flow Injection Analysis

Solutions containing 0.05 M HNO_3 and 2 M DHA in toluene were pumped through the flow injection system using a multichannel Rainin peristaltic pump. The two phases were pumped using separate channels and at the same flow rate into a tee where they were mixed. The phases were pumped through the tubing and were separated in a separator cell based on a design by Bergamin et al. (70). Flow restrictors (Anspec) were used after the separator cell to provide back pressure to the system. The two streams from the separator cell were collected after the flow restrictor.

Synthesis of N,N dibutylthioformamide

N,N dibutylthioformamide (S-DHA) was synthesized and purified using the method described by Pederson et al. (71) and Fritz et al. (72) from N,N dibutylformamide (Aldrich) and p-methoxyphenylthionophosphine sulfide. The latter compound was synthesized from anisole and P_4S_{10} (Aldrich) according to the procedure by Pederson et al. (71). The compounds were purified and tested to confirm the structure. A 1 M solution of S-DBF in toluene was made up and used in solvent extraction experiments. Extraction experiments were carried out in a similar manner to the DHA experiments.

RESULTS AND CONCLUSIONS

Instrumental Interference Effects

Initially the analysis of trace elements in uranium was performed using the ICP-MS without prior extraction. Reduced signals were seen for all the elements indicating that the ionization was suppressed by the uranium present. Figure 1 shows the signal count rate of one part per million thorium versus the concentration of uranium in solution using the Ames Laboratory instrument. The thorium signal was unaffected up to approximately 200 ppm of uranium, then the thorium signal dropped off as the uranium concentration increased. The Sciex instrument showed the same type of suppression behavior as the Ames Laboratory instrument, except that it tolerated less uranium in solution. At the experimental instrument conditions, ionization suppression was still seen at 20 ppm uranium in solution using the Sciex ICP-MS. The signal suppression was approximately an order of magnitude worse on the Sciex instrument than on the Ames Laboratory instrument. The level of suppression also varied depending upon the element being analyzed and on the instrument conditions. Douglas reported that uranium was one of the worst elements for causing ionization suppression of analytes (73). It has been theorized that the load coil may be responsible for the variations in ionization suppression. In addition, increasing the negative potential on the first ion lens reduces suppression effects (74). Because the ionization suppression effects could not be corrected for by using internal standards, sufficient extractions were carried out in order to reduce the levels of uranium to below ionization suppression levels, and standards were matrix matched. In order to reduce the uranium

Figure 1: Percentage of Signal for 1 ppm Thorium versus the concentration of Uranium on the Ames Laboratory built Instrument

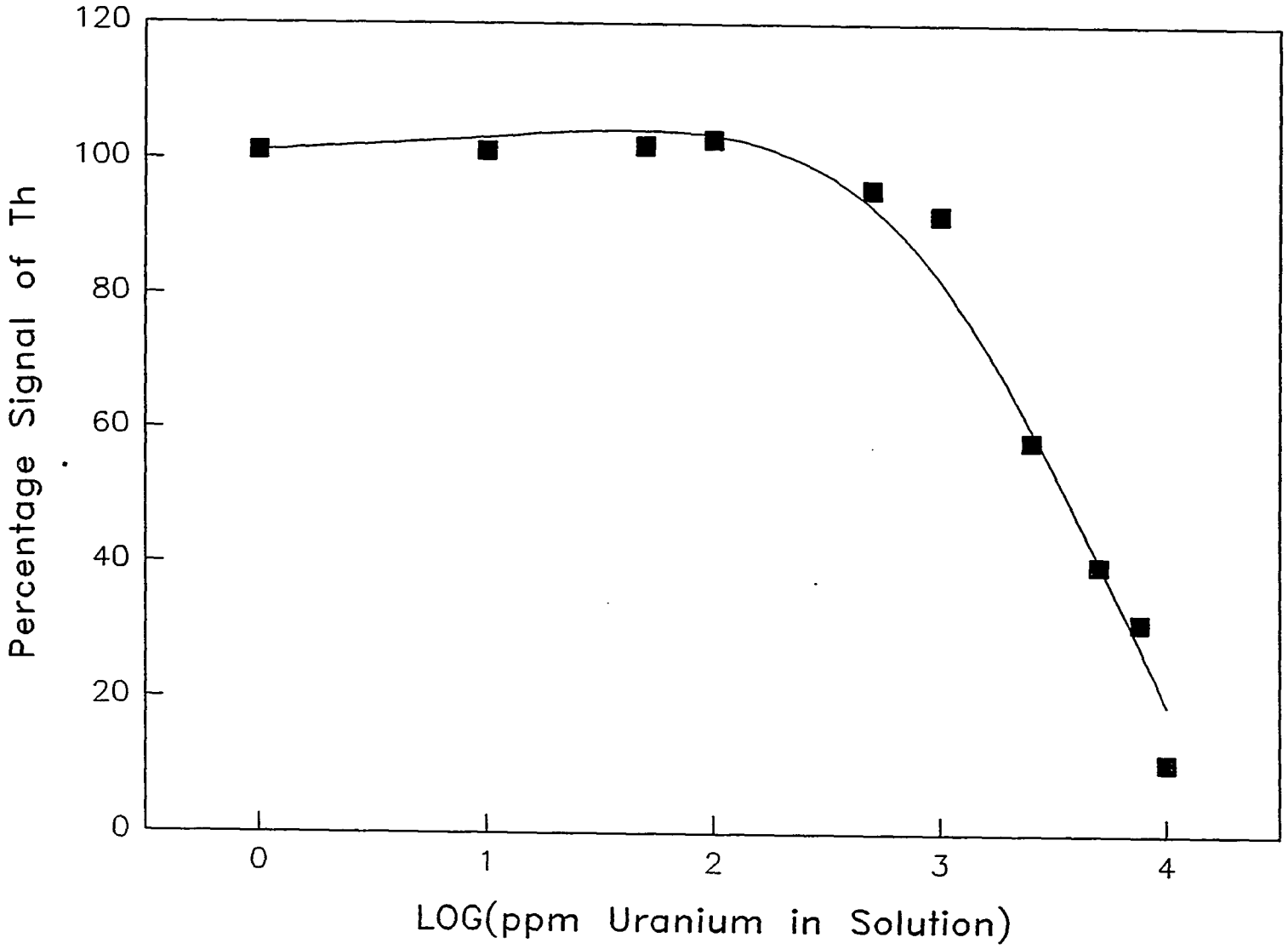
120
100
80
60
40
20
0
Percentage Signal of Th
0
1
2
3
4
LOG(ppm Uranium in Solution)

concentration to below interference levels, two extractions were performed when using the the Ames Laboratory instrument, and three extractions were performed when using the Sciex instrument for analysis.

Extraction Characteristics

The extraction of uranium using acetamides, and DHA in particular, has been studied previously. The Appendix describes the principles of solvent extraction. Orf found that the uranium complex extracts as a coordination complex consisting of the formula $UO_2(DHA)_2(NO_3)_2$ in sodium nitrate (57). The slope of the log-log plot of D_c and the DHA concentration in Figure 2 also indicates a two (1.9) to one DHA to uranium ratio for concentrations of DHA of 1 M or less in toluene. The 2 M DHA point was considerably off the line drawn through the first four points. Siddall noted that at high concentrations of amide, negative curvature was seen and suggested that this negative deviation was due to interaction between extractant molecules (52). Figure 3 shows the log D_c plotted versus the log of the nitric acid concentration. Extraction of uranium increases as the concentration nitric acid increases; at high acid levels the extraction reaches a plateau. Gasparini and Grossi (50) also found a similar curvature for other amides when the nitric acid concentration in the aqueous phase is increased. At low nitric acid concentrations ($\leq$1 M nitric acid), the slope of the straight line region is one, indicating a one to one ratio of nitrate to uranium in contrast to Orf's two to one ratio. This difference between these results and Orf's work could be due to the extraction of nitric acid with DHA interfering with the uranium extraction or due to the possible extraction of a mixed uranium nitric acid complex.

Figure 2: Log(D_c) versus Log(DHA concentration) for the uranium extraction

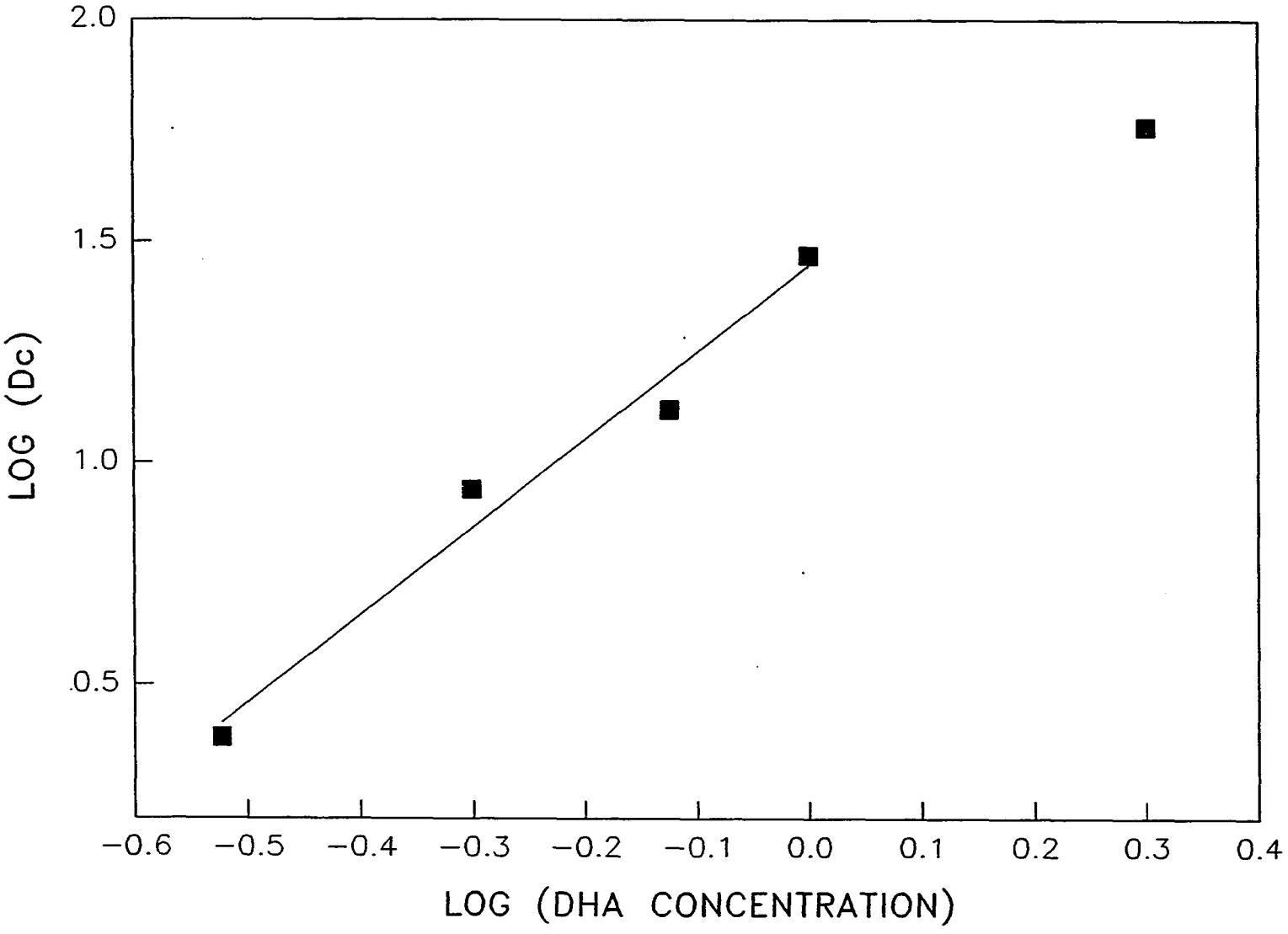
2.0
1.5
1.0
.5
LOG (Dc)
−0.6
−0.5
−0.4
−0.3
−0.2
−0.1
0.0
0.1
0.2
0.3
0.4
LOG (DHA CONCENTRATION)

Figure 3: Log(D_c) versus Log(HNO_3 concentration) for the uranium extraction

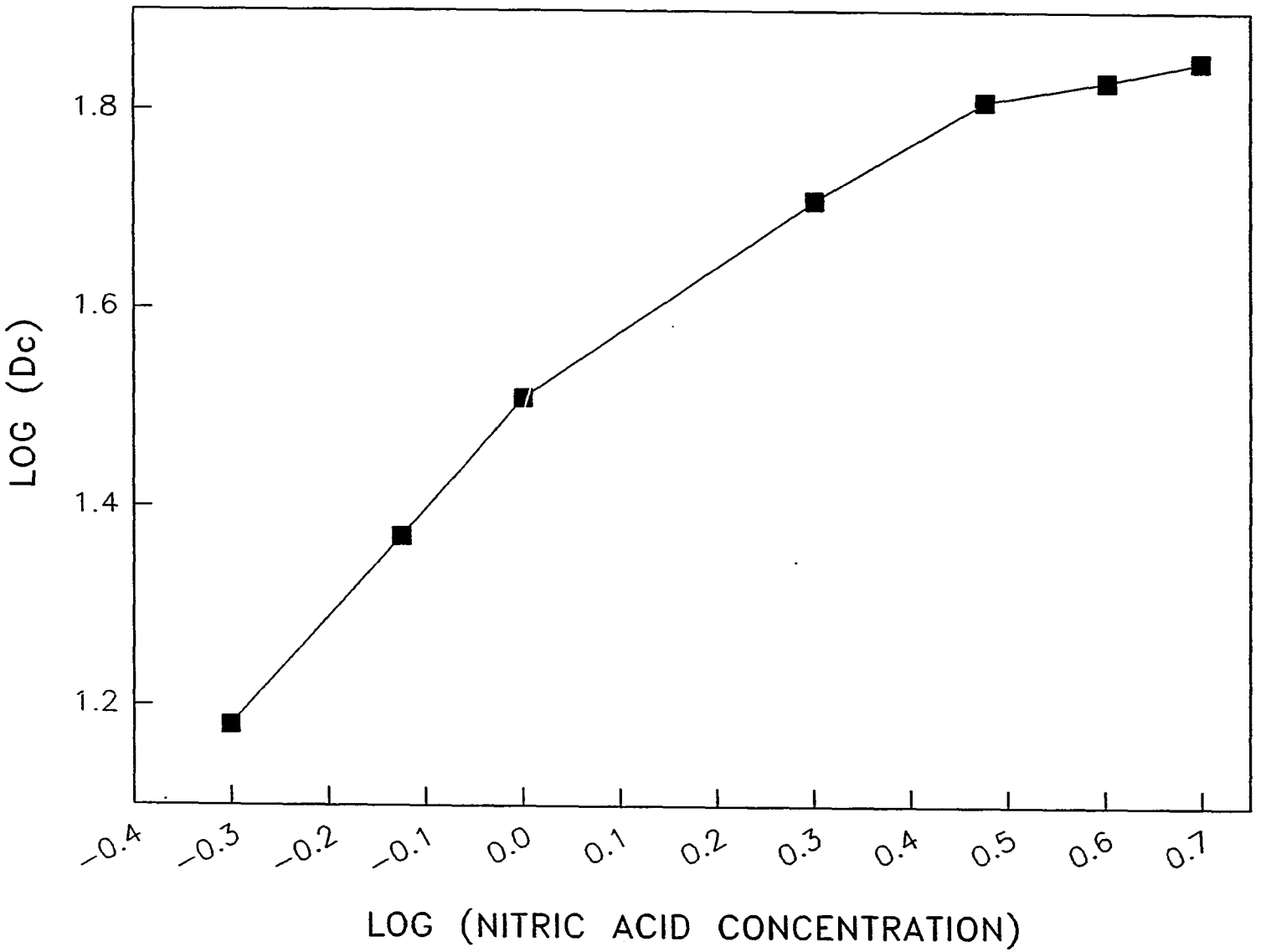
LOG (Dc)
1.8
1.6
1.4
1.2
-0.4
-0.3
-0.2
-0.1
0.0
0.1
0.2
0.3
0.4
0.5
0.6
0.7
LOG (NITRIC ACID CONCENTRATION)

Table 2 lists the distribution coefficients (D_c) for various metal ions in 2 M nitric acid with 2 M DHA in toluene as the extractant. The concentration 2 M DHA in toluene was chosen for analysis because it gave the most efficient extraction of uranium while still retaining good phase separation. At higher concentrations of DHA in the diluent, an emulsion

Table 2: Distribution coefficients for elements in 2 M HNO_3 with 2 M DHA in toluene as the extractant[a]

Metal Ion	D_c
Ag^{+}	0.054
Bi^{3+}	2.55
Hg^{2+}	0.44
Pb^{2+}	0.043
Th^{4+}	5.25
UO_2^{2+}	57.8
Zr^{4+}	0.24

[a]The following ions had D_c values less than 0.01: Cu^{2+}, Ni^{2+}, Zn^{2+}, Mn^{2+}, Co^{2+}, Cd^{2+}, La^{3+}, Tm^{3+}, Gd^{3+}, Pr^{3+}, Cs^{+}, Sr^{2+}, Ba^{2+}, Y^{3+}, Fe^{3+}, Ti^{4+}, Cr^{3+}, Al^{3+}, V^{5+}.

formed between the organic and aqueous phases. As Figure 2 shows, D_c values for the extraction of uranium were lower for the lower concentrations of DHA. The concentration of nitric acid was chosen so that a maximum of uranium was extracted while a minimum of other elements was extracted. Of the metals listed only uranium, thorium, and bismuth were extracted significantly under the chosen conditions, with uranium being extracted much more efficiently (98.3%) than the other elements. With the exception of thorium(IV) and bismuth(III), under the conditions used for analysis, recovery data for other metals can be corrected for extraction using the D_c values listed in Table 2.

Fritz and Orf (57) originally used sodium nitrate instead of nitric acid in the extraction of uranium. When using sodium nitrate instead of nitric acid, large D_c values were found for uranium. For 2 M sodium nitrate solutions extracted with 2 M DHA in toluene, Fritz and Orf reported a D_c value of 624 versus a 58 D_c value using nitric acid found in the present work. This large difference in D_c values is probably due to a salting out effect in the sodium nitrate solutions. Nitric acid is known to be extracted by amides, and the extraction of nitric acid may also lower the extraction with uranium. However, when using the ICP-MS, ionization suppression was seen due to the large concentration of sodium present. This ionization effect is further described and investigated by Olivares and Houk (75). Large concentrations of nitric acid also suppressed ionization, but it was evaporated from the sample before analysis, thereby eliminating the ionization suppression.

The extraction was fast and fairly efficient for moderate concentrations of uranium (0.05 M). Experiments showed that the uranium extracted into the organic phase with one minute of shaking, the shortest

time period tested. Separation of the two phases occurred in one to two minutes with no third phase formation seen. Other workers have reported third phase formation and precipitation for other amide uranium complexes primarily in aliphatic diluents (50).

When high concentrations of uranium were present in the aqueous phase, the extraction was still fast but was not as efficient. After two extractions of a 0.5 M uranium solution using 2 M DHA extractant, approximately 150 ppm uranium remained in the aqueous phase rather than the 34 ppm calculated to be in the aqueous phase. A single extraction of a 0.5 M uranium solution gave a D_c value of approximately 21, less than half the D_c value calculated at lower uranium concentrations. Presumably the large level of uranium saturated the organic phase, and an insufficient excess of free DHA was available to push the equilibrium towards the extraction of uranium. Most of the aqueous phase separated quickly from the organic phase. Approximately 10 to 20% of the aqueous phase was suspended in the organic phase and took longer to separate out, at least 30 minutes. After 24 hours a uranium-DHA precipitate sometimes formed in the organic phase.

The DHA was recycled for use in multiple experiments. DHA is stable to radiolytic degradation and could be reused several times without loss in extraction power. After extraction experiments, the uranium was back extracted with saturated sodium bicarbonate solution. Any nitric acid extracted was also neutralized, and after three washes with the sodium bicarbonate solution, the uranium was completely removed from the organic phase. Before reuse the DHA solution was equilibrated with 2 M nitric acid.

Recovery Determination

Tables 3 and 4 give the blank corrected recoveries for trace elements added to the uranium solution. The amount of spiked material originally added was varied according to the level of trace impurities present in the blank in order to avoid the imprecision of subtracting two numbers of nearly equal magnitude. Semiquantitative analyses of deionized water, nitric acid, and evaporated nitric acid solution have been carried out and reported elsewhere (69). The high blanks for aluminum, barium, and lead were found and are likely due to impurities in the nitric acid and have been concentrated in the evaporation step. The presence of impurities in nitric acid and native impurities in the uranyl nitrate were compensated for by running a blank with the sample. The uranium used in the recovery studies was identical to the "unknown" in Table 5. Therefore, the metals which exhibit high blanks could either be native impurities in the uranium or traces which may not have been fully back extracted from the organic phase before the extractant was reused. Thorium was extracted too efficiently to permit reliable determination of its recovery. Attempts to find recoveries for Fe and Cu at 100 $\mu g\ L^{-1}$ were precluded by significant background in the ICP-MS itself at these masses. Boron could not be determined with the ultrasonic nebulizer used, probably due to loss of boron in the desolvation system employed.

The variation in individual sample measurements was usually less than 3%, which reflects the short term stability of the instrument. The variation within a run of 3-4 samples (separately extracted) was between 3-10%. However, the day to day variation was larger, as is reflected by the confidence intervals in Tables 3 and 4. In general, those elements with lower blanks, or with one major isotope, had smaller confidence

Table 3: Recoveries of 10 ppb rare earth elements from a 119,000 ppm uranium solution[a]

Rare Earth	m/z	Average Concentration with confidence limits (ppm)[b]
La	139	9.2 ± 0.9
Ce	140	9.0 ± 0.8
Nd	146	9.0 ± 0.8
Sm	152	9.5 ± 1.1
Eu	153	9.5 ± 1.1
Gd	157	9.2 ± 0.7
Tb	159	9.5 ± 0.6
Dy	163	9.3 ± 0.3
Ho	165	9.7 ± 0.4
Er	166	9.7 ± 0.3
Tm	169	9.9 ± 0.4
Yb	174	10.0 ± 0.2

[a]Ten trials were conducted on three different days. Ten ppb is equivalent to 0.084 µg/g U.

[b]Confidence limits were calculated at the 95% probability level.

intervals in their recoveries. The elements Pb and Zr had larger confidence intervals due probably in part to differences in their extraction efficiency from sample to sample. The large amount of uranium present, especially in the initial extraction, could affect the extractability of Pb and Zr into the organic phase.

Table 4: Recoveries of other metal ions from a 119,000 ppm uranium solution[a]

Metal Ion	m/z	Number of Trials	ppb Metal Ion Spiked	Average Concentration with Confidence Limits[b]
Al	27	8	100	112 ± 18
Ti	48	14	10	8.7 ± 0.7
V	51	8	100	95 ± 11
Cr	52	11	100	107 ± 7
Mn	55	14	10	9.5 ± 0.9
Co	59	14	10	9.8 ± 1
Zn	66	8	100	99 ± 18
Sr	88	14	10	9.9 ± 0.9
Y	89	14	10	9.8 ± 0.4
Zr	90	14	10	11 ± 2
Cd	114	13	10	11 ± 1
Cs	133	14	10	9.7 ± 0.6
Ba	138	8	100	104 ± 5
Pb	208	11	100	112 ± 18

[a]Data were obtained on 3 or 4 different days. Ten ppb is equivalent to 0.084 µg/g U and 100 ppb is equivalent to 0.84 µg/g U.

[b]The confidence limits were calculated at the 95% probability level.

Sample Analysis

Once the recoveries had been demonstrated, different uranyl nitrate salts were analyzed for impurities using this extraction procedure. The first nitrate salt was analyzed for cesium using the Ames Laboratory instrument. The calibration curve is shown in Figure 4 and is linear in the analysis range. The level of cesium was found to be 2.14 μg per 1.000 g uranyl nitrate. Another uranyl nitrate salt was analyzed for impurities using the Sciex instrument. The results in ng/g U are given in Table 6. The standard deviations are rather high because of the low levels of the elements present as well as the high blanks (from the HNO_3) and drifting of the analyte signal. The detection limits for elements in a 2 mg L^{-1} uranium solution (i.e., the same U concentration as the samples) are also given in Table 6. The uranium in the standards and blanks used to determine these detection limits was not extracted. Therefore the native impurities in the uranyl nitrate were still present, but at levels below detectability. These detection limits are ten to a hundred times better than those for comparable extraction/detection experiments using ICP-AES reported in the literature (12,30,34). Thus the utility of the present method is clear, especially if precision can be improved.

Flow Injection Analysis

Because the extraction is quick and relatively efficient, this procedure could be automated using flow injection solvent extraction directly coupled to the ICP-MS. Such a procedure would limit contact of the analyst with radioactive materials. There are some restrictions which are placed on a system. First of all the organic phase must be completely removed from the aqueous phase entering the plasma. The

Figure 4: Log(Cs counts) versus Log(concentration of Cs)

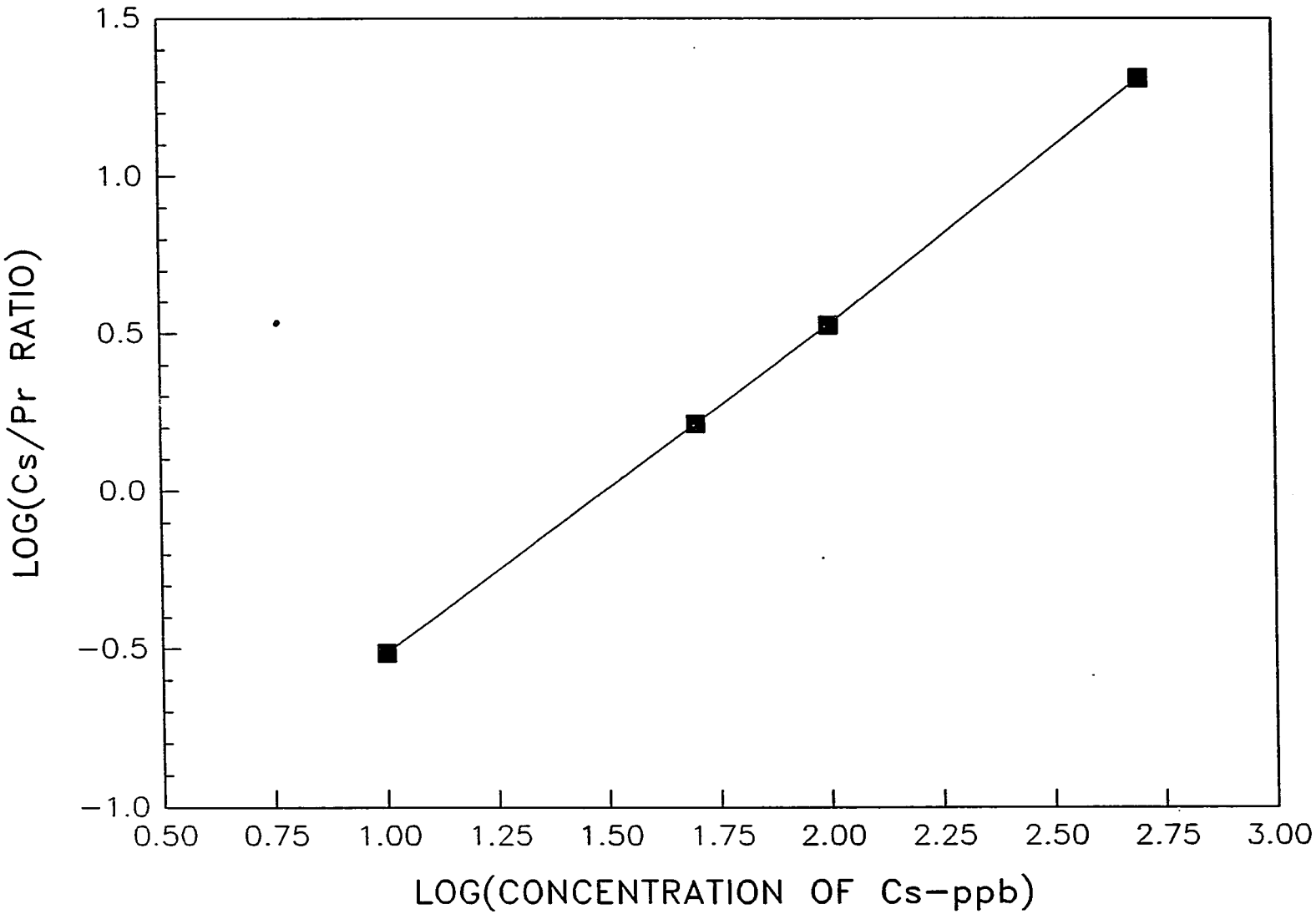
1.5
1.0
0.5
0.0
−0.5
−1.0
LOG(Cs/Pr RATIO)
0.50
0.75
1.00
1.25
1.50
1.75
2.00
2.25
2.50
2.75
3.00
LOG(CONCENTRATION OF Cs−ppb)

Table 5: Concentration of trace elements in a uranyl nitrate sample

Metal Ion	Average Concentration ng/g U	Standard Deviation[a]	Detection Limits ng/g U[b]
Al	360	220	9
Ba	940	40	0.5
Cd	31	13	2
Ce	2.8	0.7	0.3
Co	55	7	2
Cr	620	80	7
Cs	<0.3		0.3
Dy	<1.3		0.8
Er	<0.9		0.4
Eu	<0.4		0.4
Gd	<0.8		0.8
Ho	<0.1		0.1
La	<1.0		0.4
Mn	130	15	3
Nd	<2.4		0.8
Pb	400	100	0.8
Pr	<0.7		0.3
Sm	<1.3		0.8
Sr	86	11	0.2
Tb	<0.2		0.2
Ti	120	40	5
Tm	<0.5		0.2
V	110	9	4
Y	120	15	0.2
Yb	<0.3		0.3
Zn	560	330	8
Zr	67	41	0.8

[a]Standard deviation for the metal concentration determined from four separate samples, each carried through three extractions.
[b]Concentrational detection limits in µg/L are 0.088(ng/g U).

organic phase will change the signal, and the carbon generated will clog the torch. The uranium in the organic phase will cause ionization suppression. Finally a sufficient flow rate is required to sustain the plasma and produce an adequate signal.

A preliminary test of an on-line extraction cell was carried out,and a diagram of the extraction cell and the flow injection system is shown in Figure 4. The cavity in the cell is in the shape of a cone, its point oriented down. The phases are separated by gravity and the aqueous layer exits from the point. The flow restrictors provide back pressure and are used to vary the flow rate in each line exiting the separator cell. Teflon tubing and viton peristaltic pump tubing was used because toluene and nitric acid attack other types of tubing.

The system was optimized through the use of the flow rate of the pump and flow restrictors. The best separation of the two phases achieved was approximately 80-90% water and 10-20% organic modifier through the aqueous line at a flow rate of approximately one ml per minute flow rate. Addition of a second tee on the aqueous line did not increase the separation of the phases. In addition, the organic phase slowly dissolved the seals on the flow restrictors shortening the lifetime of the seals before replacement.

Extraction using S-DBF

Because amides have been shown to be efficient extractors of uranium, a thioamide, N,N-dibutylformamide (S-DBF) was synthesized and tested. S-DBF is produced by the reaction shown in Equation (2).

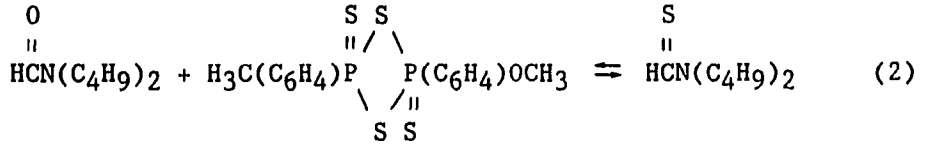

$$HCN(C_4H_9)_2 + H_3C(C_6H_4)P(S)P(S)(C_6H_4)OCH_3 \rightleftharpoons HCN(C_4H_9)_2 \qquad (2)$$

Figure 5: System used for FIA experiments

(A) Schematic of the FIA system built

(B) Flow cell diagram: A is the aqueous phase outlet

B is the organic phase outlet

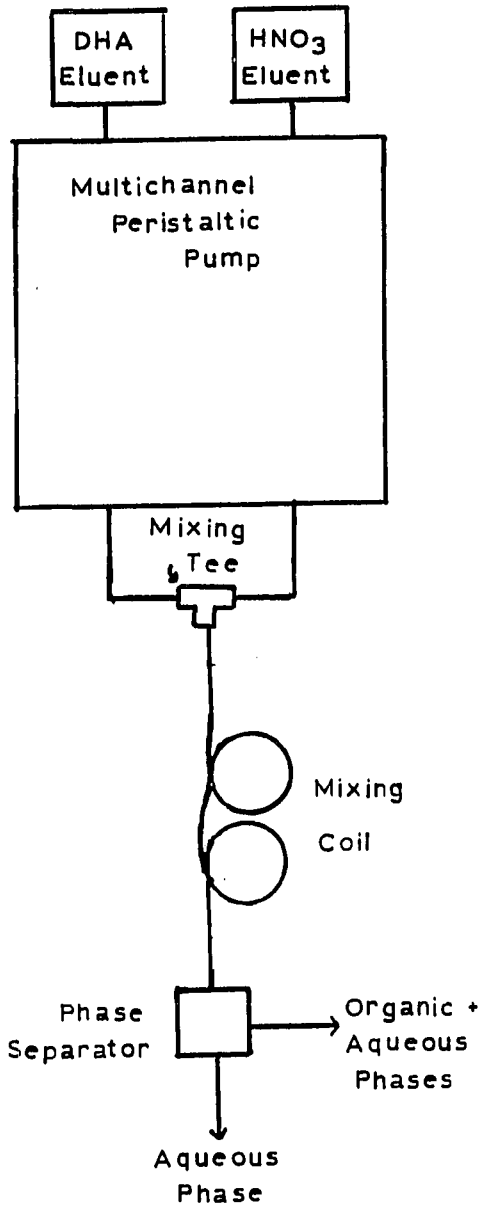
DHA Eluent
HNO_3 Eluent
Multichannel Peristaltic Pump
Mixing Tee
Mixing Coil
Phase Separator
Organic + Aqueous Phases
Aqueous Phase

(A)

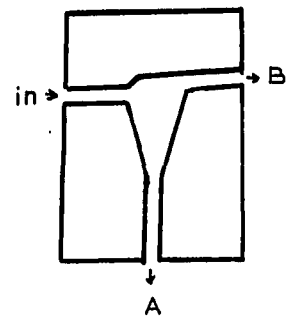
in
B
A

(B)

One problem encountered was that S-DBF seemed to polymerize with itself. A white precipitate formed upon standing and could not be dissolved with the toluene diluent. Elemental analysis indicated that the solid had the same composition as the liquid product. The liquid portion remaining was drawn off and diluted with toluene for the extraction experiments.

Uranium was the first metal tested, and in 1 and 2 M $NaNO_3$ uranium(VI) was not extracted. Lead(II) was then tested because it shows some affinity for sulfur. Table 6 shows that as the nitrate concentration increases, the extraction efficiency decreases. Increasing the pH of the aqueous phase dramatically increases the extraction of lead(II) as shown in Table 7. The hydrogen on the sulfonyl carbon is probably losing its proton at the higher pH values which enhances the extraction of the lead(II) ion. The anion present at the higher acidities would also inhibit the extraction. Sulfur loving species such as mercury(II), and silver(I) are over 99% extracted by S-DBF. A potentiometric titration indicates approximately a one to one ratio of silver to S-DBF with a formation constant of approximately 4×10^8. Once

Table 6: Study of the effect of nitrate concentration on the extraction of Pb by S-DBF. The pH is held constant at 1.7

$[NO_3]$	D_c
0.05	0.19
0.10	0.08
0.50	0.06
1.0	0.07

extracted, the metal complexes slowly precipitated out of the organic phase, and could not be back extracted. Because of the problems described, no further work was carried out on S-DBF.

Table 7: Study of the Pb-SDBF complex as a function of pH

pH	D_c
0.5	0.08
1.0	0.10
1.7	24.4
4.1	89

CONCLUSION

Several directions can be taken to expand upon the the research presented here using DHA and other related amides. Because of the chemical similarity between the trivalent actinides and the lanthanides, it should be possible to separate and determine trivalent actinides in uranium solutions using the basic procedure described here. Conversely, hexavalent and quadrivalent actinides may be extracted using amides. Gasparini and Grossi (50) have shown that plutonium and neptunium in nitric acid are extraced by amides and their data suggest that DHA could also be used to extract these actinides.

The determination of uranium in hydrochloric acid could be done using DHA as an extractant, followed by analysis using the ICP-MS. An experiment was carried out using hydrochloric acid as the extracting acid instead of nitric acid. Using 2 M hydrochloric acid and 2 M DHA in toluene extractant, the D_c for uranium was 61 and the D_c for thorium was 0.48. Uranium was efficiently extracted while the thorium was extracted over ten fold less in hydrochloric acid than in nitric acid. There was some nitrate present as the anion of the dissolved metal salts and as HNO_3 in the organic phase, both of which probably contributed to the extraction of the metals. However, too much uranium and not enough thorium was extracted for the nitrate alone to be the cause of the extraction. The low amount of thorium extracted could also be corrected for. Other papers have described the extraction of uranium from hydrochloric acid using n-octylamine and have also found that thorium was extracted to a lesser extent (34). Analysis of uranium for trace elements could be done for those elements which do not form strong

chloride complexes; such elements include the lanthanides and thorium. Those elements which form complexes with chloride could not be determined and include iron, cobalt, and zinc. Using two different acid extractions, one should be able to analyze most of the metal impurities present in uranium.

The extraction of uranium for trace element analysis could be carried out using other amides. Because uranium, thorium, and zirconium extraction is dependent upon amide structure, the use of other amides may decrease the extraction efficiency of thorium and/or zirconium without decreasing the extraction of uranium appreciably. Greater selectivity for uranium may be achieved and thorium and zirconium could be determined. Conversely, a judicious choice of amides would improve the extraction of thorium and zirconium, and these amides would give fairly selective extractions for those two elements in the presence of other elements.

Further experimentation can be carried out to develop the extraction FIA system. The experiment described here indicates that it should be feasible to separate completely the two phases for direct coupling to an ICP-MS. Because the cell originally was designed for analysis of the organic phase, further cell design changes are probably necessary (70). An organic solvent heavier than water may improve the separation of the two phases in the cell used. Finally the use of membranes may improve the separation. Other workers (76,78) have used membrane separator cells primarily for analysis of organic phases, but Fossey and Cantwell have used membranes to analyze aqueous phases (77). Some testing was done to separate the phases using a paper membrane without success; trying various papers and different organic phases may improve the separation of

the phases.

Finally, further investigation of the extraction power of other thioamides may be carried out. S-DBF does extract with metal ions which form complexes with sulfur. Other thioamides, in particular thioamides with longer organic chains, may not polymerize or their metal complexes may not precipitate out of solution, and they may be potentially useful extraction agents.

SECTION II. SYNTHESIS, CHARACTERIZATION, AND ANALYTICAL APPLICATIONS OF 2,6-DIACETYLPYRIDINE BIS(FUROYLHYDRAZONE)

INTRODUCTION

Analytical chemists have long been concerned with determining trace elements in various matrices. Metal impurities pose several problems in various samples. The impurities can affect the performance of a product, and knowledge of impurities is required by several government agencies, in particular for pharmaceuticals, food, and other consumer goods.

An element which has received considerable attention by analytical chemists is uranium. Trace uranium impurities not only compromise the integrity of a sample, but can pose health hazards. Uranium is radioactive, and ingestion of uranium has been linked to bone cancer, lung cancer, and kidney damage (79). Nuclear power plants and other industries which use or process uranium must analyze products and waste for uranium in order to prevent exposure of the public to uranium.

Uranium analysis has been carried out using a variety of procedures. By far the most popular procedures for determining uranium involve spectral methods (79). In recent years, spectroscopic methods such as ICP-AES and ICP-MS have begun to be used to determine uranium. However, many spectrophotometric analyses for uranium are still being carried out. Spectrophotometric procedures can offer some selectivity in determining uranium in the presence of other elements, and spectrophotometry does not require expensive and complicated equipment. Typically spectrophotometry is carried out by adding an organic complexing reagent to a solution containing uranium, and the uranium is determined by measuring the absorbance of the uranium complex in solution. This chapter describes a spectrophotometric method for determining uranium using the complexing agent 2,6-diacetylpyridine bis(furoylhydrazone) (H_2dapf). The reagent,

as shown below, and complexes uranium over a broad range of pH values. The spectrophotometric method is reasonably sensitive for uranium.

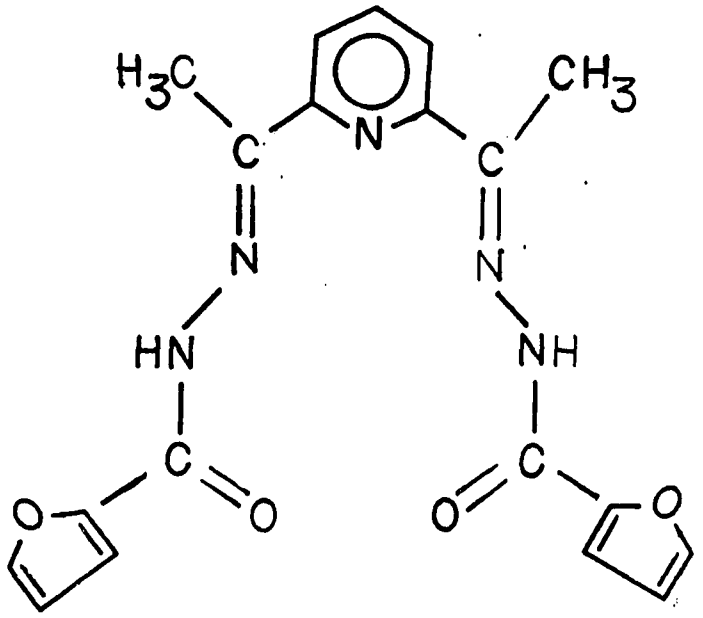

(I)

LITERATURE REVIEW

Spectrophotometry is based upon the ability of a species in solution to absorb light at a specific wavelength. The amount of light absorbed in most analtyical systems obeys the principles of Beers Law and is described in many books (80-82). According to Beers Law, for a given wavelength, the light absorbed by a species in solution is proportional to the concentration of that species. The equation form of Beers Law is

$$A = \varepsilon bc \qquad (3)$$

where A is the absorbance, b is the cell path length, c is the concentration (M), and ε is the molar absorptivity. Typically, analytical spectrophotometry uses ultraviolet or visible radiation. When determining inorganic cations, an excess of organic complexing agent is added to a sample, and the absorbance of the complex is measured at a wavelength where the complex absorbs. The wavelength is chosen such that there is a minimum of background absorbance and preferably where there is a plateau in the complex absorbance spectrum. The type of complexing agent used depends upon the type and concentration level of the analyte, and the type of sample being analyzed.

Spectrophotometric analyses for uranium using organic chelating agents have been developed by workers around the world. Literally hundreds of compounds have been tested as spectrophotometric reagents for determining uranium. A comprehensive review of spectrophotometric reagents is given in Gmelin (79) and Snell (83). Most reagents tested are not very sensitive or selective for uranium. The reagents complex primarily through nitrogen and oxygen located in functional groups. Table 8 lists the major spectrophotometric reagents used in uranium

determination and the class of compounds to which they belong. With molar absorptivity values for the uranium complexes of less than 10^4, the inorganic reagents are not very sensitive for uranium, but have seen extensive use, particularly in the 1940s and 1950s. The organic reagents listed in Table 8 have molar absorptivities for their uranium complexes ranging from 2×10^4 to 1.2×10^5 and have replaced inorganic reagents in many analyses. In order to improve selectivity for uranium, most procedures include performing an extraction or adding masking agents to the sample.

One class of compounds which has not received much attention as possible analytical complexing agents are the substituted hydrazones, in particular the hydrazone derivatives of 2,6 diacetylpyridine. Substituted hydrazones have the structure (II) where R is varied.

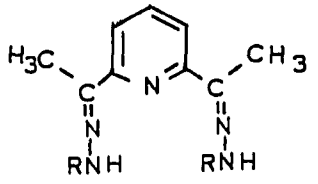

(II)

Curry et al. (104) first investigated the iron(III), cobalt(II), nickel(II), and copper(II) complexes of derivatives where the R groups are hydrogen, methyl, phenyl, and pyridyl and found that the pyridyl derivative, 2,6-diacetylpyridine(pyridylhydrazone) (H_2dapp) was a quinquedentate ligand. Webster and Palenik (105, 106) studied zinc(II) and cobalt(II) complexes, and Paolucci et al. (107, 108)) studied the uranium(VI) complex of H_2dapp. The above studies concurred with Curry's initial work that H_2dapp formed a quinquedentate ligand with the metal ion where complexation occurs through the three pyridyl nitrogens and the

Table 8: Major spectrophotometric reagents for uranium

Reagent	Reagent Class	Comments	Reference Numbers
Arsenazo I	Azo dye containing arsonic acid groups	Water soluble chelate. Greater selectivity using EDTA and tartrate as masking agents.	64,84
Arsenazo III	Azo dye containing arsonic acid groups	Water soluble chelate. Greater selectivity in acidic conditions	85-87
Dibenzoyl-methane	1,3 β diketone	Insoluble in water. Used with solvent extraction for greater selectivity	88,89
Hydrogen Peroxide	inorganic	Not very sensitive. Used for more concentrated samples	90
8-hydroxy-quinoline	nitrogen containing aromatic	Insoluble in water. Coupled with solvent extraction for greater selectivity.	91,92
Bromopyridyl-azo diethyl-aminophenol (Br-PADAP)	azo dye	Higher selectivity for Fe than PADAP. Masking agents CDTA, NaF, and sulfosalicylic acid improve selectivity.	93,94
Pyridylazo diethylamino-phenol (PADAP)	azo dye	Insoluble in water. Selective when used with MIBK extraction	95,96
1-(2-pyridyl-azo)-2 naphthol (PAN)	azo dye	Insoluble in water. Coupled with solvent extraction for greater selectivity	97,98

Table 8: Continued

Reagent	Reagent Class	Comments	Reference Numbers
Pyridylazo resorcinol (PAR)	azo dye	Water soluble chelate. Masking agents CDTA, NaF, and sulfosalicylic acid improve selectivity	99,100
Rhodamine B	ternary	Very sensitive water soluble chelate. Benzoic acid is the most common third ligand.	101
Thiocyanate	inorganic	Not very sensitive. ε is solvent dependent.	102,103

imino nitrogens.

Several groups have studied 2,6-diacetylpyridine bis(aroylhydrazone) derivatives; these derivatives have the same structure as shown in (II), with R being O=CR′ where R′ is varied. For this group of reagents, the most attention was given to 2,6-diacetylpyridine(picolinoylhydrazone) (H_2dappc) and its complexation with copper(II) (109), manganese(II) (110, 111), cobalt(II) (111), nickel(II) (111), and zinc(II) (111). Other groups have studied the tin (IV) complex of 2,6-diacetylpyridine(salicyloylhydrazone) (H_2daps) (112), the uranium(VI) complex of 2,6 diacetylpyridine(methoxy-benzoylhydrazone) (H_2dampb) (113), and the cobalt(II), nickel(II), copper(II), and zinc(II) complexes of 2,6-diacetylpyridine(benzoylhydrazone) (H_2dib) (114). Complexation of the bis(aroylhydrazone) derivatives occurs through the pyridyl nitrogen, the imino nitrogens, and the carbonyl oxygens to form four five-membered rings with the metal ion. The structure of this complex is shown in Figure 6. Recently, some analytical applications of the 2,6-diacetylpyridinebis(hydrazone) derivatives have been reported in the literature. Casoli et al. described the solvent extraction and high performance liquid chromatographic (HPLC) separation of the uranium H_2dib complex (115, 116). Garcia-Vargas et al. (117) studied the extraction of antimony(III) with H_2dib and 2,6-diacetylpyridinebis(2-hydroxybenzoylhydrazone) and determined antimony(III) spectrophotometrically using H_2dib (117).

The aroylhydrazones described are readily synthesized in alcohol and all the hydrazones studied were made following the same basic procedure. The one-step reaction occurs between 2,6-diacetylpyridine and a hydrazide as shown in the reaction below to give the hydrazone. The mixture is

Figure 6: Structure of the metal-hydrazone complex

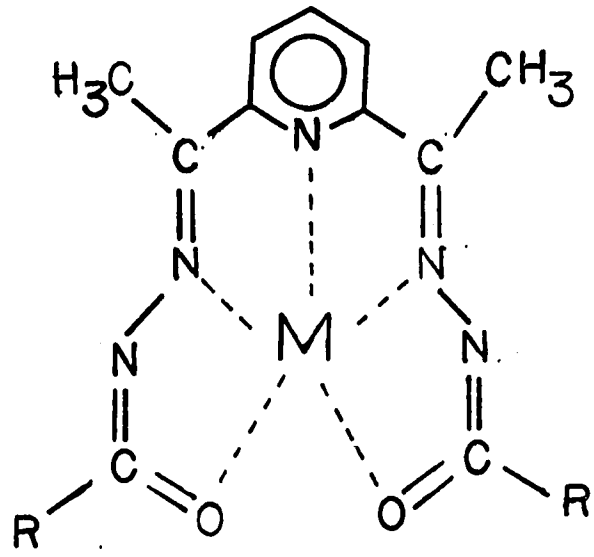
H3C
CH3
N
C
C
N
N
M
N
N
C
C
R
O
O
R

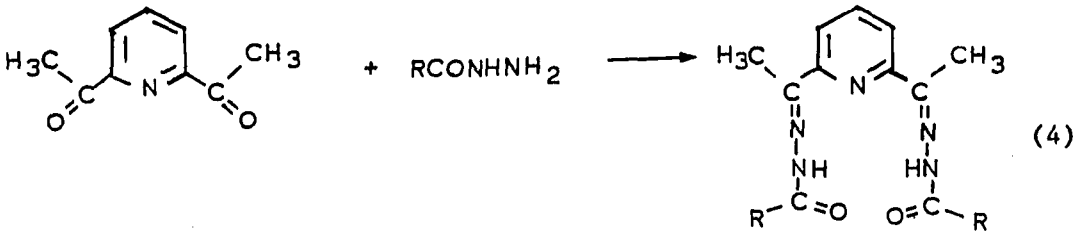

(4)

refluxed and the product precipitates out of solution for easy isolation.

EXPERIMENTAL

Synthesis of H_2dapf

To a 250 ml round bottom flask was added 0.05 M 2-furoic acid hydrazide and 0.025 M 2,6-diacetylpyridine (Aldrich) in 100 ml of absolute methanol. The mixture was heated for three hours at 40°C, cooled and filtered. The precipitate collected was crystallized in methanol as small white crystals.

The following procedures were used to characterize H_2dapf. The IR spectrum was taken using KBr pellets. The mass spectrum was obtained on a Hewlett Packard 5995A GC/MS at 70 eV using a direct insertion probe and with a scan speed of 200 amu per second. The temperature of the probe was increased from 90°C to 320°C at a rate of 64°C per minute. The NMR spectrum of the sample dissolved in $CDCl_3$ and containing TMS as the internal standard was taken using a Jeol FX90Q FT-NMR.

Complex Formation Studies

Two milliliters of 1 x 10^{-3} M metal ion solution, 2 ml of 1 x 10^{-3} M reagent in methanol, and 2 ml of buffer solution were mixed together and diluted to volume. The pH was varied from 0 to 8. Color intensity was used to determine maximum formation of the complexes.

Spectra of selected complexes were taken using a Perkin Elmer 552 UV-VIS Spectrophotometer at a pH of maximum complex formation. Solutions used in measurement of molar absorptivity contained a two-fold excess of reagent to metal ion concentration. Metal ion solutions were prepared by dissolving the nitrate or chloride salts.

Solvent Extraction Studies

For the solvent extraction experiments H_2dapf was used because it was less soluble in aqueous solutions. The metal complex was pre-formed in a methanol water solution which was buffered for maximum complex formation. The solution contained 8 x 10^{-5} M metal ion and 1.6 x 10^{-4} M H_2dapf which was then extracted once with an equal volume of CH_2Cl_2. The metal ions were then determined by established colorimetric methods (66).

Uranium Colorimetric Determination

A sample aliquot containing between 18 µg and 270 µg uranium(VI) was placed in a 30-ml beaker. To the sample was added 1.0 ml of 0.10 M EDTA, 10.0 ml of methanol, 4.0 ml of methanolic H_2dapf, and 1 ml of a 1.0 M triethanolamine (TEA) buffer. The pH (apparent pH) was adjusted to 6.0 using a Corning 125 pH meter and diluted with water to 25 ml. For the solutions analyzed at a pH of 3.3, a 2.5 ml aliquot of a 0.10 M formate buffer was used. The absorbance of the uranium complex was measured at 400 nm. The titanium studies were carried out using the procedure desrcribed for uranium except that the pH was adjusted to 2.0 using an HCl/KCl buffer.

For the sorption experiments, the gravitational flow mini-column containing 150-200 mesh XAD-4 was prepared. The column was washed with deionized water at a pH of 6.0 using the TEA buffer. A 10 ml aliquot of the sample solution containing 1 x 10^{-5} M uranium(VI) and H_2dapf in 56% methanol with an apparent pH of 6.0 was passed through the column. The column was washed with 5 ml of water, and the complex was eluted with 10 ml of 100% methanol. The eluate was collected in a 10 ml volumetric flask and the absorbance was measured at 400 nm.

In the concentration experiment 200 ml of a 2.0 x 10^{-7} M uranium(VI)

solution was placed in a 500 ml beaker containing 10 ml of methanol. To the uranium sample was added 4.0 ml of methanolic H_2dapf and 3 ml of the TEA buffer solution. The pH was adjusted to 6.0, and the solution was passed through the gravity column containing XAD-4. Five milliliters of deionized water was passed through the column, and the uranium complex was eluted with 10 ml of 100% methanol. The methanolic eluate was collected in a 25 ml volumetric flask, buffer was added, and its absorbance was measured and compared with a UO_2-H_2dapf solution of an equivalent concentration.

RESULTS

Physical Properties of the Ligands and Metal Complexes

The synthesis of H_2dapf resulted in a greater than 90% yield. The solids and most solutions of the synthesized compound was stable to light and could be kept for several months without discernible degradation; H_2dapf in basic solutions decomposed with time. The physical characteristics for H_2dapf are given in Table 9. H_2dapf is not very

Table 9: Characterization Data of H_2dapf

Molecular Weight	Melting Range, °C	IR maxima, cm^{-1}	Major mass spectral lines, M/z (%)	^1H NMR in $CDCl_3$ (no. of H)
379	238-241	3310	77(18)	8.4-8.2 (1H)
		3080	95(100)	7.6 (1H)
		1660	104(66.7)	7.4(1H)
		1580	105(15.7)	6.6(1H)
		1550	132(25.4)	2.5(3H)
		1490	145(15.4)	1.6(1H)
		1435	188(16.3)	
		1330	284(14.5)	
			379(1)	

soluble in nonpolar solvents or water, but can be readily dissolved in methanol and acetone. H_2dapf is more soluble than H_2dib due to the polar furoyl groups, but at higher concentrations (greater than one mM), methanol was used to make up the solutions. Figure 7 gives the UV- Vis spectrum of H_2dapf in its protonated, neutral, and deprotonated forms. When protonated, the spectrum of H_2dapf shows a hypsochromic shift indicating a loss of conjugation.

The metal complexes of H_2dapf and H_2dapp gave a yellow or yellow green color. Table 10 shows the pH of maximum formation for the various metals tested. The structure of H_2dapf and H_2dapp allows for the formation of up to four chelate rings for each chelate molecule bound to the metal ion. An x-ray study of the H_2dampb-uranium complex showed that the hydrazone ligand forms a quinquedentate complex with the uranyl ion (113). The large number of chelate rings gives greater complex stability than that observed for other ligands such as EDTA, tartrate, and citrate. When titrating uranium(VI) with H_2dapf, the ligand to metal ratio for the metal complexes was determined to be one to one as shown in Figure 8. This ratio agreed with results attained from x-ray crystallography experiments done on the uranyl-H_2dampb solid (113). The formation constant was determined using the graphical method outlined by Garcia (118). The absorbances (A) were measured of solutions which had been successively diluted (dilution factor=β) from a solution containing stoichiometric ratios of uranium(VI) and H_2dapf which had an initial concentration of b. For a one to one complex, a plot of $(\beta A)^{1/2}$ versus βA should yield a straight line with a slope of $(K/A)^{1/2}$. From the plot in Figure 9, the log of the formation constant for the uranyl-H_2dapf complex was determined to be approximately 5.3.

Figure 7: Spectrum of 1.25×10^{-5} M H_2dapf in 40% methanol at pH = 2.0, 5.5, and 11.2

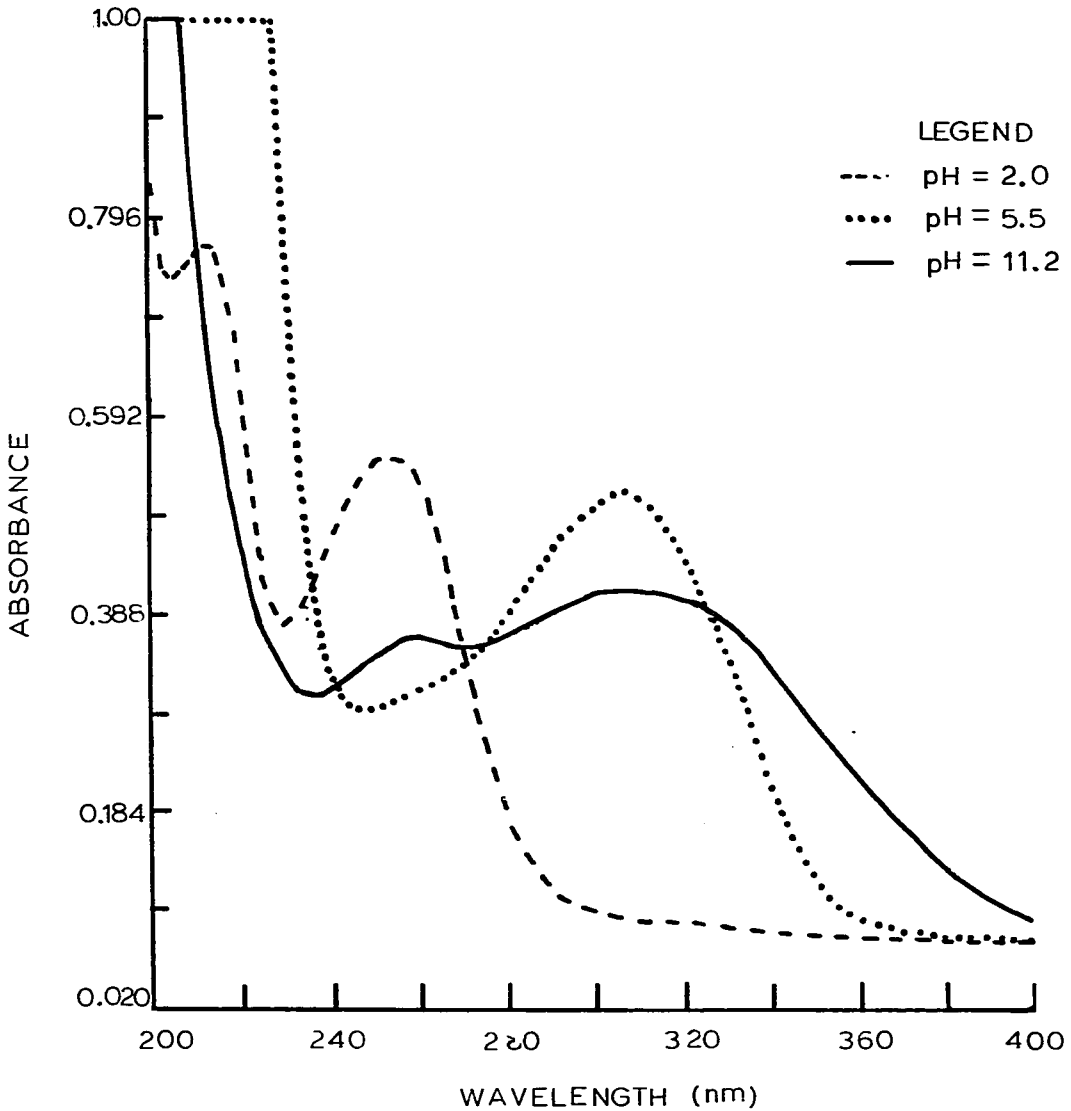
1.00
0.796
0.592
0.386
0.184
0.020
ABSORBANCE
200
240
280
320
360
400
WAVELENGTH (nm)
LEGEND
pH = 2.0
pH = 5.5
pH = 11.2

Table 10: pH of maximum formation and molar absorptivity of peak maxima of the metal complexes of H_2dapf and H_2dapp versus a reagent blank[a]

metal ion	pH_{max}	λ_{max}	ε
Fe^{3+}	1	334	3.0×10^4
Ti^{4+}	2	378	2.2×10^4
Zr^{4+}	2	358	1.0×10^4
UO_2^{2+}	3	354	3.5×10^4
		400	1.5×10^4
Cu^{2+}	4	350	2.0×10^4
Th^{4+}	4	350	3.2×10^4
		397	1.7×10^4
Tm^{3+}	5	349	2.8×10^4
Ni^{2+}	6	373	3.2×10^4
Tb^{3+}	6	350	2.5×10^4
Y^{3+}	6	352	2.8×10^4
Hg^{2+}	7	353	2.0×10^4
Mn^{2+}	7	348	2.2×10^4
		382	1.3×10^4
Ag^{+}	8	354	0.4×10^4
Co^{2+}	8	352	3.5×10^4
Pb^{2+}	8	360	1.1×10^4
		408	1.0×10^4
Eu^{3+}	9	351	2.1×10^4

[a]The samples were made up in 60% methanol and 40% water and an excess of complexing agent. The pH measured was the apparent pH.

Figure 8: Photometric titration of 5.0×10^{-5} M uranium with 1.0×10^{-3} M H_2dapf

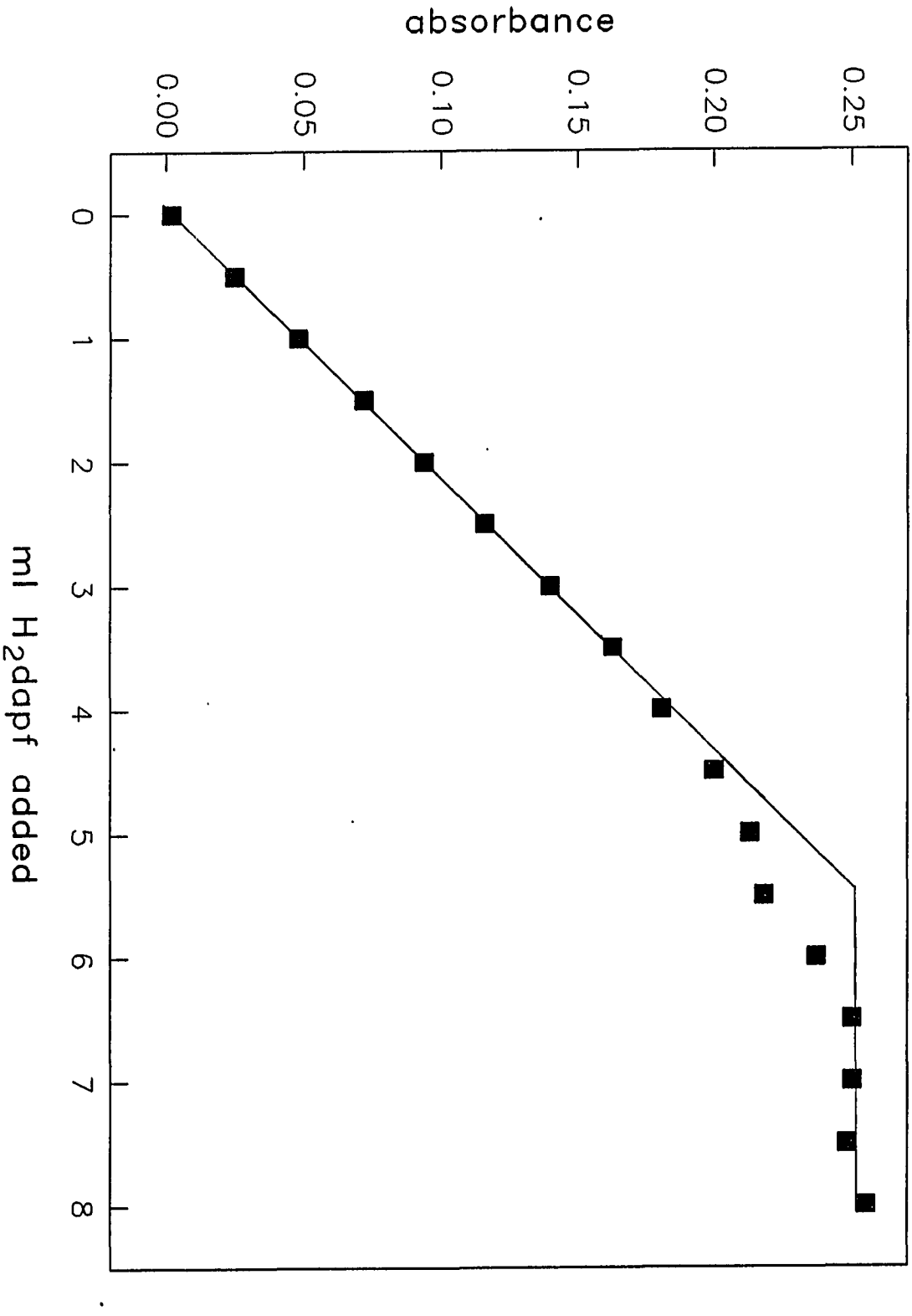
absorbance
0.00
0.05
0.10
0.15
0.20
0.25
0
1
2
3
4
5
6
7
8
ml H2dapf added

Figure 9: Determination of $UO_2(H_2dapf)$ formation constant by the graphical method of Garcia

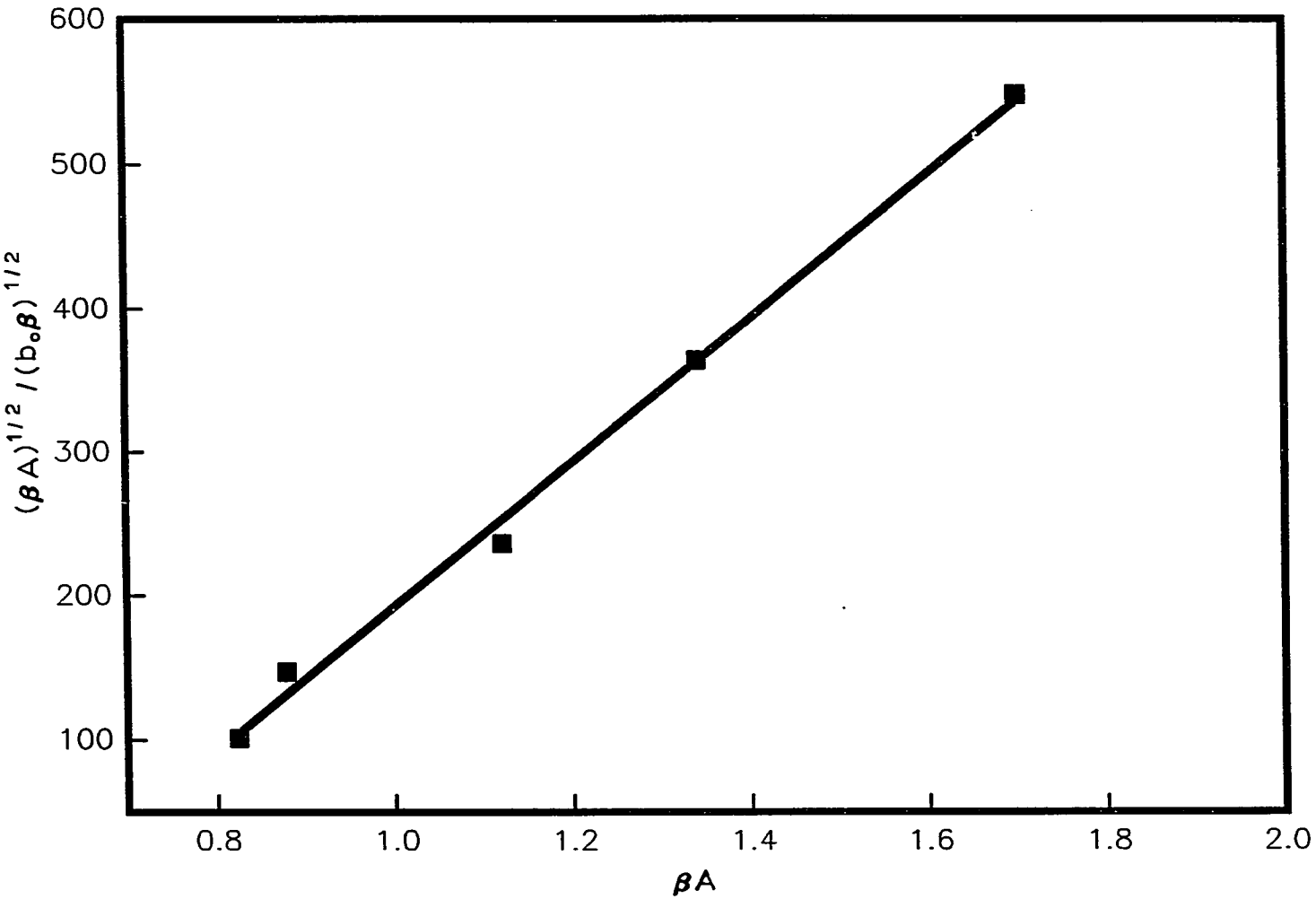
600
500
400
300
200
100
$(\beta A)^{1/2} / (b_o \beta)^{1/2}$
0.8
1.0
1.2
1.4
1.6
1.8
2.0
βA

Solvent extraction studies in methylene chloride were carried out using H_2dapf for uranium(VI), copper(II), and lanthanum(III), and Figure 10 gives the results. For efficient extraction the complex was preformed in aqueous solution; solvent extractions using organic phases containing H_2dapf resulted in poor efficiencies of extraction of the metals. A two to one ratio of H_2dapf to metal ion gave an efficient extraction (>99%) of the uranyl and copper(II) complexes. For a 98% extraction of lanthanum(III) at a pH of 7.6, a 10 to 1 molar ratio of H_2dapf to lanthanum(III) was required.

Uranium Colorimetric Determination and Interference Study

The yellow uranyl-H_2dapf complex formed instantaneously and remained stable for several hours. Figure 11 gives the UV-VIS spectra of H_2dapf and the uranyl-H_2dapf complex at a pH of 2.8. The uranyl-H_2dapf complex had two maxima: one at 340 nm and the other at 400 nm with molar absorptivities of 2.9×10^4 and 1.57×10^4 respectively. Figure 12 gives the Beers Law plot for uranium(VI) at 400 nm; the plot is linear from 2×10^{-6} to 4×10^{-5} M uranium(VI). At 341 nm there was still considerable absorbance by the H_2dapf ligand, and a high background for the uranium complex was consequently seen. In addition, the percentage of methanol in the solution affected the absorbance spectrum. As the percentage of methanol increased, the absorbance spectrum shifted to longer wavelengths, and at the 341 band the absorptivity increased. However, at 400 nm the absorptivity remained constant. Because of the dependence of molar absorptivity on the percentage of methanol in solution and a higher background at 341 nm, 400 nm was the preferred wavelength for analysis. At least 20% methanol is required to keep the

Figure 10: Graph of percentage of extraction of the UO_2^{2+}, Cu^{2+}, and Tb^{3+} H_2dapf complexes at different pH values with an organic phase of methylene chloride

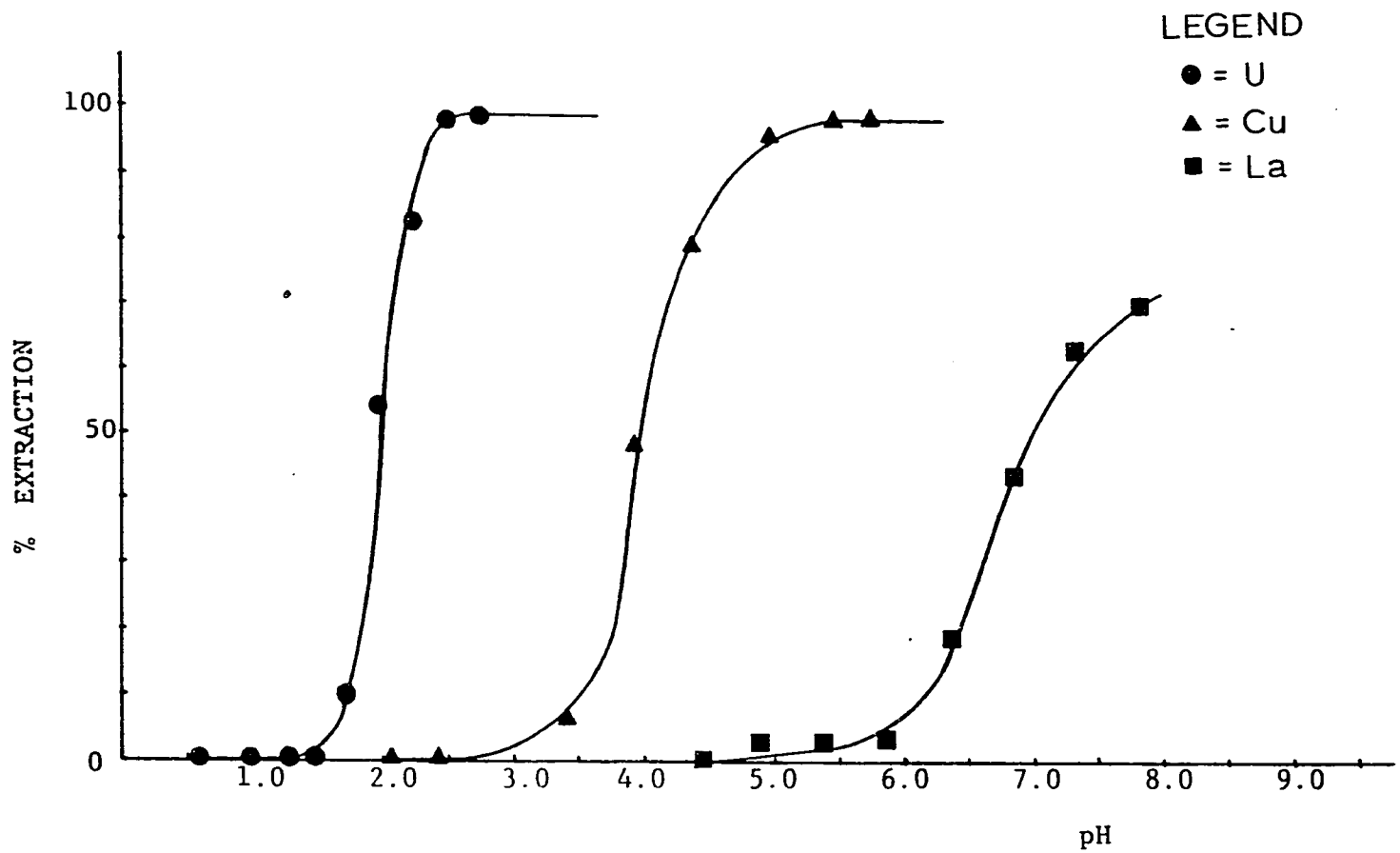
LEGEND
● = U
▲ = Cu
■ = La
100
50
0
% EXTRACTION
1.0
2.0
3.0
4.0
5.0
6.0
7.0
8.0
9.0
pH

Figure 11: UV-vis spectra of the following solutions made up in 28% methanol at a pH of 2.8:

Curve 1- 2.5×10^{-5} M H_2dapf versus water

Curve 2- 1.0×10^{-5} M UO_2^{2+} and 2.5×10^{-5} M H_2dapf versus water

Curve 3- 1.0×10^{-5} M UO_2^{2+} and 2.5×10^{-5} M H_2dapf solution of 2.5×10^{-5} M H_2dapf

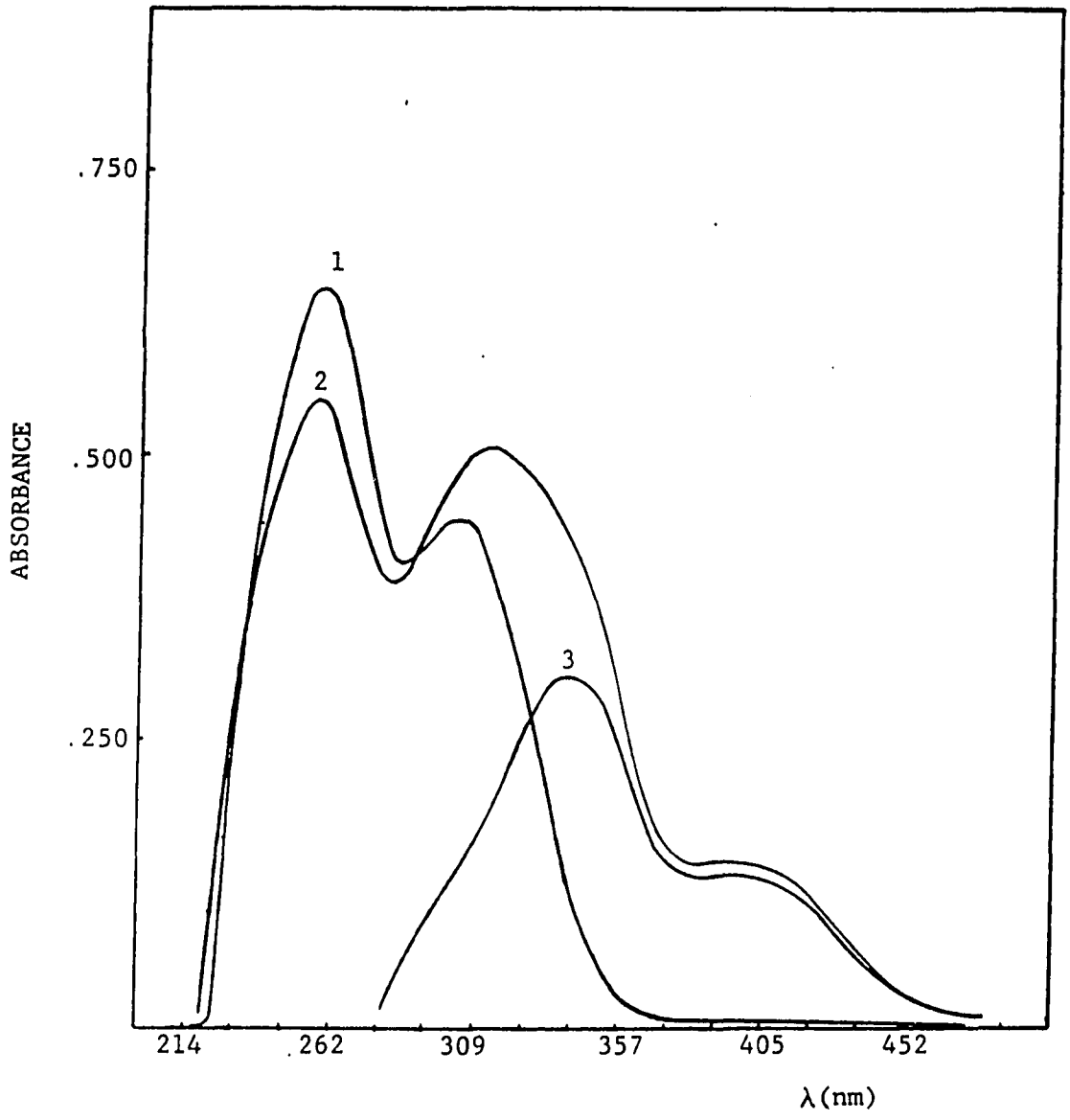
.750
.500
.250
ABSORBANCE
1
2
3
214
262
309
357
405
452
λ(nm)

Figure 12: Beers law plot of the uranyl-H_2dapf complex

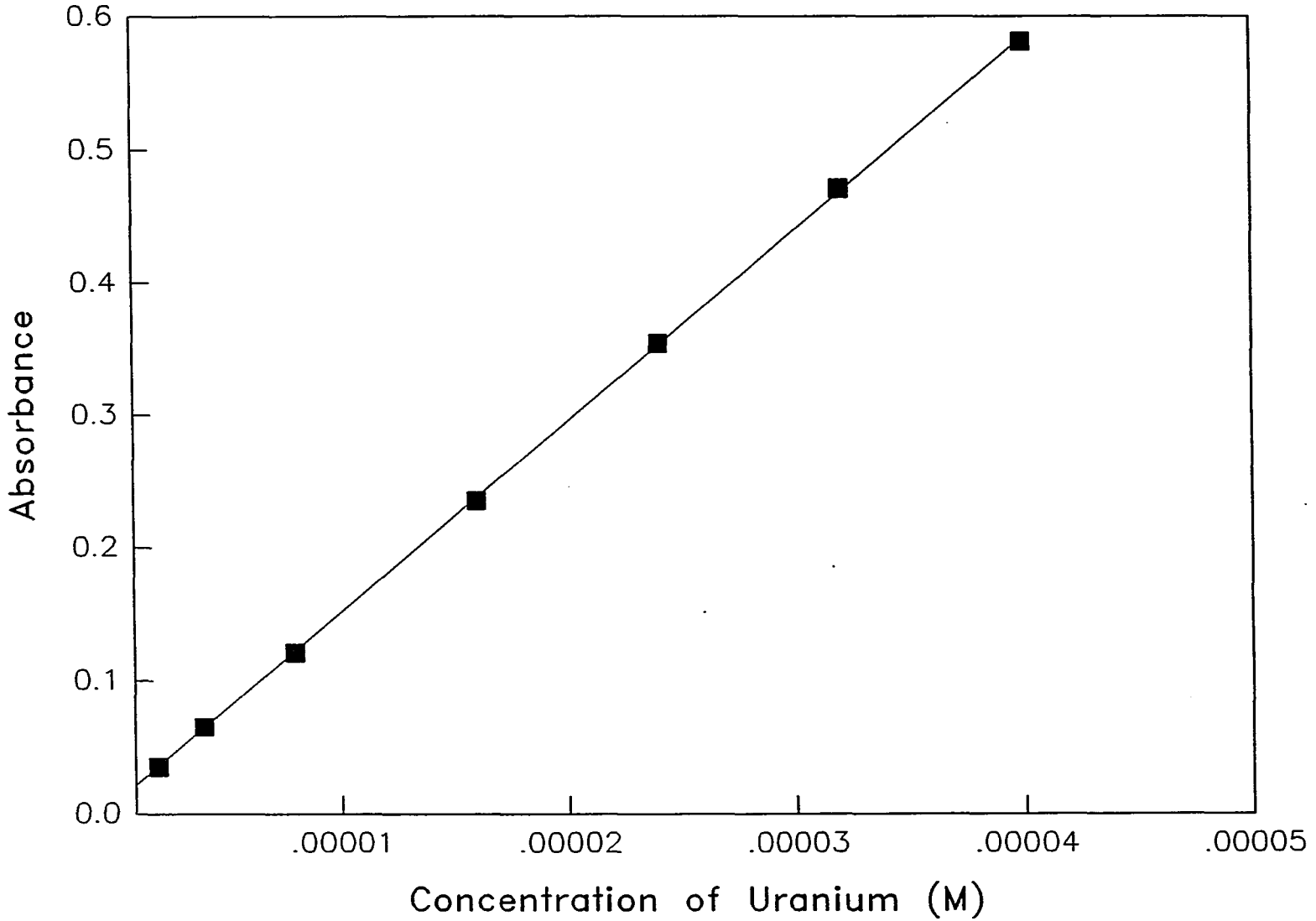
0.6
0.5
0.4
0.3
0.2
0.1
0.0
Absorbance
.00001
.00002
.00003
.00004
.00005
Concentration of Uranium (M)

uranyl-H_2dapf complex from precipitating. To maintain maximum absorptivity, the pH must be between 3.3 and 8.0.

Because H_2dapf forms complexes with many metals, there was considerable interference in the uranium determination from several other metal ions. At low pH values, thorium(IV), zirconium(IV), iron(III), copper(II), and titanium(IV) severely interfere with uranium(VI) when present in low concentrations. Many masking agents for these metals were either not particularly strong or they precipitated at low pH values. Low concentrations of lanthanide metals in solution were tolerated to a greater extent because at low pH values, very slight complexation occurs between H_2dapf and lanthanides. The masking effect of ethylenediamine tetraacetic acid (EDTA) on possible interferents was then tested at pH 6.0 to minimize precipitation of the EDTA in solution. Addition of EDTA to the solution eliminated interference from other metals with the exception of iron(III), zirconium(IV), and titanium(IV). Table 11 gives the maximum allowable concentrations of metal ions at pH 6.0 which can be present in solution without interference. EDTA masked zirconium(IV) and titanium(IV) at low concentration metal concentrations, but was ineffective at higher interferent levels. The interference from iron(III) after the addition of EDTA was due primarily to the absorption of the iron-EDTA complex at the same wavelength. A method used to correct for iron(III) interference required the preparation of two blanks: one containing sample and EDTA only and the other blank for the standard containing EDTA. Above a concentration of 4×10^{-4} M iron, the iron began to form a complex with the H_2dapf and a second blank could no longer be used.

Table 11: Maximum allowable concentration of metal ions present in the determination of a 2.0×10^{-5} M uranium solution using EDTA as a masking agent[a]

Metal Ion	Max. allowable conc. M	Mole ratio mole metal/ mole U
Al^{3+}	1.8×10^{-3}	91
Ca^{2+}	2.4×10^{-4}	12
Cd^{2+}	4.0×10^{-3}	200
Co^{2+}	4.9×10^{-4}	25
Cu^{2+}	3.0×10^{-3}	150
Fe^{3+}	1.2×10^{-5}	0.60
	4.0×10^{-4} [b]	20
Hg^{2+}	2.0×10^{-3}	100
La^{3+}	3.3×10^{-3}	166
Mn^{2+}	2.0×10^{-3}	100
Na^{+}	1.2×10^{-3}	60
Ni^{2+}	4.8×10^{-4}	24
Pb^{2+}	1.4×10^{-3}	72
Th^{4+}	6.0×10^{-4}	30
Ti^{4+}	2.0×10^{-4}	10
Y^{3+}	2.0×10^{-3}	100
Zn^{2+}	3.4×10^{-4}	168
Zr^{4+}	1.2×10^{-4}	6.0

[a]Determinations was made at pH = 6.0 using a TEA buffer. Each solution contained 0.004M EDTA. The maximum allowable concentrations of metals gave a 3% or less deviation in the uranium analysis.

[b]U analysis was done at pH = 3.3 using a formic acid buffer. The Fe interference was corrected for by the preparation of a second blank.

Resin sorption experiments were done to determine if the uranyl-H_2dapf complex could be concentrated from solution using a resin column. A solution containing 2 x 10^{-5} M uranium(VI) and an excess of H_2dapf was passed through a resin column, and the complex was then eluted off the column with 100% methanol. The average recovery of the uranium complex was 97.5%. A concentration experiment was then performed by following the previous procedure. A 250 ml solution of uranium(VI) was concentrated by a factor of ten, and an average recovery of 97% was attained. This experiment shows that H_2dapf is an effective chelating agent in analysis procedures requiring the preconcentration and determination of ultra-trace levels of uranium.

Investigation of the Titanium-H_2dapf Complex

In addition to uranium(VI), titanium(IV) formed a complex with H_2dapf at low pH values, and this complex was studied to see if it could be used as a spectrophotometric reagent for titanium. The titanium-H_2dapf complex had maximum color formation between the pH values of 2 and 3 and the spectrum for the complex is shown in Figure 13. The spectrum is dependent upon the methanol content; as the percentage of methanol increases, the UV peak at 350 nm shifts towards longer wavelengths. This solvatochromatic shift suggests that increased methanol content improves the charge delocalization through the complex, possibly by entering the coordination sphere of the complex. Since absorbance of the H_2dapf complex is methanol-dependent in most of the absorbance range, exact knowledge of the methanol content must be known when making up the complex.

A Job's plot study of the titanium-H_2dapf complex gave a 1.7 to one ratio of H_2dapf to titanium(IV), indicating a two to one ligand to metal

Figure 13: Absorbance spectrum of 2.5×10^{-5} M Ti-H_2dapf complex at pH = 2.0 in 8%, 44%, and 77% methanol

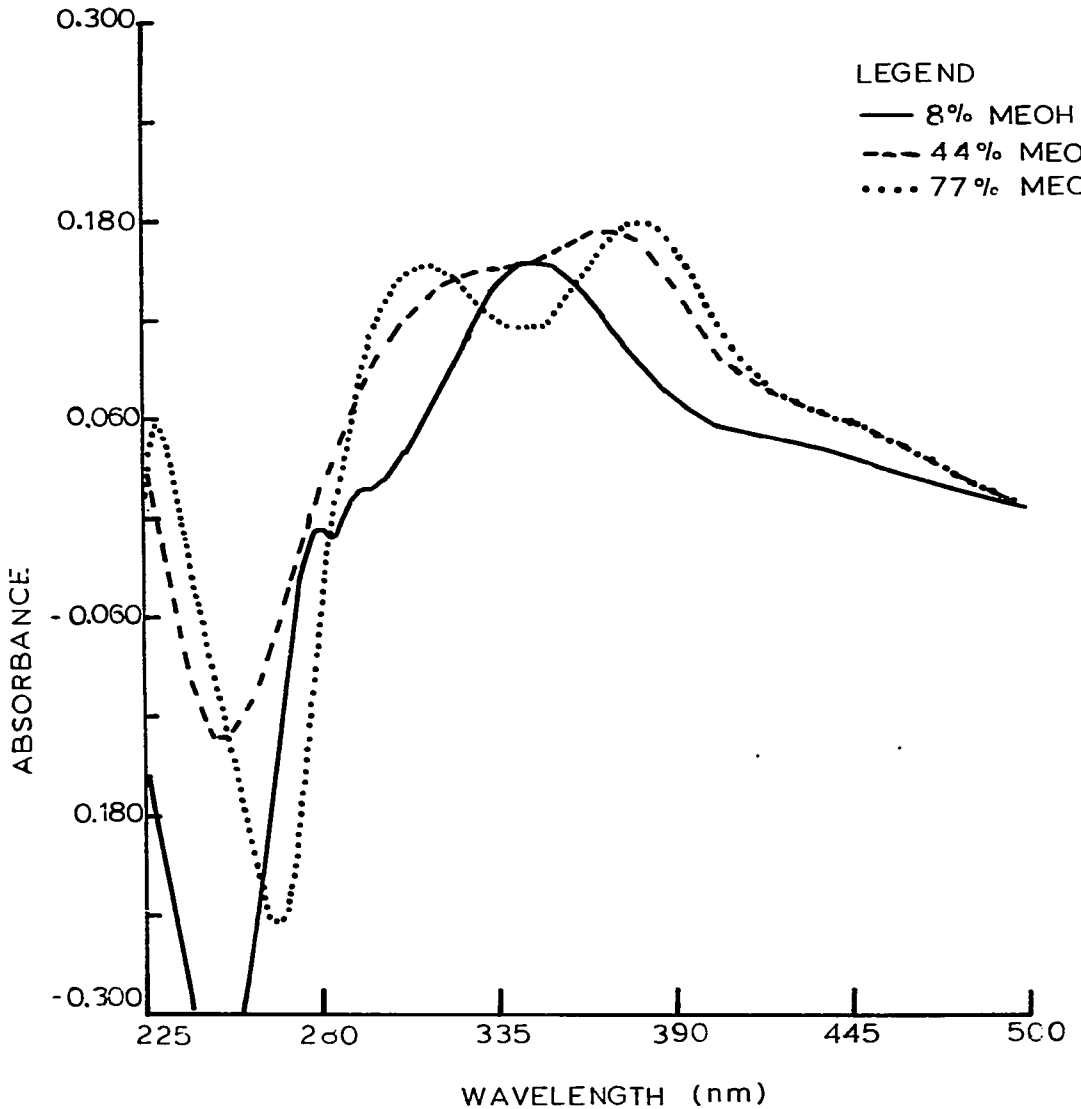
0.300
0.180
0.060
- 0.060
0.180
- 0.300
ABSORBANCE
225
280
335
390
445
500
WAVELENGTH (nm)
LEGEND
8% MEOH
44% MEOH
77% MEOH

complex. Titanium- H_2dapf solutions in 40% methanol were made up at pH 2.0, and at 400 nm, a Beers Law plot showed a linear range of 1 $x10^{-6}$ to 4.8 x 10^{-5} M titanium with a molar absorptivity of 1.6 x 10^4. The absorbances of different solutions containing the same amount of Ti(IV) and H_2dapf differed considerably from each other, and the linear calibration curve range varied each time a Beer's law study was carried out. Further investigation showed that the titanium-H_2dapf complex is not stable over time. Titanium-H_2dapf solutions were made up in varying percentage methanol content, and absorbances were measured over time. Over a 24 hour period, approximately a 20% decrease in absorbance was seen, with greatest decrease in absorbance occurring in the first hour. The solutions with the greatest methanol content initially had the slowest decrease in absorbance, but after 24 hours, the percentage decrease in the absorbance was simlar in all solutions. This decrease in absorbance is probably due to the hydrolysis of titanium. Titanium(IV) hydrolyzes very easily even at low pH values, and hydrolysis would cause a decrease in absorbance. The high methanol content in some of the solutions probably slowed down the initial hydrolysis of the titanium(IV).

Finally some masking agents were tested in order to see if other metal ions could be masked. No masking agent was found which did not interfere with the formation of the titanium-H_2dapf complex; the masking agents competed with the H_2dapf for the titanium.

CONCLUSION

H_2dapf has some use as a colorimetric reagent for the determination of uranium. Other reagents such as Arsenazo compounds (84-87) and Br-PADAP (99,100) are more sensitive for uranium than H_2dapf. With the addition of masking agents, these reagents are also selective for uranium. Because H_2dapf forms complexes with uranium(VI) at lower pH values than with the rare earth metals and many divalents, some natural selectivity occurs. At higher pH values uranium can be determined without interference using H_2dapf and EDTA. This complex is most useful, however, when preconcentration and determination of the uranium needs to be done. H_2dapf and its uranium complex can be concentrated and then eluted from a resin-based concentrator column. Many colorimetric reagents, such as the Arsenazo compounds irreversibly adsorb to hydrophobic resins making them useless for preconcentration procedures. The preconcentration of uranium using resin-based columns is preferable to solvent extraction because the latter method can be messy and time consuming. The masking of other metal ions present in a solution by EDTA in conjunction with the addition of H_2dapf to the sample followed by sorption of the complex onto a resin would allow selective preconcentration and determination of uranium.

Possible future work with this complexing agent could include performing HPLC of the uranium complex. Casoli et al. (115) showed that uranium could be separated from other elements using H_2dib and it should be feasible to separate uranium from other elements using H_2dapf. With H_2dapf it may be feasible to separate other metal ion complexes separated especially at higher pH values. The high molar absorptivites of the

complex would allow sensitive direct detection of the complexes. In addition, other substituted hydrazones could be evaluated as possible spectrophotometric reagents, such as H_2dampb, H_2dappc, and H_2daps.

SECTION III. DETERMINATION OF METAL IONS BY HIGH PERFORMANCE LIQUID CHROMATOGRAPHIC SEPARATION OF THEIR 1,3-DIMETHYL-4-ACETYL-2-PYRAZOLIN-5-ONE CHELATES

INTRODUCTION

The HPLC separation of metal organic compounds up has not been extensively studied up until recently. Two types of metal-organic compounds have been separated by HPLC: organometallic compounds and coordination complexes. Coordination complexes have received the most attention because of the wide availability of organic complexing reagents. Typically the organic reagents tested were originally developed as extractants or spectrophotometric reagents for metal ions. Many different types of organic complexing agents have been tested for use in the HPLC separation of metals; several reviews on the HPLC separation of metal complexes have been written (119-127).

Potential complexing agents for HPLC are evaluated on the basis of the following characteristics: formation of stable metal chelates, solubility of the complex in the mobile phase, complexation with a large number of metal ions, and a means of sensitively detecting metal ions (120). The most important consideration in choosing the complexing agent is the stablility of the metal complex. The metal complex must be stable enough to remain together while travelling through the HPLC column. Often, inert complexes are used because of their slow dissociation; kinetically labile complexes will break up on the column without special precautions. In general, five-membered chelate rings give the most stability, but four- and six-membered rings of several complexes also can be stable. The complex should be soluble in the mobile phase;if it is not, on-column precipitation will occur. For HPLC of metal complexes, a chelating agent which complexes a large number of metal ions is preferred so that a large number of metals can be separated in one run. The metal

chelates should have a characteristic property which can be detected by some sort of detector. The most common properties used to detect metal complexes are UV-vis absorptivity and electrochemical activity. Element specific detectors can be used to detect metal complexes.

This chapter will describe the HPLC separation of 1,3-dimethyl-4-acetyl-2-pyrazolin-5-one (DMAP) metal complexes. DMAP is a heterocyclic β-diketone and has the structure given below (III):

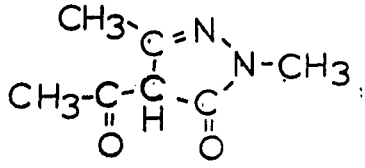

(III)

DMAP complexes a large number of metal ions and forms relatively strong complexes. Because DMAP and its complexes are water-soluble, they are ideal for use in reversed phase HPLC (RP-HPLC); precipitation of the metal complexes on the column at low organic modifier levels is avoided.

LITERATURE REVIEW

Chemistry of the 4-acyl-2-pyrazolin-5-ones

DMAP belongs to a general class of reagents called β-diketones. β-Diketones have the general structure shown in Equation (5) and in solution are in two forms: the enol and keto forms. β-Diketones have been extensively studied as chelating agents. Complexation of the β-diketones with metal ions takes place with the enolic form;

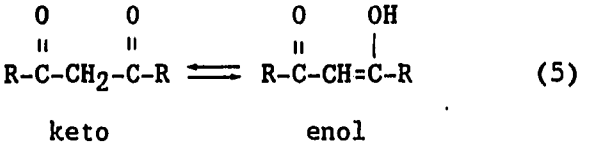

keto enol (5)

the subsequent complexes are neutral due to the loss of the acidic hydrogen (128). β-Diketones form six-membered rings with the metal ions, and in general complex with a large number of metal ions at varying pH values. Most of the β-diketones have been used as gravimetric, extraction, and spectrophotometric reagents. Some volatile fluoro-β-diketones have been synthesized for use in gas chromatographic separations. Several reviews have been written on the chemistry of β-diketones and their metal complexes (128-130).

DMAP belongs to a particular group of β-diketones called 4-acyl-2-pyrazolin-5-ones. 4-Acyl-2-pyrazolin-5-ones, are heterocyclic β-diketones, and the general structure is shown below. Stoltz synthesized

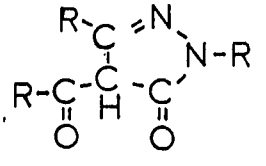

(IV)

the first 4-acyl-2-pyrazolin-5-one derivative in 1897. Since that time, many derivatives have been synthesized; Wiley and Wiley have reviewed the different procedures developed for synthesizing 4-acyl-2-pyrazolin-5-one derivatives (131).

Jenson first reported the analytical chelating properties of the 4-acyl-2-pyrazolin-5-ones in a series of articles (132-134). Complexation of the 4-acyl-2-pyrazolin-5-ones with metal ions occurs in a similar fashion to other β-diketones. Various 4-acyl-2-pyrazolin-5-ones have been tested as gravimetric, photometric, and extraction reagents for several different metal ions. One of the most intensively studied pyrazolone reagents, 1-phenyl-3-methyl-4-benzoyl-2-pyrazolin-5-one (PMBP), has been tested with many metal ions (128, 135, 136). Applications of the complex formation of PMBP with metal ions are shown in Table 12. Much of the early work using PMBP, particularly that involving actinide ions, has been conducted in the Soviet Union.

The complexing agent under present investigation, DMAP, was synthesized and characterized by King (136). King found that unlike other 4-acyl-2-pyrazolin-5-ones, both DMAP and its metal complexes display moderate solubility in water. The complexes sorbed readily onto a hydrophobic XAD-4 resin; in particular, the DMAP complexes of copper(II), iron(III), lanthanum(III), thorium(IV), uranium(VI), and zirconium(IV) were found to sorb quantitatively onto the resin at varying pH ranges. King also found that uranium(VI) formed the complex $UO_2(DMAP)_2$ with DMAP. He developed a method for concentrating and separating uranium(VI) from a solution by forming the uranium-DMAP complex and sorbing it onto XAD-4 resin. The complex was then eluted from the resin with an organic solvent and analyzed by spectrophotometry.

TABLE 12: Applications of 1-phenyl-3-methyl-4-benzoyl-2-pyrazolin-5-one to metal analysis

Metal Ion	Subject Studied	Reference
Ac(III)	Extraction with PMBP	137
Al(III)	Extraction with PMBP in various solvents	138
Am(III)	Extraction with PMBP	137-141
Am(III),Bk(III)	Extraction with PMBP	142
Am(III),Eu(III)	Extraction with PMBP and TOPO	143
Bi(III)	Extraction with PMBP and TBP or TOPO	144
Ca(II)	Extraction with PMBP	145
Cd(II)	Extraction with PMBP	146
Cu(II)	Extraction with PMBP and TBP	147
Eu(III)	Extraction with PMBP and TBP or TOPO	148
Fe(III)	Extraction and spectrophotometric determination Extraction from various mineral acids	149 150
Ga(III)	Separation from Tl(II) and In(III) Extraction with PMBP	151 152
Hf(IV)	Extraction studies with PMBP	153-157
In(III)	Extraction with PMBP	158
In(III).Sc(III),Y(III)	Extraction with PMBP	159

TABLE 12: Continued

Metal Ion	Subject Studied	Reference
Nb(V)	Extraction with PMBP and SCN^- or catechol	160
Ni(II)	Extraction with PMBP	161,162
	Extraction with PMBP and ClO_4^-	163
Np(III)	Extraction with PMBP	164,165
Pa(V)	Extraction with PMBP	163
Pb(II)	Extraction with PMBP	166
Pu(IV)	Extraction with PMBP from various mineral acid solutions	167
Sc(III)	Extraction with PMBP	168
Sr(II)	Extraction with PMBP	168
Ta(V)	Extraction from 9 M HCl	169
Th(IV)	Separation from Eu(III)	170
	Substoichiometric extraction	171
Ti(IV)	Extraction with PMBP	172,173
U(VI)	Extraction with PMBP	174–177
V(IV)	Spectrophotometric determination	178
Zn(II)	Extraction with PMBP and TBP or TOPO	179
Zr(IV)	Extraction from various mineral acids using PMBP	180

Liquid Chromatography of the β-Diketones

One of the most studied groups of complexing agents for separating metal chelates by HPLC are the β-diketones. In 1972, Huber et al. carried out the first HPLC separation of metal complexes using acetylacetone (acac) and trifluoroacetylacetone (tfaa) as chelating reagents (181). Using a liquid liquid normal phase system consisting of water, 2,2,4-trimethylpentane, and ethanol, Huber separated copper(II), aluminum(III), chromium(III), ruthenium(III), cobalt(III), and beryllium(III) acac complexes. The peaks initially were quite tailed; upon the addition of acac to the eluent, peak symmetry improved. Upon standing, aluminum-acac peaks gave multiple peaks; these multiple peaks were attributed to the hydrolysis of the aluminum complex. Tollinche and Risby (182) investigated the separation of the metal chelates of acac, tfaa, 2,2′,7,7′-tetramethyl-3,5-heptanedione (thd), and 1,1′2,2′,3,3′-heptafluoro-4,6-octanedione (fod). Normal and reverse phase chromatography were carried out using various solvents and column packings in the separation of beryllium(III), aluminum(III), chromium(III), iron(III), cobalt(III), nickel(II), copper(II), zinc(II), zirconium(IV), and ruthenium(III). Silica gel was found to give better separations than the alumina, bonded phase, and polyurethane columns tested. Order of elution and peak shape depended upon the column, stationary phase, β-diketone, and mobile phase composition. Schwedt also separated the beryllium(III)-acac complex by GC, TLC, by normal phase HPLC (183). Schewdt detected down to 150 pg beryllium using silica column and a methylene chloride acetonitrile eluent.

Three other normal phase separations have been reported in the literature on the separations of isomers of metal-β-diketone complexes.

Uden et al. separated tfaa and hexafluoroacetylacetone (hfaa) complexes of chromium(III) on a silica gel column using an acetonitrile-methylene chloride eluent (184). He found that pure and mixed chromium(III) complexes of tfaa and hfaa and the isomers of the tfaa complexes could be separated. Cobalt(III) isomers of benzoylacetylacetone (baa) and tris (2,2-dimethylhexane-3,5 dione) were also separated by normal phase HPLC. Yamazaki et al. reported the separation of cis and trans isomers of cobalt(III), chromium(III), and rhodium(III) of baa and tfaa on alumina and silica gel, respectively (185). Calibration curves for the complexes were linear for three orders of magnitude. Cardwell et al. separated brominated and nitrated cobalt(III), chromium(III), and rhodium(III) acac complexes by GC and HPLC (186). The cobalt derivatives were thermally unstable and were separated on a silica gel column in order of increasing substitution of bromine and nitrate groups. Finally, an interesting separation was reported by Bleyker on the separation of copper(II), nickel(II), and zinc(II) ions (187). The stationary phase was a tfaa bonded silica, and the mobile phase of acetone contained tfaa. Visible detection was achieved using a post column reactor system containing PAR.

Several papers on the separation of β-diketone metal complexes by gel chromatography using various polymeric gels have been published by Saitoh et al. (188-192). In the first paper, chromium(III) acac and tfaa complexes were separated, and it was found that separation of these complexes occurred on the basis of the size of the chelate and that there was negligible contribution from absorption and partition (188). In the following paper, acac complexes of nickel(II), cobalt(III), chromium(III), aluminum(III), and beryllium(III) were separated (189). In this case, interaction of the β-diketone with the gel were seen, in

particular with those complexes which were planar. Chromium complexes of acac, tfaa, baa, furoyltrifluoroacetone, benzyoltrifluoroacetone, thenoyltrifluoroacetone, and dibenzoylmethane were separated on several gels in the third paper (190). Separation of the chromium chelates was determined by the chelates' interaction with the gel and not by size or molecular weight. Saitoh et al. reported in 1977 that the variation of the mobile phase solvent changed the retention characteristics of the acac complexes of aluminum(III), chromium(III), iron(III), cobalt(III), and beryllium(III) (191). It was postulated that several of the complexes formed adducts with the mobile phase which would affect the retention. Finally beryllium(III) complexes of acac and tfaa were separated (192). A mixed acac-tfaa complex formed when the two pure complexes were together in solution, and the three forms were separated by HPLC.

Three studies were carried out using reversed phase HPLC of acac metal complexes. Willett and Knight determined chromium(III) in orchard leaf using a C-18 column and an acetonitrile-water eluent (193). Studies using nonbonded silica column showed silanol interactions with the complex. Gurira and Carr separated cobalt(III), beryllium(III), rhodium(III), chromium(III), ruthenium(III), palladium(III), and platinum(III) complexes on a C-18 column using acetonitrile or methanol as the organic modifier (194). Metal complexes were chosen which were kinetically stable in order to reduce dissociation of the complexes. Nickel(II) and copper(II) complexes were labile and decomposed on the column. Inversions of retention were also seen when different organic modifiers were used. The chromium(III) and cobalt(III) complexes were also shown to have linear calibration curves for over two orders of magnitude. Wenclawiak et al. separated chromium(III) and cobalt(III)

isomers of 2,2,7-trimethyloctane-3,5-dione (tod) on a C-18 column (195). The normal phase separation was also tested, but the four isomers could not be separated from one another. The researchers also investigated some fluoronated β-diketones and found that an inversion of elution order was seen between the cis and trans forms of the complexes.

One study has been carried out using a 4-acyl-2-pyrazolin-5-one as a complexing agent for the separation of trace metals by HPLC. Morales and Bartholdi separated uranium(VI), iron(III), thorium(IV), copper(II), zirconium(IV), and neptunium(IV) complexes of PMBP using a C-18 column and an acetonitrile-water eluent (196). A high percentage of organic modifier was required (>90%) because the complexes were very hydrophobic and were insoluble in water. The researchers also found that the addition of a small amount of PMBP to the eluent improved peak shape of the complexes.

EXPERIMENTAL

Synthesis of DMAP and Preparation of Solutions

DMAP was synthesized from 1,3-dimethyl-2-pyrazolin-5-one and acetyl chloride, and 1,3-dimethyl-2-pyrazolin-5-one was synthesized from methylhydrazine and ethylacetoacetate according to the procedures described by King (136). All organic reagents were purchased from Aldrich. Solutions of DMAP were prepared by dissolving DMAP in water.

Metal ion stock solutions were made from metal ion salts or from the metal. The salts and metals were obtained from various sources. Uranium(VI), copper(II), thorium(IV), and iron(III) solutions were made from the nitrate salt. Vanadium(IV) solution was prepared by dissolving vanadyl sulfate. Aluminum and gallium metals were dissolved in hydrochloric acid and nitric acid solutions respectively. Stock solutions used in the interference studies were made from nitrate, perchlorate, chloride, and sodium salts.

LC Studies

The chromatographic system consisted of a Milton Roy Simplex Mini Pump, Milton Roy Pulse Dampener, pressure release valve, 10 cm x 4 cm saturator column, Rheodyne 7010 injector, 0.2 μm Rheodyne inline filter, and a Tracor 560A UV-vis scanning detector. The saturator column was hand packed with silica gel (Amico) or XAD 16 (Rohm and Haas). Two types of columns were used: a 3 μm Zorbax C-18 silica column (40 mm x 6 mm) from Du Pont and a PLRP-S 5 μm polystyrene divinylbenzene (150 mm x 4.6 mm) column (PS-DVB) from Polymer Laboratories.

Eluents were prepared from Fisher HPLC grade acetonitrile, tetrahydrofuran, or methanol, and from water purified with a Barnstead

Nanopure II system. Acids and buffers were reagent grade or better. Eluent components were mixed together and filtered using a 0.2 or 0.45 µm Nylon 66 (Rainin) or PTFE filters (Nuclepore). Eluents were made fresh every day. For all eluents except those containing tetrahydrofuran, the flow rate was set at one ml per minute. When tetrahydrofuran was the organic modifier, the flow rate was reduced to 0.6 ml per minute, due to the high back pressure which formed when those eluents were delivered. For direct detection the detector wavelength was set at 318 nm. The eluents used for the majority of the studies contained 5×10^{-4} M DMAP and either 0.02 M pyridine or acetate (HAc) buffer. Apparent pH values of the eluent were measured using a Corning 125 pH meter and adjusted using nitric acid or NaOH solutions.

For the post-column reactor studies, an LKB 2150 HPLC pump delivered a post column reagent solution of 2.5×10^{-4} M Arsenazo I (Kodak) at approximately the same flow rate as the eluent. Organic modifier was added to the post-column reagent solution to prevent formation of air bubbles when the reagent and eluent were mixed together. The solution contained 0.2 M triethanolamine (TEA)-nitric acid buffer adjusted to pH 7.8. The tee was a standard low pressure fitting tee. After mixing the eluent and the post-column reagent, the pH of the resulting mixture was 7.6.

RESULTS

Spectral Studies for Detection

Ultraviolet absorption spectra were taken of the metal DMAP complexes versus a DMAP solution. The spectra showed that the complexes absorbed weakly between 300 and 345 nm, and most had molar absorptivities of less than 3000. Initially 330 nm was chosen for detection. When peaks were seen, the final detector wavelength was chosen by injecting the DMAP complexes and measuring peak height and background noise. A wavelength of 318 nm was chosen because it gave a maximum of signal and minimum of background noise. The background absorbance of the DMAP eluent at 318 nm was approximately 0.600 and was subtracted electronically.

Chromatographic Conditions

According to King's sorption studies of metal ion complexes onto XAD-4, an initial pH of 5 was chosen for the eluent buffer (136). At this pH, the largest number of metal ions formed complexes with DMAP and were either quantitatively or significantly sorbed onto the XAD resin. Initial testing was carried out using the PLRP-S column, a polystyrene divinylbenzene gel, because of its similarity to XAD resins and because it has no reactive column sites. The initial acetonitrile-water eluents tested contained no DMAP; no metal-DMAP complexes eluted. Upon addition of DMAP into the eluent, metal ion peaks were seen. When the concentration of DMAP in the eluent was varied, there were no significant changes in retention times. However, as the DMAP concentration in the eluent decreased, the peaks of the eluents became broader, and below 1×10^{-4} M DMAP, the peak for thorium disappeared. A concentration of 5×10^{-4} M DMAP was chosen for the eluent because it gave peaks for all

the metals, and because below that concentration, increases in peak width were noted. Figure 14 gives a chromatogram showing a separation of iron(III), gallium(III), uranium(VI), thorium(IV), copper(II), and vanadium(IV) complexes at pH 5. The thorium(IV) peak is broad for an early eluting peak, indicating that the thorium-DMAP complex may not be stable. In addition to the metal ion complexes shown in Figure 14, other metal complex peaks were seen. The aluminum(III) peak eluted as a broad peak at the same retention time as the thorium peak. Zirconium(IV) coeluted with uranium(VI) under these conditions. A titanium(IV) peak was sometimes seen eluting between thorium(IV) and uranium(VI); it was unstable and its retention time and appearance changed over time.

Different pH values of the eluent were tested to see if the separation could be improved or if different DMAP complexes could be seen. At higher pH values, direct detection was not possible due to the increased absorbance of the anionic form of DMAP, and eluents with higher pH values were not tested (181). As the pH of the eluent was lowered, the metal peaks began to elute earlier. In Figure 15, the chromatogram at pH 4, the thorium(IV) peak coeluted with copper(II), and gallium(III) eluted approximately two minutes earlier and partially overlapped with uranium(VI). Uranium(VI), zirconium(IV), and iron(III) retention times remained approximately the same. The aluminum(III) peak eluted as a broad and tailed peak at the same time as copper(II) and thorium(IV). As shown in Figure 16, when the pH of the eluent was lowered to 3 the iron(III) peak was not affected to a great extent, but the other peaks eluted much earlier. The copper(II), thorium(IV), and aluminum(III) peaks disappeared, while vanadium(IV), which coeluted with copper(II) at higher pH values, was still retained. Gallium(III) now eluted earlier

Figure 14: Separation of Cu(II), V(IV), U(VI), Ga(III), and Fe(III) DMAP complexes at pH 5.0 on a PLRP-S column

[V] = 1×10^{-4} M, [Cu] = 2.5×10^{-5} M, [Th] = 2×10^{-4} M, [U] = 2×10^{-4} M, [Ga] = 1×10^{-4} M, [Fe] = 1×10^{-4} M

Eluent conditions: 30% CH_3CN, 70% H_2O, 0.02 M HAc, 0.5 mM DMAP, flow rate = 1.0 ml per minute, detection at 318 nm

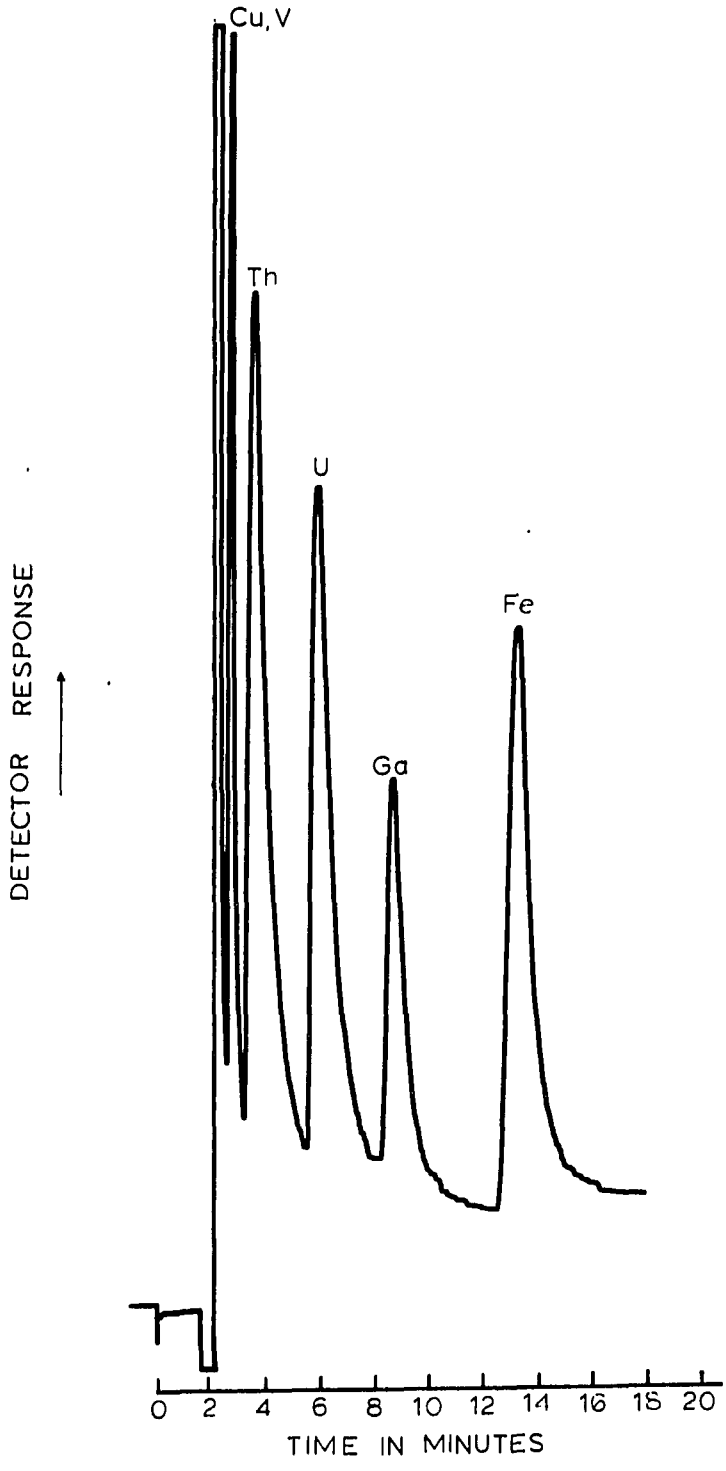
Cu, V
Th
U
Ga
Fe
DETECTOR RESPONSE
0 2 4 6 8 10 12 14 16 18 20
TIME IN MINUTES

Figure 15: Separation of Cu(II), Th(IV), U(VI), Ga(III), and Fe(III) DMAP complexes at pH 4 on a PLRP-S column

[Cu] = 2.5×10^{-5} M, [Th] = 2×10^{-4} M, [U] = 2×10^{-4} M, [Ga] = 1×10^{-4} M, [Fe] = 1×10^{-4} M

Eluent conditions: 28% CH_3CN, 72% H_2O, 0.02 M HAc, 0.5 mM DMAP, flow rate = 1.0 ml per minute, detection at 318 nm

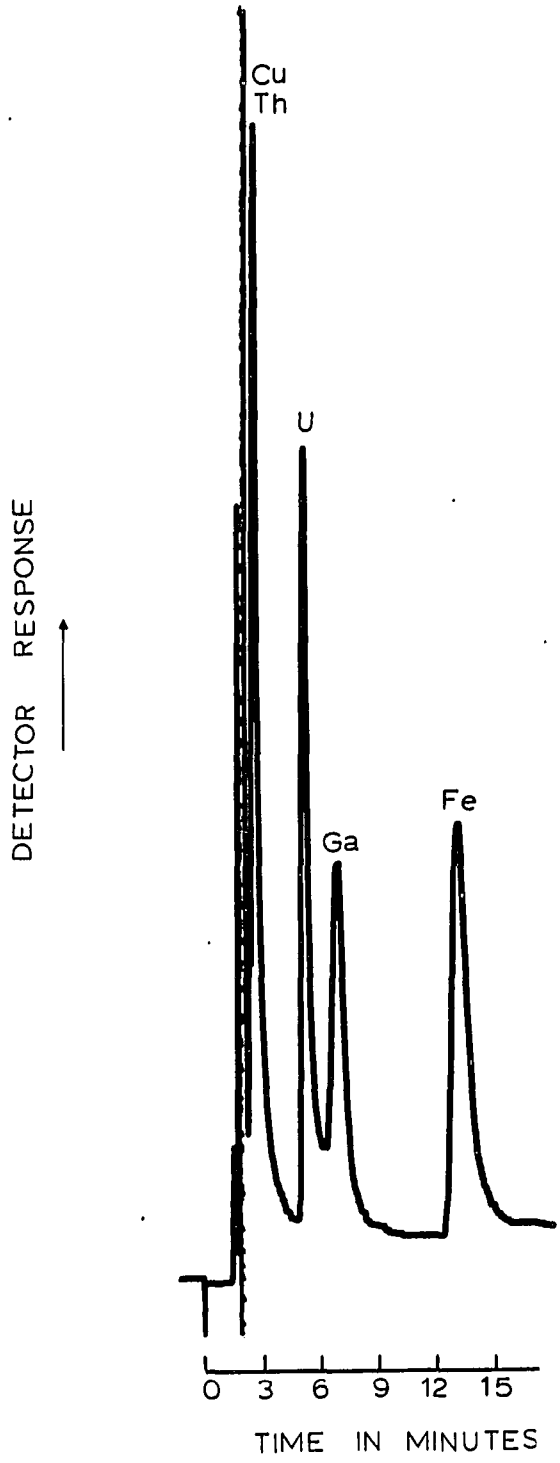
Cu
Th
U
Ga
Fe
DETECTOR RESPONSE
0 3 6 9 12 15
TIME IN MINUTES

Figure 16: Separation of V(IV), Ga(III), U(VI), and Fe(III) DMAP complexes at pH 3.0 on a PLRP-S column

[V] = 1×10^{-4} M, [Cu] = 2.5×10^{-5} M, [Th] = 2×10^{-4} M, [U] = 2×10^{-4} M, [Ga] = 1×10^{-4} M, [Fe] = 1×10^{-4} M

Eluent conditions: 25% CH_3CN, 75% H_2O, 0.02 M formate, 0.5 mM DMAP, flow rate = 1.0 ml per minute, detection at 318 nm

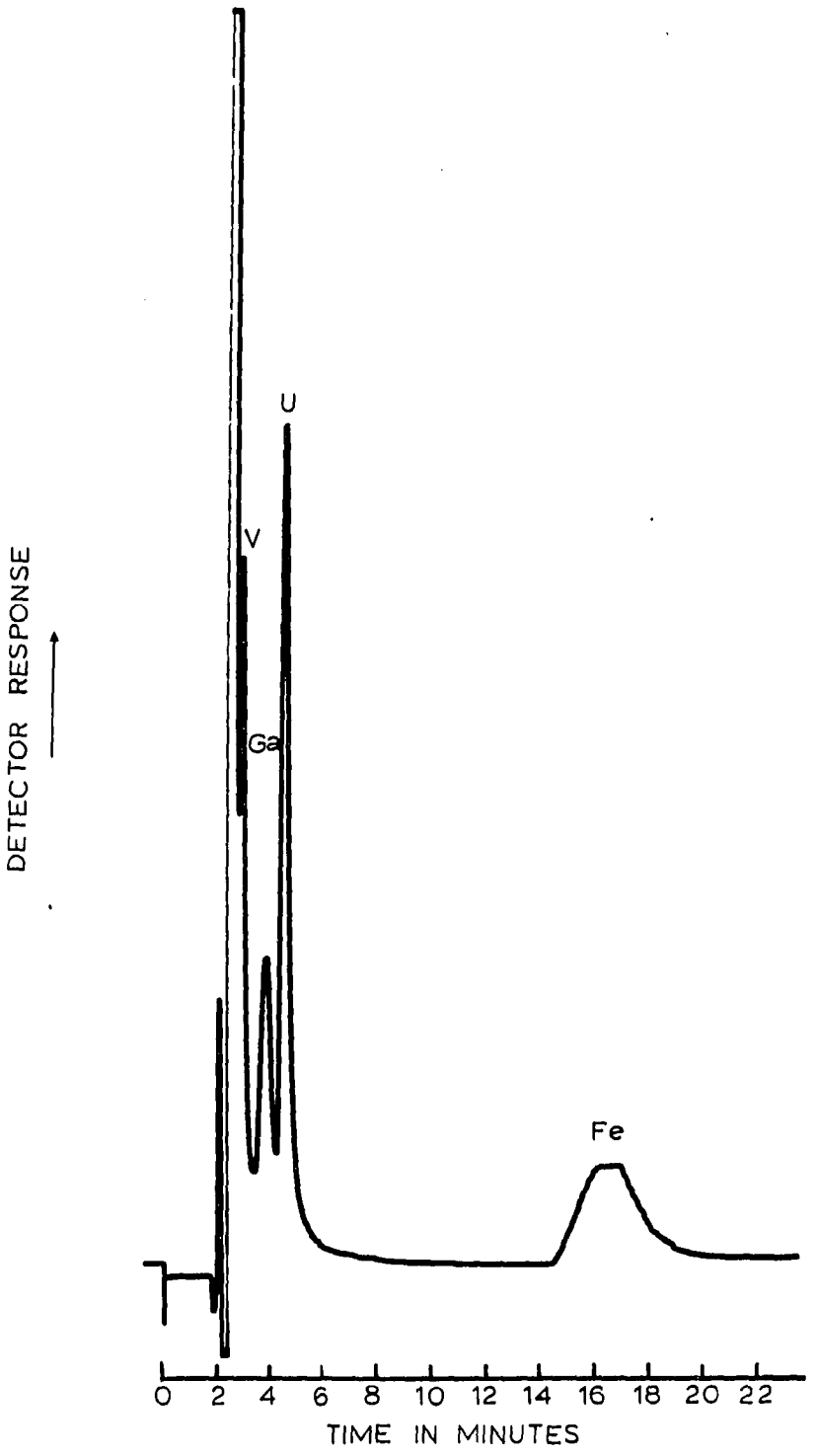
DETECTOR RESPONSE
V
U
Ga
Fe
0 2 4 6 8 10 12 14 16 18 20 22
TIME IN MINUTES

than uranium(VI), but zirconium(IV) still coeluted with uranium(VI). Of the metals tested at pH 2, only uranium(VI) and iron(III) were seen, and the peaks coeluted. The remainder of the studies were carried out at pH 5.0.

Different buffer solutions were tested to see the effect of the buffer on the separation. Pyridine, acetic acid, nicotinic acid, and hexamethylenetetramine buffers were tested for metal complex elution effects. Little difference was seen in retention or peak response when using pyridine, HAc, and hexamethylenetetramine. Nicotinic acid, however, affected the elution of gallium(III) as shown in Figure 17. Gallium(III) eluted earlier, and had a smaller and broader peak than when eluted in the other buffers. Eluent modifiers were also tested to see their effect on the retention of the complexes. In Figure 18, tetraethylammonium bromide was added, and the uranium(VI) peak became broader and overlapped with the gallium(III) peak. Addition of sodium perchlorate caused the thorium(IV) peak to elute under the uranium(VI) peak as shown in Figure 18.

Column Investigation

Because so many HPLC separations are carried out using modified silica columns, the metal-complex separation was tested on a C-18 column. Figure 19 gives the metal-DMAP complex separation using acetonitrile as the organic modifier. Retention order is different using the C-18 column. The gallium-DMAP complex elutes earlier than uranium(VI) and copper(II) complexes and coelutes with the vanadium(IV) complex. The thorium(IV) peak is no longer seen on the chromatogram. A small, broad thorium peak is seen at low acetonitrile concentrations on the C-18

Figure 17: Effect of eluent buffer on the DMAP complex separation at pH 5 on the PLRP-S column

[Th] = 2×10^{-4} M, [U] = 2×10^{-4} M, [Ga] = 1×10^{-4} M, [Fe] = 1×10^{-4} M

(A) Eluent conditions: 28% CH_3CN, 72% H_2O, 0.02 M nicotinic acid, 0.5 mM DMAP, flow rate = 1.0 ml per minute, detection at 318 nm

(B) Eluent conditions: 28% CH_3CN, 72% H_2O, 0.02 M HAc, 0.5 mM DMAP, flow rate = 1.0 ml per minute, detection at 318 nm

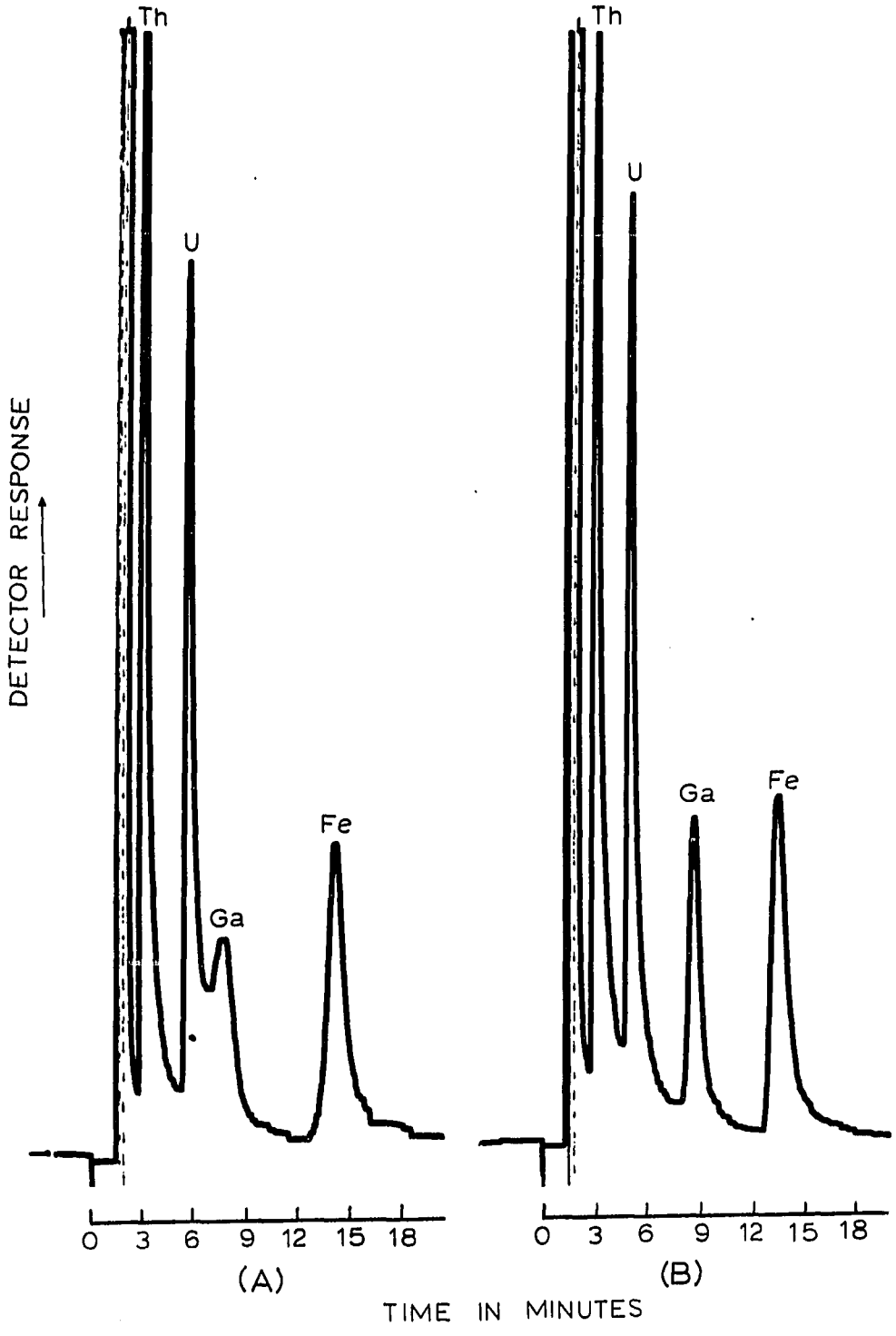
Th
U
Ga
Fe
DETECTOR RESPONSE
0 3 6 9 12 15 18
(A)
Th
U
Ga
Fe
0 3 6 9 12 15 18
(B)
TIME IN MINUTES

Figure 18: Effect of various salts in the eluent on DMAP complex retention at pH 5.0 using the PLRP-S column

[Cu] = 2.5×10^{-5} M, [Th] = 2×10^{-4} M, [U] = 2×10^{-4} M, [Ga] = 1×10^{-4} M, [Fe] = 1×10^{-4} M

A. Eluent conditions: 28% CH_3CN, 72% H_2O, 0.027 M $NaClO_4$, 0.02 M HoAC, flow rate = 1.0 ml per minute, detection at 318 nm

B. Eluent conditions: 28% CH_3CN, 72% H_2O, 0.050 M tetraethylammonium bromide, 0.02 M HoAC, flow rate = 1.0 ml per minute, detection at 318 nm

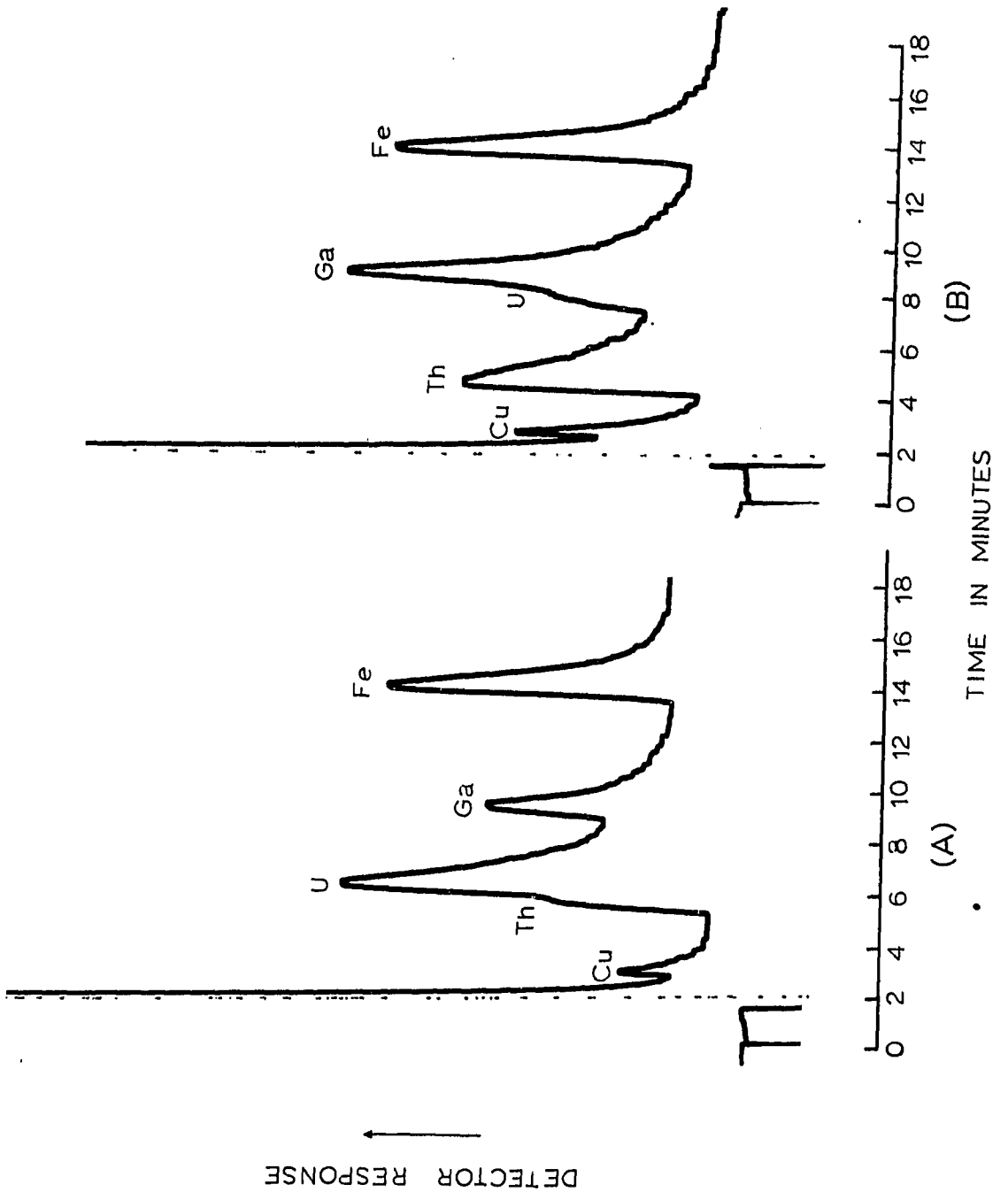
Fe
Ga
U
Th
Cu
Fe
Ga
U
Th
Cu
0 2 4 6 8 10 12 14 16 18
(B)
0 2 4 6 8 10 12 14 16 18
(A)
TIME IN MINUTES
DETECTOR RESPONSE

Figure 19: Separation of V(IV), Ga(III), Cu(II), U(VI), and Fe(III) DMAP complexes at pH 5.0 on a C-18 column

[V] = 1×10^{-4} M, [Cu] = 2×10^{-4} M, [Th] = 2×10^{-4} M, [U] = 2×10^{-4} M, [Ga] = 1×10^{-4} M, [Fe] = 1×10^{-4} M

Eluent conditions: 23% CH_3CN, 77% H_2O, 0.02 M HAc, 0.5 mM DMAP, flow rate = 1.0 ml per minute, detection at 318 nm

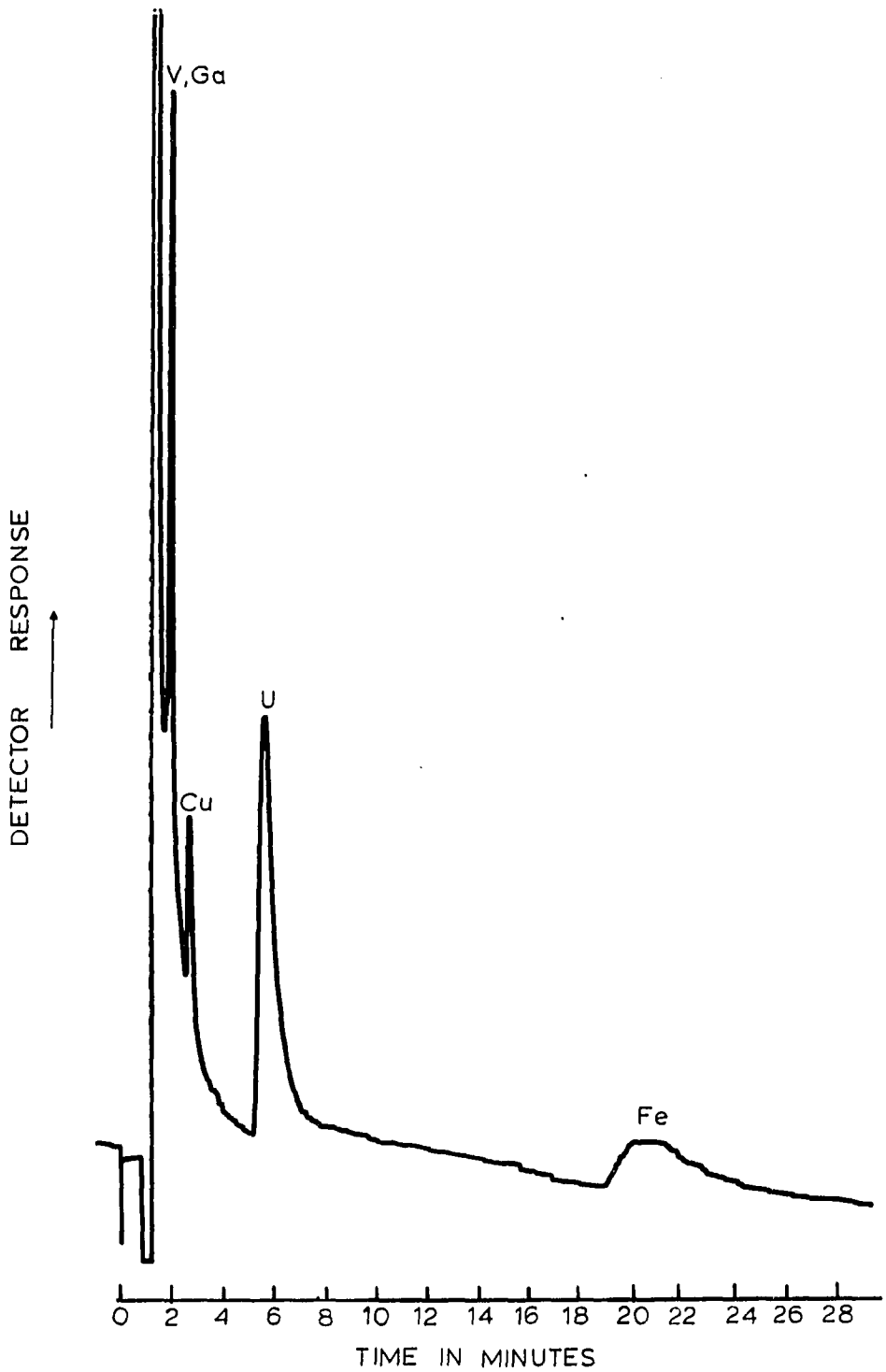
V,Ga
Cu
U
Fe
DETECTOR RESPONSE
0 2 4 6 8 10 12 14 16 18 20 22 24 26 28
TIME IN MINUTES

column, suggesting that another interaction is occurring which breaks up the thorium DMAP complex. Other researchers have reported that silanol groups on the silica interact with metal complexes (196-200). The silanol group is probably breaking up the thorium complex causing the complex to elute earlier as shown in Equation 6.

$$-Si-O^- + Th(DMAP)_n \rightleftharpoons -Si-O-Th^{4+} + DMAP \qquad (6)$$

Studies were carried out to investigate the effect of varying the acetonitrile percentage in the eluent and compare the retention between the two columns. Figures 20 and 21 show a plot of the log(k′) versus the percentage acetonitrile in the eluent for both the C-18 and the PLRP-S columns. The term k′ is the capacity factor and is related to the retention time by Equation (7), where t_r is the retention time of a

$$k' = (t_r - t_o)/t_o \qquad (7)$$

compound and t_o is the time for an unretained compound to travel through the column. For all the complexes tested, a nonlinear relationship was seen. With the exception of gallium(III), for the same eluent percentages, the k′ values were greater for the C-18 column, indicating that the C-18 column is more hydrophobic than the PLRP-S column for this separation system.

Effect of the Organic Modifier

The type of organic modifier used was varied in order to test its effect on the retention of the DMAP complexes. Methanol was first used, and Figure 22 gives a separation of the DMAP complexes on the PLRP-S column. Separation of vanadium(IV) and copper(II) is seen, but thorium(IV) and uranium(VI) are no longer separable. The uranium peak elutes earlier relative to gallium(III) and iron(III). For this separation, over twice the percentage of methanol as compared to

Figure 20: Dependence of log(k') on percentage acetonitrile concentration in the eluent for the PLRP-S column

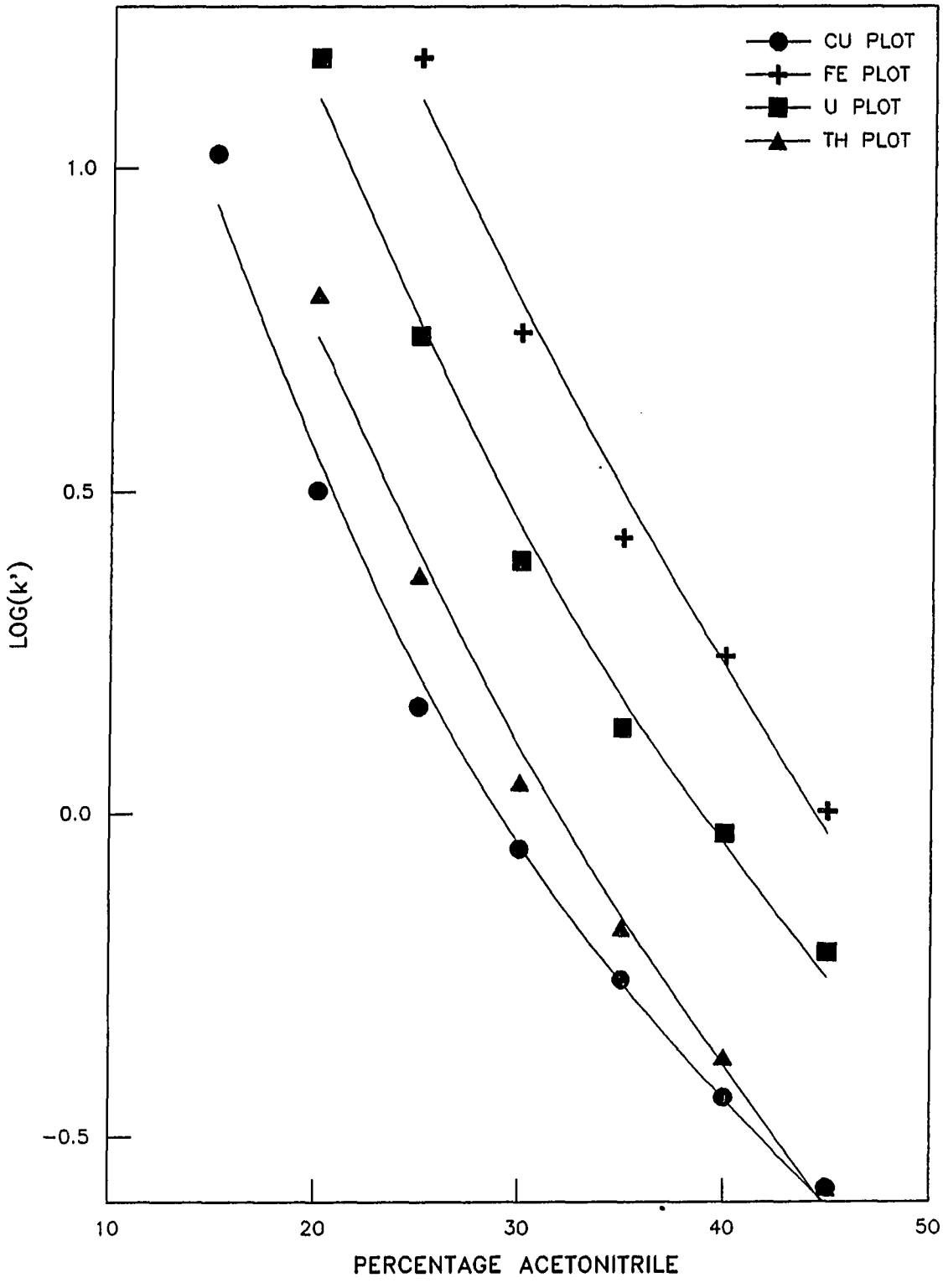
CU PLOT
FE PLOT
U PLOT
TH PLOT
1.0
0.5
0.0
−0.5
LOG(k')
10
20
30
40
50
PERCENTAGE ACETONITRILE

Figure 21: Dependence of log(k′) on percentage acetonitrile concentration in the eluent for the C-18 column

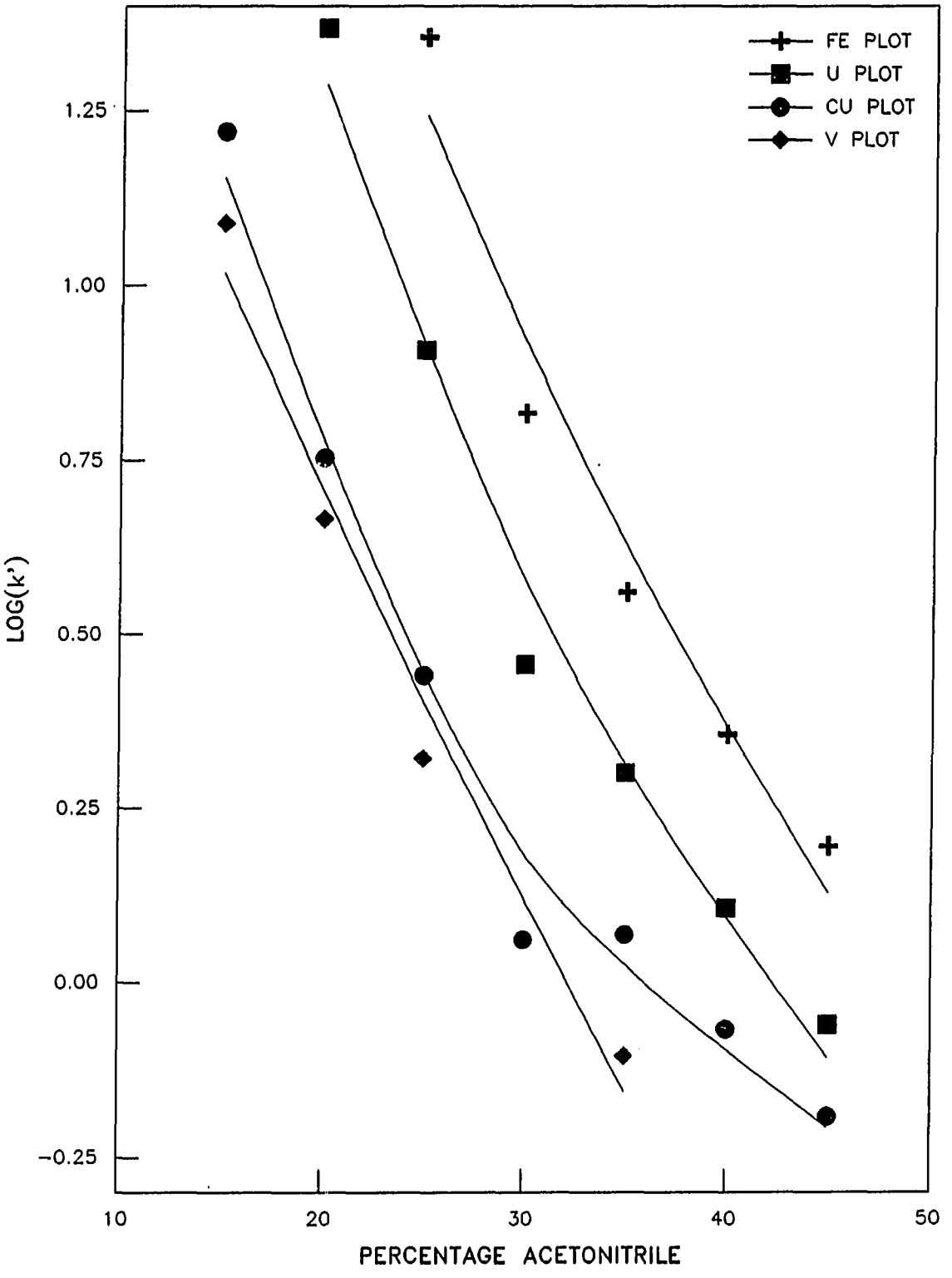
FE PLOT
U PLOT
CU PLOT
V PLOT
1.25
1.00
0.75
0.50
0.25
0.00
-0.25
LOG(k')
10
20
30
40
50
PERCENTAGE ACETONITRILE

Figure 22: Effect of methanol on the separation of V(IV), Cu(II), Th(IV), U(VI), Ga(III), and Fe(III) DMAP complexes at pH 5.0 on the PLRP-S column

[V] = 1×10^{-4} M, [Cu] = 2×10^{-4} M, [Th] = 2×10^{-4} M, [U] = 2×10^{-4} M, [Ga] = 1×10^{-4} M, [Fe] = 1×10^{-4} M

Eluent conditions: 77% MeOH, 23% H_2O, 0.02 M HAc, 0.5 mM DMAP, flow rate = 1.0 ml per minute, detection at 318 nm

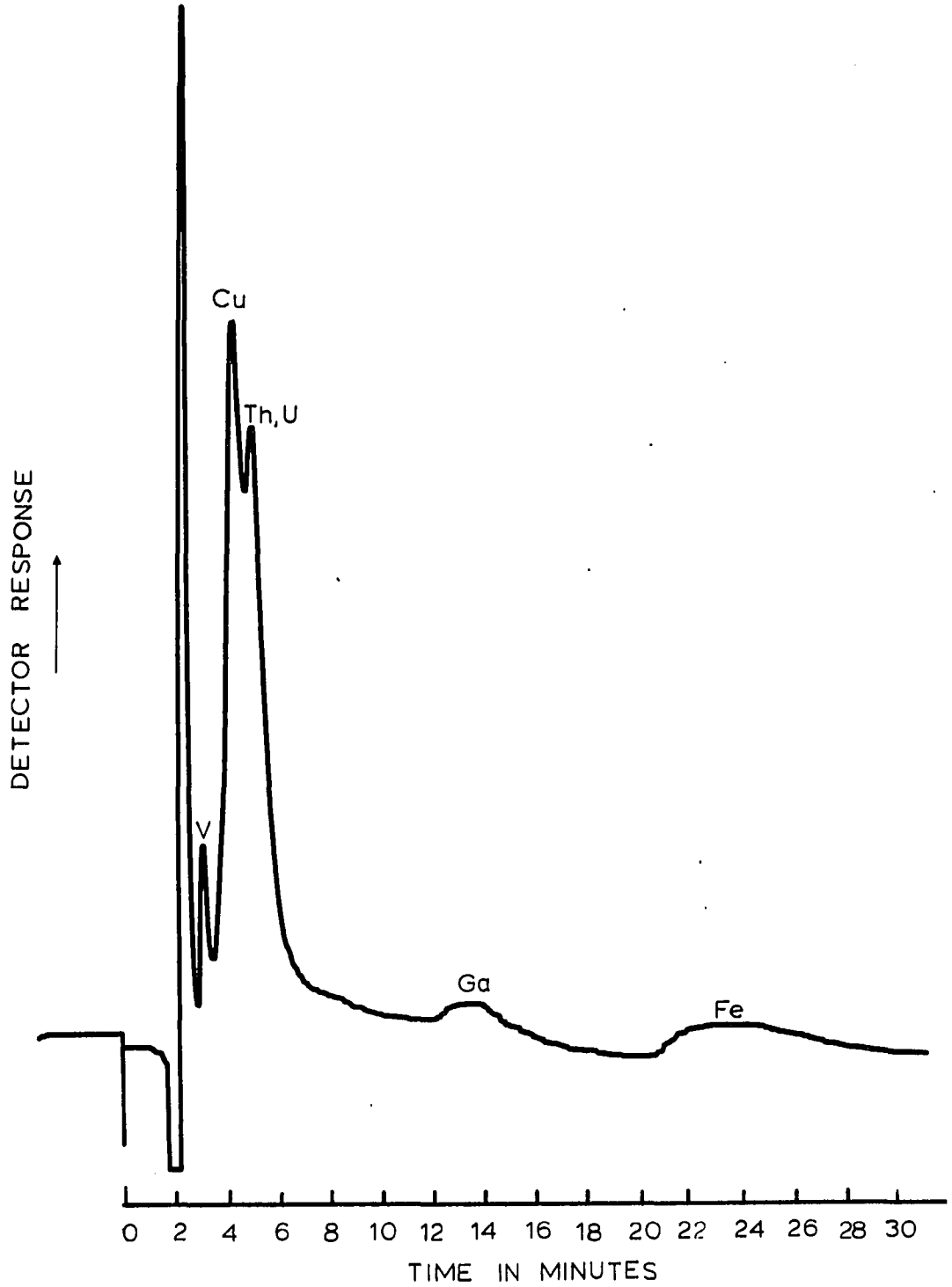
Cu
Th, U
V
Ga
Fe
DETECTOR RESPONSE
0 2 4 6 8 10 12 14 16 18 20 22 24 26 28 30
TIME IN MINUTES

acetonitrile was required in order to elute the complexes at approximately the same k' values. There are two possible reasons for the large amount of methanol required. First the resin is not wetted as well with methanol as with acetonitrile; other researchers have reported that methanol is not a good wetting agent for the resin (201). Secondly, the complexes may have different affinities for methanol and acetonitrile relative to the stationary phase. To test the second hypothesis, the separation was carried out using methanol as the organic modifier on the C-18 column. Figure 23A shows the separation of DMAP metal complexes on the C-18 column using methanol as the eluent. Gallium(III) eluted at the end of the DMAP peak as part of the void. Copper(II) under these conditions eluted after uranium(VI), the first time copper(II) was a later eluting peak. More methanol was required in order to elute the DMAP complexes at approximately the same k' value as achieved using acetonitrile than was predicted by Snyder and Kirkland (202). The inversion in retention order and the retention times indicate that the organic modifiers interacted with the DMAP complexes.

Tetrahydrofuran was also used as an organic modifier to see its effect on the DMAP separation. Figures 24 and 23(B) give the separation of the copper(II), iron(III), gallium(III), and uranium(VI) complexes on the PLRP-S and the C-18 column respectively. On the PLRP-S column the thorium(IV) peak was broad and had variable retention times when it was seen. The peaks eluted at approximately the same percentage of tetrahydrofuran in the eluent as predicted, in order to give the same k' values found in the acetonitrile eluent (202). There was one exception; uranium(VI) became the last peak to elute in the tetrahydrofuran eluent on both columns.

Figure 23: Effect of organic modifier on the separation of DMAP complexes on the C-18 column at pH 5.0

(A) [Cu] = 8.4×10^{-5} M, [U] = 1×10^{-4} M, [Ga] = 2×10^{-4} M

Eluent conditions: 45% MeOH, 55% H_2O, 0.02 M HAc, 0.5 mM DMAP, flow rate = 1.0 ml per minute, detection at 318 nm

(B) [Cu] = 8.4×10^{-5} M, [U] = 1×10^{-4} M, [Fe] = 5.1×10^{-5} M

Eluent conditions: 15% THF, 85% H_2O, 0.02 M HAc, 0.5 mM DMAP, flow rate = 1.0 ml per minute, detection at 318 nm

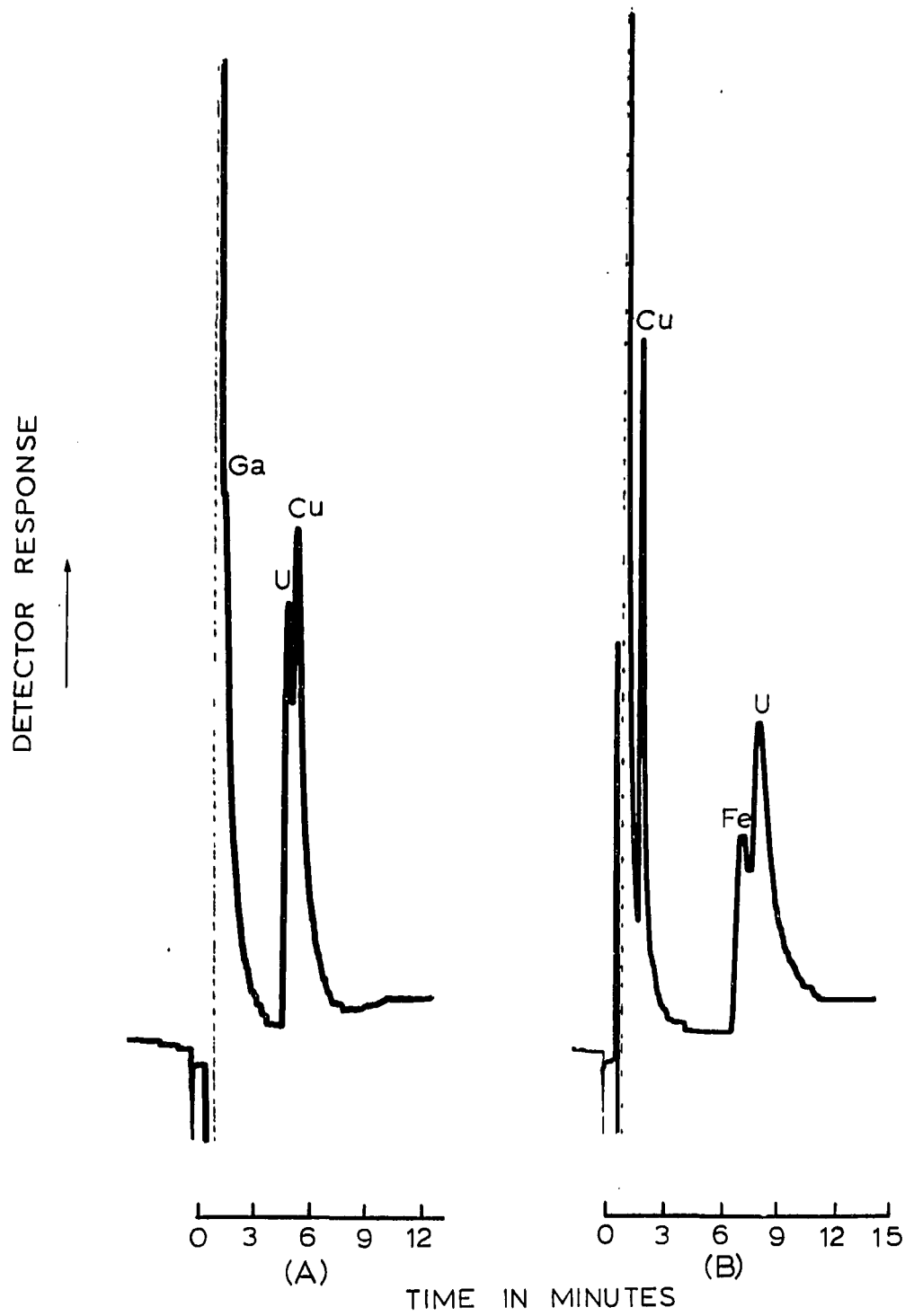
DETECTOR RESPONSE
Ga
Cu
U
Cu
U
Fe
0 3 6 9 12
(A)
0 3 6 9 12 15
(B)
TIME IN MINUTES

Figure 24: Effect of THF on the separation of Cu(II), Ga(III), U(VI), Fe(III) DMAP complexes at pH = 5.0 on the PLRP-S column

[Cu] = 2.5×10^{-5} M, [U] = 2×10^{-4} M, [Ga] = 1×10^{-4} M, [Fe] = 1×10^{-4} M

Eluent conditions: 23% THF, 77% H_2O, 0.02 M HAc, 0.5 mM DMAP, flow rate = 0.6 ml per minute, detection at 318 nm

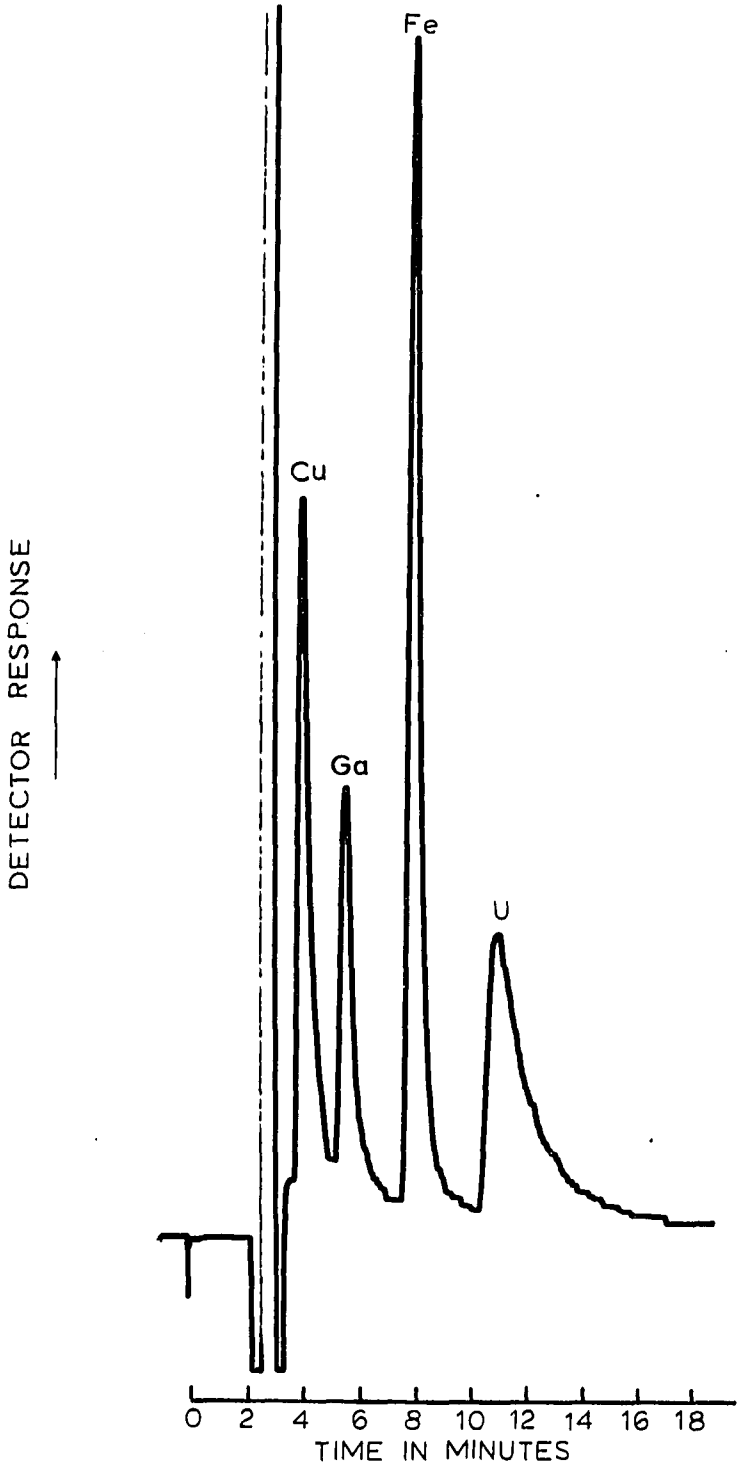
Fe
Cu
Ga
U
DETECTOR RESPONSE
0 2 4 6 8 10 12 14 16 18
TIME IN MINUTES

Discussion of Separation

As described previously, β-diketones form neutral complexes with metal ions. These complexes are separated according to their distribution between the mobile and stationary phases. The metal-DMAP complexes are kinetically labile, as evidenced by the peak decay when no DMAP was present in the eluent. Addition of DMAP also prevents hydrolysis of the complex as reported by Huber et al. (181). The presence of buffer and ionic reagents affected the structure of the metal complex as indicated by the peak shape, height, and retention time. These reagents probably competed with the DMAP or interacted with the complex, thus altering the retention characteristics. The column used had an impact on the retention order of the complexes. The difference in the elution of the gallium(III) was probably due to the difference in selectivity for gallium-DMAP complex between the C-18 and the PLRP-S columns. The disappearance of the thorium(IV) peak on the C-18 column was probably due to interaction with silanol.

For many compounds separated by HPLC, log(k′) versus percentage organic modifier is linear, which indicates that the retention mechanism is due primarily to the equilibrium of the analyte between the stationary and mobile phases (203). The metal complexes may have different affinities for the organic modifiers tested causing some changes seen in the retention characteristics. The nonlinear log(k′) versus percentage acetonitrile plots, and differences in peak shape and relative retention also indicate complex interaction with the mobile phase. Metal complexes of β-diketones are known to form adducts with certain solvents which may be responsible for the inversions of retention (129) described for uranium(VI) and copper(II) complexes. The inversion of retention for the

uranium-DMAP complex when using a tetrahydrofuran eluent is not surprising. Researchers using tetrahydrofuran as a solvent in combined ion exchange-solvent extraction reported greater complexation between tetrahydrofuran and uranium (204) than with other solvents. Other ethers have also been used as extractants for uranium (22-25). Tetrahydrofuran may be entering the coordination sphere of uranium, causing the complex to become more hydrophobic and thus increasing the retention. Spectra of the uranium-DMAP complex were run in 35% acetonitrile and 35% tetrahydrofuran and increased absorbance at 318 nm was seen for the uranium-DMAP complex in tetrahydrofuran, supporting the theory of tetrahydrofuran interaction with uranium. Other LC studies of β-diketone complexes have also reported inversions of retention when the organic modifier was varied (183,191,204).

Hydrolysis also played an important role in the retention characteristics of some of the complexes. The thorium-DMAP complex exhibited variable retention and poor peak shape on the PLRP-S column due probably to hydrolysis. Theoretically a 4 to 1 DMAP to thorium(IV) complex is formed and should elute late because of its hydrophobicity. This behavior was not seen and the early retention coupled with the broad peaks indicated that the thorium was hydrolyzing. In the tetrahydrofuran eluent, the thorium peak was probably not seen due to both hydrolysis and interaction with tetrahydrofuran. Hydrolysis was also responsible for the broad aluminum(III) peaks and the variable titanium(IV) peaks. Huber reported the hydrolysis of the aluminum-acac complex (181). Titanium(IV) hydrolyzes very easily under mildly acidic conditions.

The separations reported here show differences in the retention order compared to the separations of PMBP complexes (196). Using acetonitrile

as an organic modifier, the order of retention on the PLRP-S column was $V^{4+} < Cu^{2+} < Th^{4+} < UO_2^{2+} < Ga^{3+} < Fe^{3+}$ and on the C-18 column the order was $V^{4+}, Ga^{3+} < Cu^{2+} < UO_2^{2+} < Fe^{3+}$. The retention order for the PMBP complexes on a C-18 column using acetonitrile were $UO_2^{2+} < Cu^{2+} < Ga^{3+}, Th^{4+}, < Fe^{3+}$. The metal ions gallium(III), uranium(VI), and copper(II) exhibited different retention orders for the two complexing agents. The three DMAP complexes also exhibited varying retention orders when the column and organic modifier were varied. The differences in retention order between the DMAP and PMBP complexes were probably due to several effects. First, there was the selectivity difference due to the difference in affinity of the columns for the PMBP and DMAP complexes. Secondly, the interaction of the complexes with the organic modifier caused a difference in the affinity of the complex for the mobile phase. The differences between the DMAP complex elution order and the PMBP elution order is probably due to the nature of the metal complex and its interaction with the organic modifier. Finally, the stability of the complexes played a role in the changing retention order. The early elution of the thorium(IV) complex in the DMAP separation probably was due at least in part to the hydrolysis of the thorium complex. Assuming that the thorium(IV) hydrolysis is proportional to the water content in the eluent, the thorium-PMBP complex should elute later than the thorium-DMAP complex, relative to the other ions. The separation of the thorium-PMBP complex was carried out in 95-98% acetonitrile, while the separation of the thorium-DMAP complex was carried out in 25-35% acetonitrile. The thorium-PMBP peak does elute later relative to the other ions suggesting that greater hydrolysis occurred in the DMAP system.

Sample Preparation

Before being chromatographed, an excess of DMAP and buffer were added to the sample. Pre-derivatization ensured that the DMAP complex formed and prevented hydrolysis of the ions in the solution. Samples with and without DMAP and buffer were injected as shown in Figure 25. The underivatized sample gave smaller peaks with shoulders, and the peaks overlapped. The pH of the sample was also investigated for its effects on the peak shape and area of uranium(VI), gallium(III), and iron(III) peaks. At or above pH 3, no changes in sample peak shape or area were seen; below pH 3, the peak heights and areas began decreasing but with little change in retention time. These results indicate that prederivatization is reqiured before sample injection.

Quantitative Aspects of the Separation

The DMAP complexes were then investigated to determine if the separation could be used as a method for determining trace metal ions. Mobile phase composition was adjusted for each metal such that the metal complex eluted at approximately five minutes. The five minute elution was chosen because the peaks were sharp and narrow with little tailing, and completely resolved from the void volume. Table 13 gives the eluent conditions, linear calibration curve range, and detection limits for copper(II), uranium(VI), gallium(III), and iron(III). The detection limit was defined as the metal ion concentration which gave a peak height three times larger than the standard deviation of the background. Depending upon the metal ion, the calibration curves were linear for approximately one to two orders of magnitude. Uranium(VI) determination using tetrahydrofuran as the eluent had larger linear ranges and lower detection limits due to the increased absorption of the uranium-DMAP

Figure 25: Effect of prederivatization on peak shape of the U(VI), Ga(III), and Fe(III) DMAP complexes at pH = 5.0 on the PLRP-S column

[Cu] = [U] = 2×10^{-4} M, [Ga] = 1×10^{-4} M,

[Fe] = 1×10^{-4} M

Eluent conditions: 30% CH_3CN, 7% H_2O, 0.02 M HAc, 0.5 mM DMAP, flow rate = 1.0 ml per minute, detection at 318 nm

(A) Prederivatized sample

(B) Underivatized sample

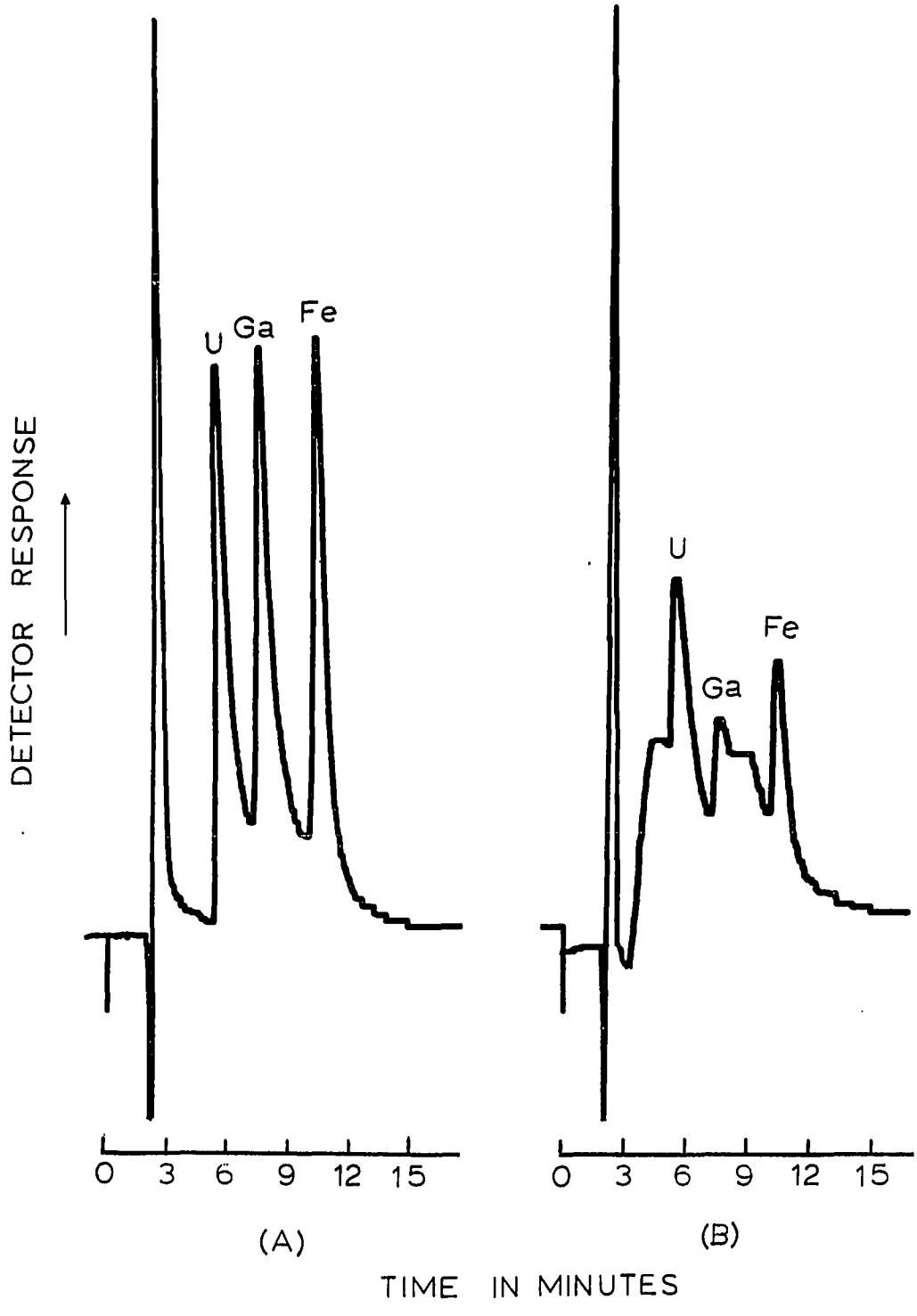
DETECTOR RESPONSE
U
Ga
Fe
0 3 6 9 12 15
(A)
U
Ga
Fe
0 3 6 9 12 15
(B)
TIME IN MINUTES

Table 13: Eluent conditions for determination of various metals by HPLC using DMAP as complexing agent

Metal Ion	Elution Conditions[a]	Linear Calibration Curve Range (M)	Detection Limit (M)
Fe	40% CH_3CN 60% H_2O 0.050 mM DMAP 0.02 M HAc	$5x10^{-4}$-$6x10^{-6}$	$2x10^{-6}$
Cu	25% CH_3CN 75% H_2O 0.50 mM DMAP 0.02 M HAc	$7.8x10^{-4}$-$3.1x10^{-5}$	$6.3x10^{-6}$
Ga	35% CH_3CN 65% H_2O 0.50 mM DMAP 0.02 M HAc	$2x10^{-4}$-$1.3x10^{-5}$	$4x10^{-6}$
U	35% CH_3CN 65% H_2O 0.50 mM DMAP 0.02 M HAc	$5x10^{-4}$-$5x10^{-5}$	$5x10^{-6}$
	35% THF 65% H_2O 0.50 mM DMAP 0.02 M HAc	$5x10^{-4}$-$1x10^{-5}$	$2x10^{-6}$

[a]For all eluents UV detection; λ = 304 nm; injection volume = 20 µl CH_3CN and THF eluent flow rates were 1.0 and 0.6 ml/min respectively.

complex in tetrahydrofuran. No linear calibration curve for thorium(IV) was obtained. As the concentration of thorium(IV) decreased, the thorium(IV) peak broadened out and the peak area and height decreased nonlinearly. No further analytical studies were carried out on thorium.

Tables 14 and 15 give the results on the interference studies carried out for uranium(VI), gallium(III), and iron(III). No cations were tested

Table 14: Percentage decrease in peak area of iron and uranium in the presence of excess of interferent ion[a]

Ion[b]	% Decrease Fe	% Decrease U
F^-	9.2%	16.2%
SO_4^{2-}	3.6%	< 3%
PO_4^{2-}	68%	No Peak

[a]Eluent conditions: 30% CH_3CN, 70% H_2O, $5x10^{-4}$ M DMAP 0.02 M HAc, pH=5.0 flow rate = 1.0 ml/min, λ= 318 nm, [Fe] = $1x10^{-4}$ M, [U] = $2x10^{-4}$ M, [interferent] = 0.02 M.

[b]The following ions tested had less than a 3% difference in peak area: K^+, Na^+, Ba^{2+}, Ca^{2+}, Cd^{2+}, Co^{2+}, Mn^{2+}, Ni^{2+}, Pb^{2+}, Zn^{2+}, La^{2+}, Sm^{3+}, Cl^-, ClO_4^-, NO_3^-.

Table 15: Percentage decrease in peak area of gallium in 200 fold excess of interferent when preparing samples at pH = 3.0 and pH = 5.0[a]

Ion [b]	% Difference pH = 5.0	% Difference pH = 3.0
La^{3+}	>99	7.4
Ni^{2+}	28	8.4
Zn^{2+}	12	< 2
Sm^{3+}	99	10
Co^{2+}	9.5	5.8
Mn^{2+}	12	< 2
F^-	4.1	----
HPO_4^{2-}	62	----
Pb^{2+}	3.5	----

[a]Eluent conditions: 30% CH_3CN, 70% H_2O, 0.02M HAc, $5x10^{-4}$M DMAP, pH = 5.0 Flow rate = 1.0 ml/min, λ= 318 nm, [Ga] = $1x10^{-4}$M, [interferent] = $2x10^{-2}$M.

[b]The following ions tested gave less than 3% decrease in peak area for Ga when tested: K^+, Na^+, Ba^{2+}, Ca^{2+}, Cd^{2+}, NO_3^-, Cl^-, ClO_4, SO_4^{2-}. The concentration of each of these ions was also 0.02 M.

that were retained on the column because high concentrations of these ions gave very large peaks which swamped out the signal of the analyte. High concentrations of the DMAP-metal complexes also precipitated out of the sample solution. With the exception of gallium(III), cations and the anions perchlorate, nitrate, chloride, and sulfate had no effect on the peak area. Copper(II) was also tested for the same cations and chloride, perchlorate, and nitrate, and no interference was found. Gallium(II), however, had interference from several cations. These cations begin to form complexes with DMAP at pH 5; the gallium-DMAP complex is not as strong as the copper(II), uranium(VI), and iron(III) complexes and the large excess of cations interfere with the formation of the gallium(III) complex in the sample. The pH of the sample was varied in order to attain maximum gallium-DMAP complex formation and a minimum interferent-DMAP formation. By reducing the pH to 3.0, the formation of the interferent-DMAP complex was inhibited, while the formation of the gallium-DMAP complex remained unchanged. The reduction in the interference of the cations is seen in Table 15. The major source of interference came from the anions; the complexing anions fluoride, and phosphate interfered with the gallium(III), uranium(VI) and iron(III) peaks. Phosphate complexes fairly strongly with uranium and the disappearance of the uranium peak is somewhat expected. Fluoride interference of uranium disappeared when the concentration of the anion was reduced to 0.001 M.

Post-Column Reactor Detection System

The calibration curve range and detection limits reported in Table 13 are not very sensitive, and low levels of ions could not be detected. Use of a post-column reactor was then investigated in an attempt to

increase the sensitivity of detection. Very few spectrophotometric reagents can form highly colored complexes with all of the metal ions separated; Arsenazo I at pH 7.8 is one of the few reagent systems which reacts with all the metal ions, and it was used as the post-column reagent. Spectral studies indicated that for a minimum of reagent background noise and a maximum of analyte signal, a wavelength in the range between 570 and 600 nm. Injections of a mixture of iron(III), gallium(III), uranium(VI), thorium(IV), and copper(II) were made with and without the addition of the post-column reagent at 590 and 318 nm respectively, at the same detector sensitivity. The chromatograms are shown in Figure 26. For the post-column reactor, a large increase of peak height was seen for the thorium and uranium peaks; the gallium(III) peak disappeared and the copper(II) and iron(III) peaks were very small, indicating that the DMAP masked the copper(II), gallium(III), and iron(III). King reported that DMAP does not affect the formation of the uranium-Arsenazo I complex (136). The results of this study suggested the possibility of selectively determining uranium by HPLC using post-column detection.

The post-column reactor system was tested for its properties. The tee and detector cell exhibited a high back pressure, approximately 150 psi; this high back pressure and the use of a low pulsing dual piston pump for delivering the Arsenazo I lowered the background noise so that it was not significantly different from the background for direct detection. Cassidy et al. reported that high back pressure decreased the noise in the system (205). The efficiency of the tee was measured by comparing the number of theoretical plates for the uranium peak with and without the post-column reactor. With the tee on-line and no Arsenazo I

Figure 26: Effect of peak response of Cu(II), Th(IV), U(VI), Ga(III), and Fe(III) DMAP complexes when post column reactor is used

[Cu] = 4×10^{-5} M, [Th] = 4×10^{-5} M, [U] = 4×10^{-5} M, [Ga] = 4×10^{-5} M [Fe] = 4×10^{-5} M

Eluent conditions: 30% CH_3CN, 70% H_2O, 0.02 M HAc, 0.5 mM DMAP, flow rate = 1.0 ml per minute

Post column reactor conditions: 20% CH_3CN, 80% H_2O 0.20 M TEA/HNO_3, 2.5×10^{-4} M Arsenazo I, flow rate = 1.0 ml per minute

(A) No post column reactor, detection at 318 nm

(B) Post column reactor, detection at 590 nm

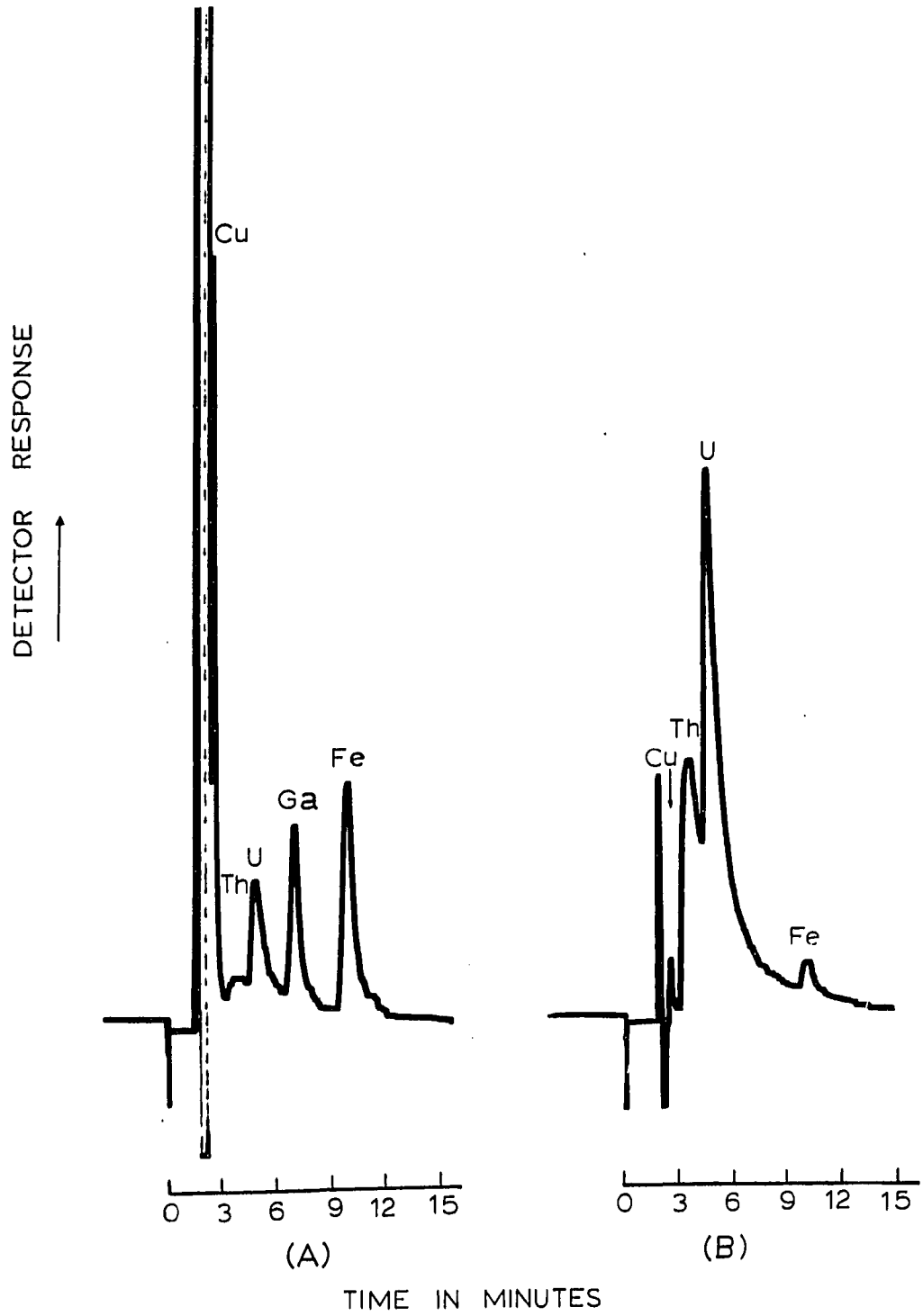
DETECTOR RESPONSE
Cu
Th
U
Ga
Fe
0 3 6 9 12 15
(A)
Cu
Th
U
Fe
0 3 6 9 12 15
(B)
TIME IN MINUTES

being pumped through the system, the efficiency was lowered approximately 15%; when the reagent was pumped, the efficiency was lowered approximately 34%.

The analytical properties for selectively determining uranium were investigated. The tetrahydrofuran eluent was chosen because uranium was the last peak to elute, and there was no overlap or coelution of other DMAP complexes. The uranium(VI) peak with and without the post column reactor are shown in Figure 27. The calibration curve study in Figure 28 indicated that the uranium(VI) peak response was linear for almost three orders of magnitude. In Table 16 the detection limits were four times lower for uranium(VI) and five times lower for thorium when using the post column reactor. An interference study using a uranium(VI)

Table 16: Comparison of detection limits for uranium and thorium with and without the post column reactor[a]

Ion	Direct Detection (ng)	Post Column Reaction (ng)
U	10	2
Th	200	40

[a]Elution and post column reactor conditions for uranium and thorium are listed in Figures 27 and 26 respectively.

Figure 27: Enhancement of uranium signal when post column reactor is used

[U] = 3×10^{-5} M

Eluent conditions: 35% THF, 65% H_2O, 0.02 M HAc, 0.5 mM DMAP, flow rate = 0.6 ml per minute, detection at 318 nm

Post column reactor conditions: 35% CH_3CN, 65% H_2O 0.20 M TEA/HNO_3, 2.5×10^{-4} M Arsenazo I, flow rate = 0.6 ml per minute

(A) No post column reactor, detection at 318 nm

(B) Post column reactor, detection at 590 nm

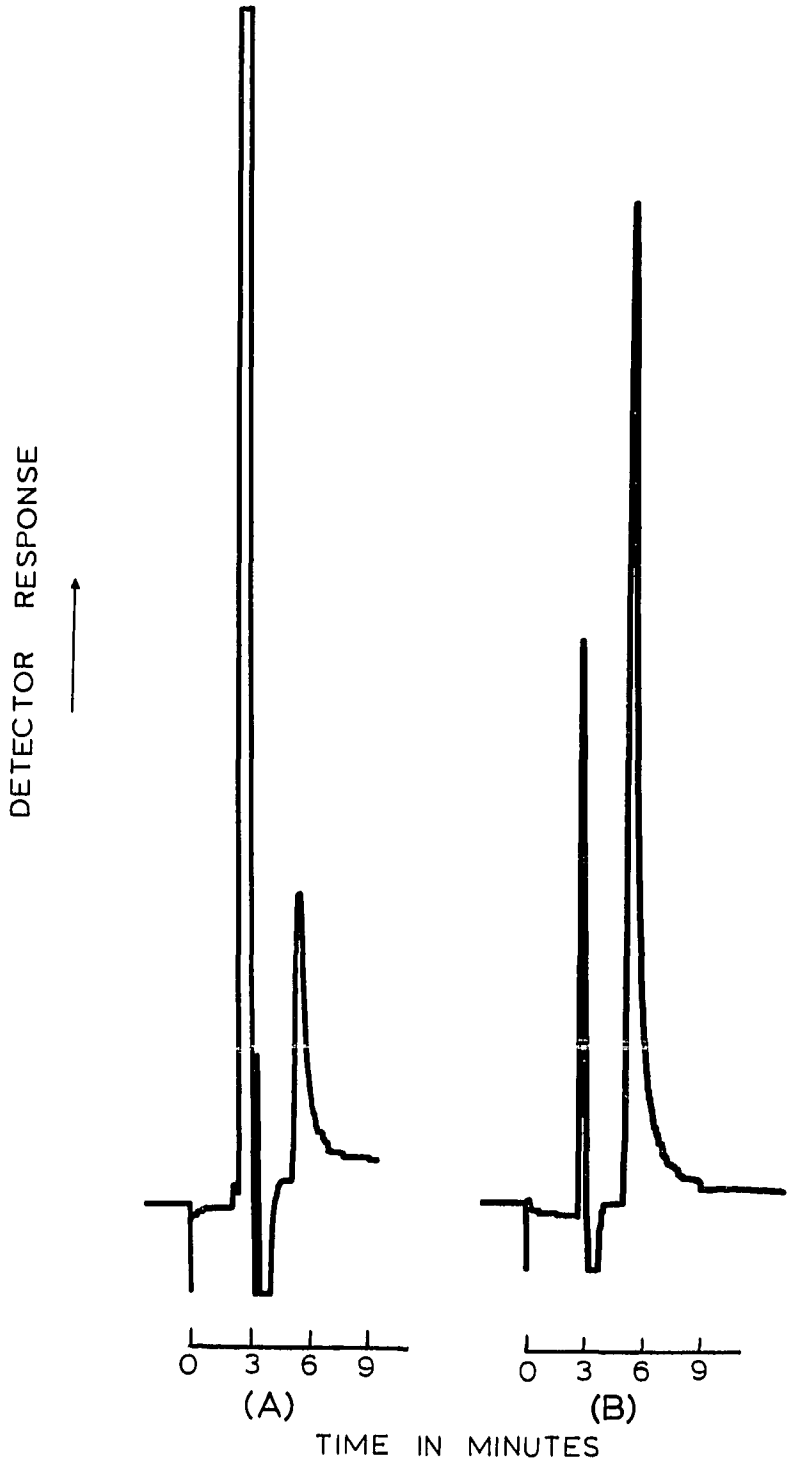
DETECTOR RESPONSE
0 3 6 9
(A)
0 3 6 9
(B)
TIME IN MINUTES

Figure 28: Calibration Curve for the determination of uranium when using a post column reactor

Eluent conditions: see Figure 27

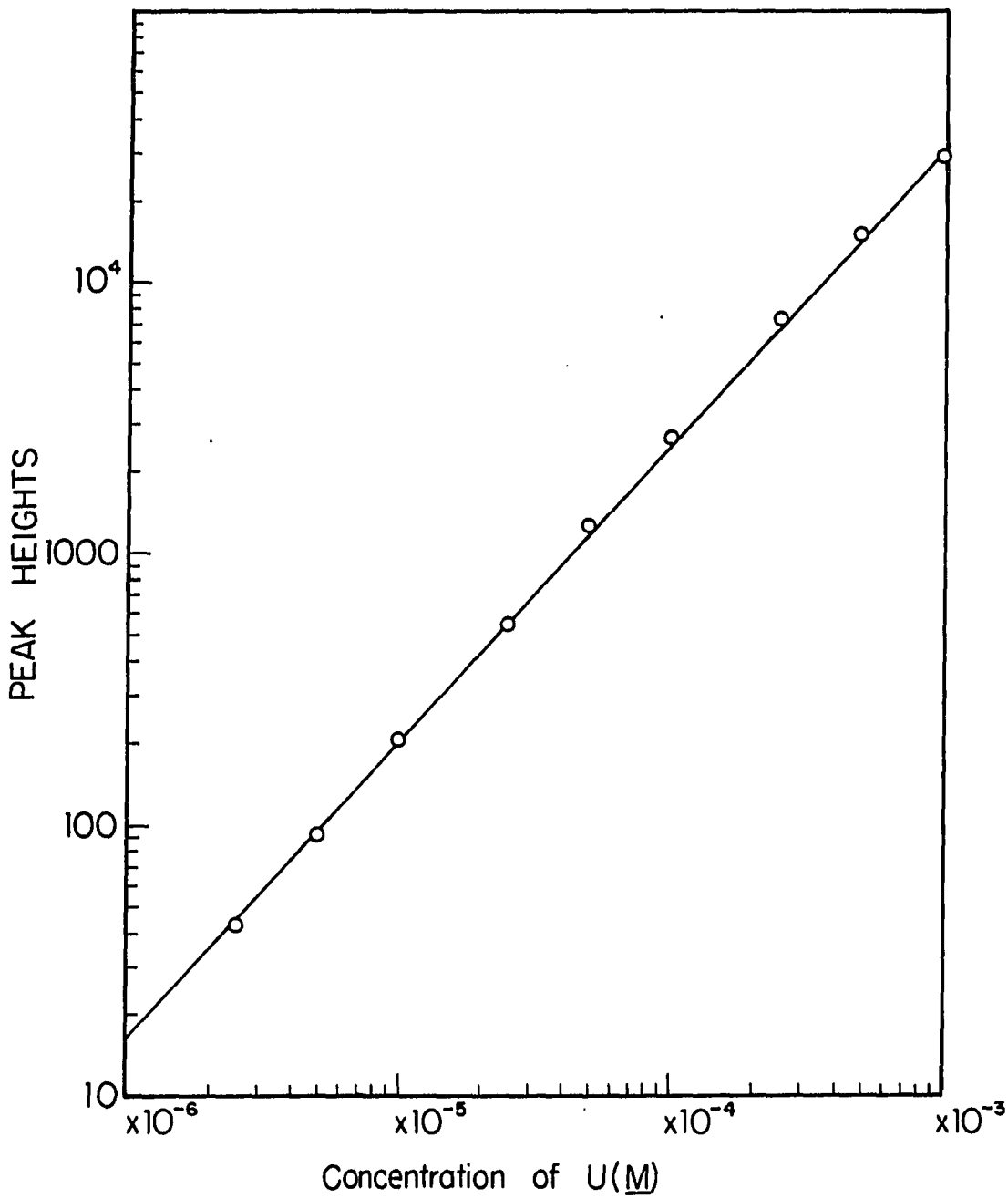
PEAK HEIGHTS
10^4
1000
100
10
$x10^{-6}$
$x10^{-5}$
$x10^{-4}$
$x10^{-3}$
Concentration of U(M)

concentration of 5×10^{-5} M was carried out on the same ions tested in the direct detection interference study. The results were similar to those obtained using direct detection and acetonitrile as the eluent modifier, except when the rare earth ions were tested. The rare earth ions form strongly absorbing complexes with Arsenazo I, and the rare earth broad peak overlapped with the uranium(VI) peak. Decreasing the tetrahydrofuran concentration to increase the uranium(VI) retention time helped to separate the complex and the interferent, but there was still considerable overlap. Enough EDTA was added so that its concentration was the same as that of the rare earth, and the broad rare earth peak became much smaller. Uranium(VI) was now baseline separated from the interferents as shown in Figure 29. Approximately a five percent decrease in peak height of uranium was seen under the given conditions due probably to some uranium-EDTA complexation, but the addition of a greater amount of DMAP to the sample should eliminate the decrease in peak height.

Figure 29: Effect of the addition of EDTA on samarium peak interference when determining uranium

[U] = 5×10^{-5} M, [Sm] = 2×10^{-2} M

Eluent conditions: 30% THF, 65% H_2O, 0.02 M HAc, 0.5 mM DMAP, flow rate = 0.6 ml per minute, detection at 318 nm.

Post column reactor conditions: 20% CH_3CN, 80% H_2O 0.20 M TEA/HNO_3, 2.5×10^{-4} M Arsenazo I, flow rate = 0.6 ml per minute

(A) No EDTA

(B) 2×10^{-2} M EDTA added

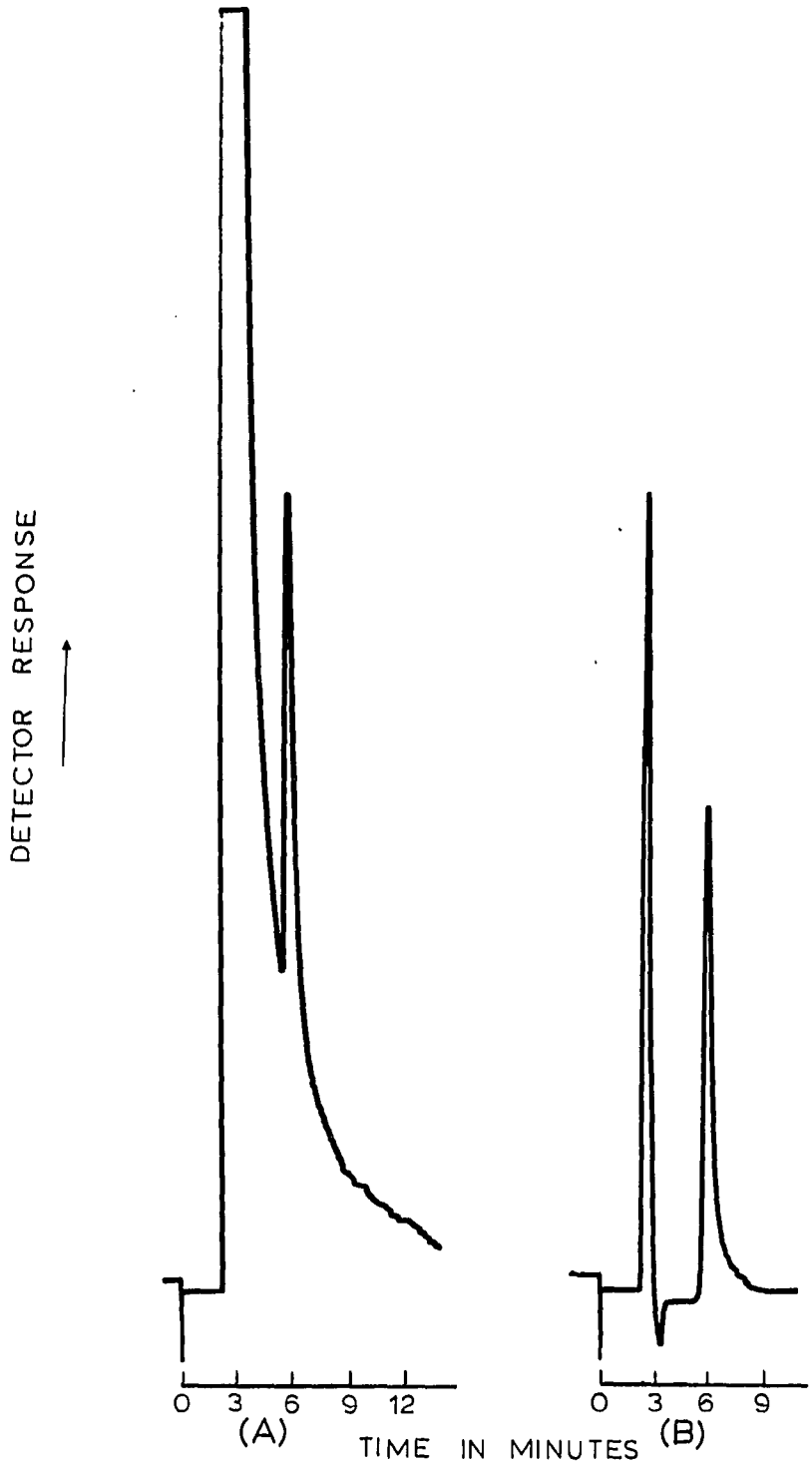
DETECTOR RESPONSE
0 3 6 9 12
(A)
0 3 6 9
(B)
TIME IN MINUTES

CONCLUSIONS

The work presented describes the feasibility of separating metal complexes using DMAP. One extension of the research presented is to increase the number of metal ions separated by HPLC. In particular, transition metals which form DMAP complexes at higher pH values could be tested for HPLC separation. DMAP separations were not tried at pH values greater than 5. The DMAP anion displays considerable absorbance in the UV range, and the high background from the DMAP eluent precluded direct detection of the metal complex. Using a post-column reactor system, one could investigate DMAP complex separations at higher pH values.

Improvement of the post-column reactor detector system could also be carried out. Use of a zero dead volume tee would decrease the overlap of closely eluting peaks, particularly the thorium and uranium peaks. In order to increase the linear calibration curve range and the limits of detection of the metals, testing other colorimetric reagents which react with all the metals could be carried out. Use of an element-specific colorimetric reagent would also allow the selective determination of one the metal ions separated in this system. The post-column reactor system for uranium could be improved by using a more sensitive colorimetric reagent such as PAR, PADAP, or Arsenazo III.

Finally, to achieve lower limits of detection, an on-line or off-line concentrator column could be included in the sample system. By passing a sample to which DMAP has been added through the mini-column, the metal complexes are sorbed onto the resin and separated from the sample. The DMAP complexes are eluted from the concentrator column with a minimum of

solvent thereby concentrating the metals. The concentrated sample is then passed through the HPLC system for final separation and detection.

SECTION IV. DETERMINATION OF METAL IONS BY HIGH PERFORMANCE LIQUID CHROMATOGRAPHIC SEPARATION OF THEIR N-METHYLFUROHYDROXAMIC ACID CHELATES

INTRODUCTION

A traditional classical separation which has been a challenge for chemists to carry out is the separation of zirconium and hafnium. Zirconium and hafnium are cogeners, have nearly the same atomic and ionic radii, and chemically behave very similarly. While the two elements tend to react in a similar manner, they have different mechanical and physical properties. Because hafnium has a high neutron capture cross section, it can be used in the manufacture of nuclear reactor control rods. Zirconium, on the other hand, has a low neutron capture cross section, which is a desirable quality for nuclear reactor construction material. In addition, hafnium shows promise as a possible aerospace construction material; it can absorb or lose heat twice as fast as zirconium and titanium (206).

The separation of zirconium and hafnium has been accomplished using a variety of methods (206). Fractional crystallization and precipitation of zirconium and hafnium complexes have been carried out successfully, but the methods are time consuming and tend to be limited to separations of large amounts of the two elements. Separation of the elements by distillation has been achieved because of the difference in volatility in the chloride compounds. Electrolysis has also been used to separate zirconium and hafnium. The most common analytical methods for separating zirconium and hafnium are ion exchange and solvent extraction. Solvent extraction methods of separation take advantage of differences in the extraction efficiency of the two elements. Multiple extractions are carried out, with the organic phase becoming enriched in one element. Solvent extraction is a major method of separating large amounts of

zirconium and hafnium. Ion exchange separations have been extensively studied, and several methods for separating zirconium and hafnium have been reported (206). Most of the methods utilize gravity flow systems and are often carried out under acidic conditions in the presence of complexing anions such as fluoride, sulfate, and citrate.

Very little work has been carried out using HPLC as a means of separating and determining zirconium and hafnium. One paper reported the normal phase HPLC separation of zirconium and hafnium organometallic compounds (207). In this section, a chromatographic method for separating and determining zirconium(IV) and hafnium(IV) by HPLC will be presented. In addition to zirconium(IV) and hafnium(IV), the ions aluminum(III), iron(III), niobium(V), and antimony(III) will be separated as complexes of N-methylfurohydroxamic acid (NMFHA) using reversed phase HPLC. NMFHA belongs to a class of acidic complexing agents called hydroxamic acids; the structure of NMFHA is shown as structure (V). Conditions for separating the metals, and the potential analytical applications for determining these elements by HPLC will be discussed.

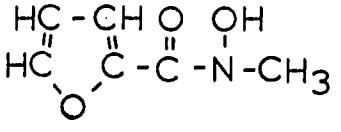

(V)

LITERATURE REVIEW

NMFHA belongs to the general organic class known as substituted hydroxylamines, and the specific group of hydroxylamines to which NMFHA belongs is called N-hydroxylamide or hydroxamic acid. Hydroxamic acids are related to the complexing agent cupferron and have the structure (VI) shown in Equation (8). Hydroxamic acids are weak acids; the hydroxyl proton is lost between pH 8 and 10 to form the hydroxamate ion (VII).

$$\underset{\text{(VI)}}{R\text{-}C(=O)\text{-}N(OH)\text{-}R'} \rightleftharpoons \underset{\text{(VII)}}{R\text{-}C(=O)\text{-}N(O^-)\text{-}R'} + H^+ \qquad (8)$$

For the case of benzohydroxamic acid, spectroscopic evidence indicates that at least three tautomers form in solution as shown in Equation (9).

$$C_6H_5\text{-}C(=O)\text{-}N(O^-)\text{-}H \rightleftharpoons C_6H_5\text{-}C(O^-)=N \rightleftharpoons C_6H_5\text{-}C(=O)\text{-}\bar{N}\text{-}OH \qquad (9)$$

Lossen discovered oxalohydroxamic acid over 100 years ago, and since that time many hydroxamic acids have been synthesized and/or discovered to be naturally occurring. Typically, hydroxamic acids are synthesized by reacting a substituted hydroxyl amine with a compound containing a reactive acyl group, such as an acid chloride or an anhydride. The general chemistry and biology of hydroxamic acids is described in a book edited by Kehl (208).

The ability of hydroxamic acids to complex metal ions has been extensively studied. Hydroxamic acids are similar to cupferron in complexing ability, but are much more stable to acid, light, and heat than cupferron. Like cupferron, hydroxamic acids preferentially complex high valence metal ions such as iron(III), vanadium(V), zirconium(IV),

hafnium(IV), tantalum(V), niobium(V), tin(IV), titanium(IV) etc. in acidic solutions. Transition metals and rare earth ions complex at higher pH values, typically between pH 4 and 9. Several reviews and a book have been published describing the synthesis of various hydroxamic acids and their complexation characteristics with metal ions (209-213).

Most of the hydroxamic acids synthesized have been used as gravimetric, spectrophotometric, and extraction reagents for metal ions. Several hydroxamic acids have been tested for use as potential analytical reagents; most have found use in determining a specific metal ion. The most extensively studied hydroxamic acid is N-benzoylphenylhydroxamic acid (BPHA). First synthesized by Bamburger in 1919 (209), BPHA has been used as an all-purpose, general analytical reagent, and over two thirds of the elements are known to form complexes with BPHA (210). Like most of the hydroxamic acids synthesized and used as analytical reagents, BPHA has been used primarily as a gravimetric or extraction agent because its metal complexes are insoluble in water. Table 17 lists selected applications of BPHA to metal ion analysis. Fritz and Sherma have also separated BPHA-metal complexes by paper chromatography (257).

The structure of metal-hydroxamic acid complexes has been under extensive study. Complexation of the hydroxamic acid (HA) with the metal ion occurs through the carbonyl and hydroxyl oxygens, forming a five membered ring with the metal ion. At moderate pH values (4-10) for most metal ions, the hydroxyl hydrogen is lost and the neutral metal-hydroxamic acid complex $M(HA)_n$ is formed, where n is the charge on the metal ion. Fouche et al. investigated the BPHA complexes of zirconium(IV), hafnium(IV), and germanium(IV) and found that under acidic conditions, these ions formed ion paired complexes of the structure

TABLE 17: Analytical applications of benzoylphenylhydroxamic acid

Metal Ion	Subject Studied	Reference
Al(III)	Separation and determination in stainless steel and other materials	214
	Precipitation from Be(II),Co(II),Mn(II),Ni(II),U(VI)Zn(II)	215
Be(II)	Precipitation from Al(III),Fe(III),Ti(IV)	216
Bi(III)	Extraction with BPHA	217
	Precipitation from Al(III),As(V),Be(II),Cd(II),Co(II),Cu(II),Fe(III), Hg(II),La(III),Mn(II),Mo(VI),Ni(II),Pb(II),Pd(II),Sb(III), Sn(IV),Th(IV),Ti(IV),U(VI),V(V),W(VI)	218
Cd(II)	Precipitation with BPHA	219
	Extraction with BPHA	220,221
Co(II)	Extraction using BPHA	220,221
	Precipitation from Cu(II)	222
Cr(III)	Extraction with BPHA	220,221
Cu(II)	Extraction with BPHA	220,221
Cu(II),Fe(III)	Separation and determination in brass and bronze	223
Ga(III)	Precipitation from Al(III),Be(II),Ce(III),Cu(II),Fe(II),In(III), Ti(IV),U(VI),Zr(IV)	224
	Extraction with BPHA	225
Ge(III)	Extraction with BPHA	217
Hf(IV)	Extraction with BPHA	226-231

TABLE 17: Continued

Metal Ion	Subject Studied	Reference
Hg(II)	Extraction from Ag(I),Cd(II),Cu(II),Mo(VI),Pb(II),Th(IV),Ti(IV), V(V),U(VI),Zn(II),Zr(IV)	232
In(III)	Extraction with BPHA	217,233
La(III)	Extraction with BPHA Precipitation from Al(III),Be(II),Co(II),Fe(II),Fe(III),Ga(III), In(III),Ni(II),Sc(III),Th(IV),U(VI),Zn(II)	234 235
Mg(II)	Precipitation form Al(III), Be(II),Co(II),Cu(II),Fe(III),Ni(II), Th(IV),Zn(II)	236
Mo(VI)	Extraction with BPHA	237
Nb(V)	Extraction from Al(III),Bi(III),Ba(II),Bi(III),Cd(II),Co(II),Cr(III), Cu(II),Fe(III),K(I),Li(I),Mg(II),Mn(II),Mo(VI),Na(I),Ni(II), Pt(IV),Si(IV),Sn(II),Th(IV),U(VI),W(VI),Zn(II),	238-240
Np(IV)	Extraction with BPHA	241
Pa(IV)	Extraction from Al(III),Fe(III),Hf(IV),Mn(II),Nb(V),Ta(V),Th(IV), Ti(IV),Zr(IV),rare earths	240,242
Pb(II)	Extraction with BPHA	220
Pu(IV)	Extraction from Am(III),U(VI),Zr(IV) and other fission products	240
Sb(III)	Extraction with BPHA	224
Sc(III)	Extraction from La(III)	243

TABLE 17: Continued

Metal Ion	Subject Studied	Reference
Sn(IV)	Precipitation from Cu(II),Pb(II),Zn(II)	244
	Extraction with BPHA	224,245
Ta(V)	Extraction from steel	246
	Extraction from Pa(IV)	239
Ti(IV)	Extraction with BPHA	248
Th(IV),U(VI)	Extraction with BPHA	247
U(VI)	Extraction and spectrophotometric analysis	249,250
V(V)	Extraction and photometric determination	251,252
W(VI)	Extraction from Al(III),As(V),Bi(III),Ba(II),Cr(III),Cu(II),Fe(III) Ni(II),Pb(II),Sb(III),Ti(IV),U(VI),V(V)	253
Zr(IV)	Precipitation from Al(III),Cr(III),Fe(III),Nb(V),Ta(V),Ti(IV), V(V),rare earths	254
	Extraction with BPHA	255,230, 232
Zr(IV),Ti(IV)	Extraction from Sc(III)	256

$M(BPHA)_iX_{4-i}$, where X is a monovalent anion (258-259). Benzohydroxamic acid (BHA) complexes display a different complexing behavior for vanadium(V) and iron(III) in acidic solutions (260-261). Iron(III) and vanadium(V) benzohydroxamic acid complexes are cationic at low pH values, and as the pH increases the number of BHA molecules complexing with the metals increase. At alkaline pH values, the iron(III) complex is anionic. Under highly acidic conditions for some metal ions, the ion, the neutral hydroxamic acid, and an anion form mixed complexes;the structure of the complex depends upon the metal (213).

The hydroxamic acid under investigation, N-methylfurohydroxamic acid (NMFHA), was synthesized by Al-biaty and Fritz in 1982 (262). NMFHA complexes with a wide variety of metal ions, and both the hydroxamic acid and its metal complexes display moderate solubility in water. Al-biaty and Fritz conducted resin sorption studies on the NMFHA metal complexes and determined conditions for quantitatively preconcentrating over 20 metal ions from an aqueous solution. Several metal ions were also separated from concentrated salt solutions, by sorbing the NMFHA complexes onto an XAD-4 gravity column.

EXPERIMENTAL

Synthesis

NMFHA was synthesized following the procedure described by Al-biaty and Fritz (262) using N-methylhydroxylamine and 2-furoyl chloride from Aldrich. Two modifications of the procedure were used: the reaction mixture was brought to dryness using a rotovaporator instead of a steam bath, and the final product was crystallized from cold water rather than from a 1:1 methanol solution. Dilute ($<10^{-2}$) solutions of NMFHA were prepared by dissolving the NMFHA solid in a few milliliters of acetonitile or methanol and diluting with water. The final percentage of organic solvent in the stock solution was approximately 5% or less.

Metal ion stock solutions were made from metal ion salts or from the metal which were obtained from various sources. Zirconium(IV) and hafnium(IV) solutions were dissolved from the oxychlorides, while iron(III) solutions were made from the nitrate salt. Aluminum and Sb_2O_3 were dissolved in hydrochloric acid, and niobium was dissolved in hydrofluoric acid and nitric acid and then fumed in H_2SO_4 to eliminate the fluoride from solution. Stock solutions used in the interference studies were made from nitrate, perchlorate, and sodium salts. Titanium was dissolved from the metal using nitric acid and sulfuric acid.

LC Studies

The chromatographic system consisted of a Milton Roy Simplex Mini Pump, Milton Roy Pulse Dampener, pressure release valve, 10 cm x 4 cm saturator column, Rheodyne 7010 injector, Rheodyne inline filter, and a Tracor 560A UV-vis scanning detector. The saturator column was hand packed with silica gel (Amico) or XAD 16 (Rohm and Haas). Three

analytical columns were tested: an EM Science C-18 10 µm (250 mm x 4.6 mm), a 3 µm Du Pont Zorbax C-18 (40 mm x 6 mm) column, and a PLRP-S 5 µm polystyrene divinylbenzene (150 mm x 4.6 mm) column from Polymer Laboratories.

Eluents were prepared from Fisher HPLC grade acetonitrile or methanol, and from water purified with a Barnstead Nanopure II system. Acids and buffers were reagent grade or better. Eluent components were mixed together and filtered using a 0.2 or 0.45 µm Nylon 66 (Rainin) or PTFE filter (Nuclepore). Eluents were made fresh every day. The flow rate was set at one ml per minute unless otherwise noted, and for direct detection, the detector wavelength was set at 304 nm. The post column reactor was based on a design by Cassidy and Elchuck (263) and the rest of the system is described by Sevenich and Fritz (264). A Rainin peristaltic pump was used to pump post-column reagent solution of 0.125% PAR in a buffer containing 2.0 M ammonium hydroxide and 1.0 M ammonium acetate. Wavelength detection with a Kratos 783 detector was set at 535 nm.

The antiperspirant sample was prepared by refluxing between 0.10 and 0.40 g of solid antiperspirant overnight with nitric acid, fuming with hydrofluoric acid, and finally fuming with perchloric acid several times to eliminate all fluoride. All wet digestions were done in platinum crucibles. Samples were diluted to 50 ml with water containing NMFHA to prevent hydrolysis of the zirconium(IV). One ml aliquots of the solution were taken, diluted to 10 ml and analyzed for zirconium(IV) by HPLC. The eluent contained 25% acetonitrile, 75% water, 0.01 M perchloric acid, and 0.001 M NMFHA.

The digested antiperspirant samples were also analyzed by ICP-MS. The digested samples were diluted, and yttrium was added as an internal standard. The samples were analyzed by the Sciex ICP-MS using ultrasonic nebulization.

In the analysis of zirconyl oxide containing 0.99% hafnyl oxide, the same sample preparation procedure was followed as described for the antiperspirant sample, except that the samples were not refluxed overnight. An aliquot of the dissolved oxide was then chromatographed using an eluent of 20% acetonitrile, 80% H_2O, 1 $x10^{-3}$ M NMFHA, and 0.1 M perchloric acid at a flow rate of 0.52 ml per minute. The wavelength for detection was set at 304 nm.

Rare Earth Determination in Uranium

Solutions containing 100 $\mu g l^{-1}$ uranium, varying concentrations of rare earth ions, 2.4 x 10^{-4} M NMFHA and 1 x 10^{-4} M EDTA were made up between pH 5 and 8. For the off-line separation experiments, the solutions were passed though a gravity column containing XAD-16 resin from Rohm and Haas. The effluent was collected, a rare earth internal standard was added, and the solution was analyzed for the rare earth ions using the Ames Laboratory ICP-MS. The instrument conditions were described in reference 75. The on-line system consisted of a Hamilton PRP 10 µm polystyrene divinylbenzene column (150 mm x 4.1 mm), a Varian 2010 HPLC pump, a Rheodyne 7125 injector with a 200 µl sample loop, and a Sciex ICP-MS with ultrasonic nebulization. The ICP-MS operating conditions are described by Jiang et al. (265). The eluent consisted of a 1% methanol solution containing 0.001 M NMFHA, and a 0.01 M pyridine-nitric acid buffer at pH 5.0, and the flow rate was 1.2 ml per minute.

RESULTS

Absorbance and Spectral Studies

NMFHA and its metal chelates exhibited UV absorbance, the major absorbance band for both complexing agent and metal chelates being at 258 nm. Figure 30 gives the spectrum of NMFHA and the zirconium(IV) NMFHA complex. Other metal ion NMFHA complexes exhibited a similar UV spectrum. The metal complexes did not shift the wavelength maximum in the UV, but displayed increased absorption at the long wavelength end of the band. The molar absorptivities of the complexes at 304 nm were approximately 1.5×10^4 $lcm^{-1}mol^{-1}$. For direct detection in the HPLC studies, the UV detector was set at 304 nm to take advantage of this increased absorptivity; all the elements tested could be detected at 304 nm. Iron(III), uranium(VI), vanadium(V), and copper(II) complexes also displayed weak visible absorption bands. The iron(III) visible band maximum shifted in the hypsochromic direction as the pH increased. The maximum was at 525 nm at pH 1.0; at pH 5.0, the maximum shifted to 455 nm. The band maxima for copper were at 740 and 360 nm, and a slight shoulder was seen between 420 and 440 nm for the uranium-NMFHA complex. The molar absorptivities of the visible bands were too low to sensitively detect the metal complexes.

Figure 31 gives the UV spectrum of the neutral and anionic forms of NMFHA. Direct UV detection could not be done at high pH values because the anionic form of NMFHA displayed greater absorptivity at longer wavelengths. The possibility of using a post-column reactor to enhance detection of metal ions was tested, and it was found that most metal ions reacted with the post column reagent in the presence of NMFHA. Due to

Figure 30: Absorbance spectra of NMFHA and Zr-NMFHA at pH=2

[NMFHA] = 5.0×10^{-5} M [Zr] = 1×10^{-5} M

------ NMFHA ——————Zr-NMFHA

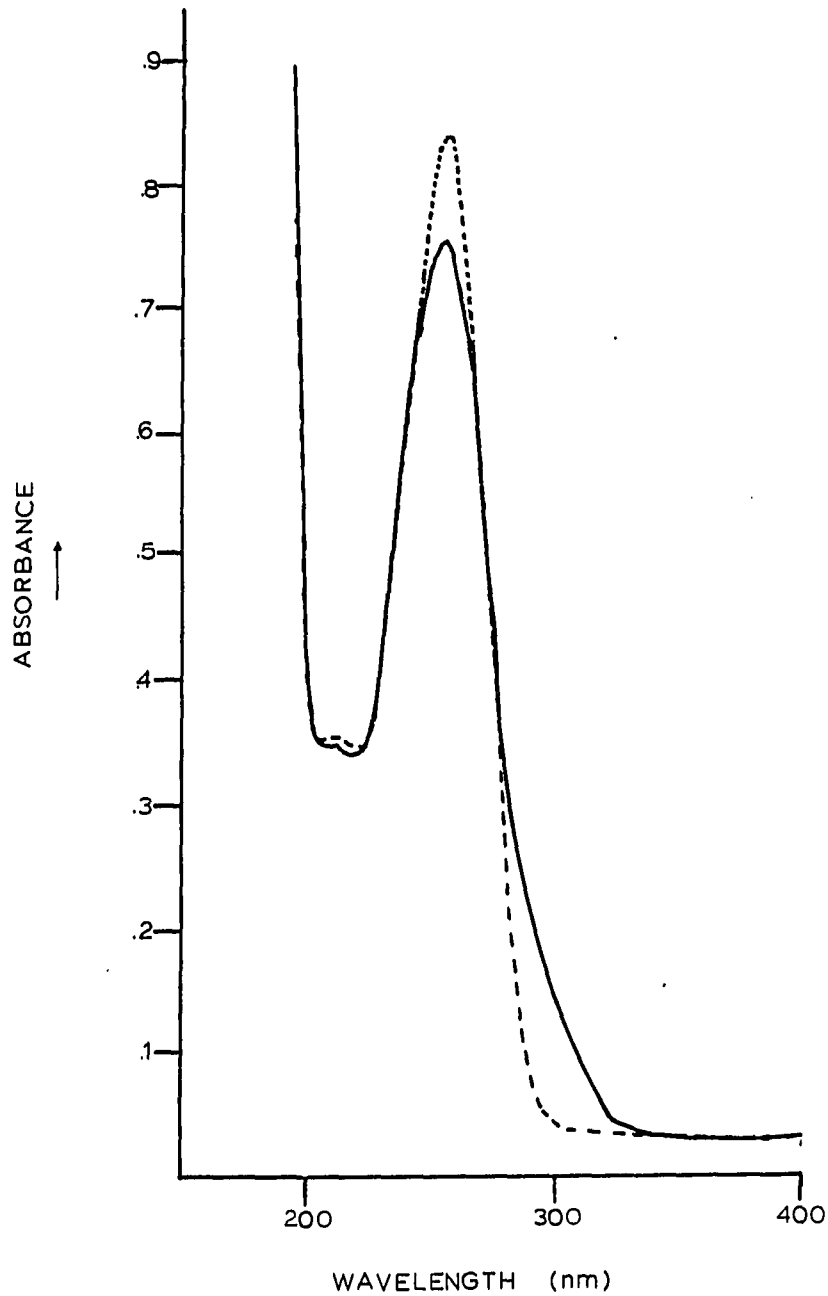
.9
.8
.7
.6
.5
.4
.3
.2
.1
ABSORBANCE
200
300
400
WAVELENGTH (nm)

Figure 31: UV spectrum of 2.5×10^{-5} M NMFHA at pH 2 and pH 11

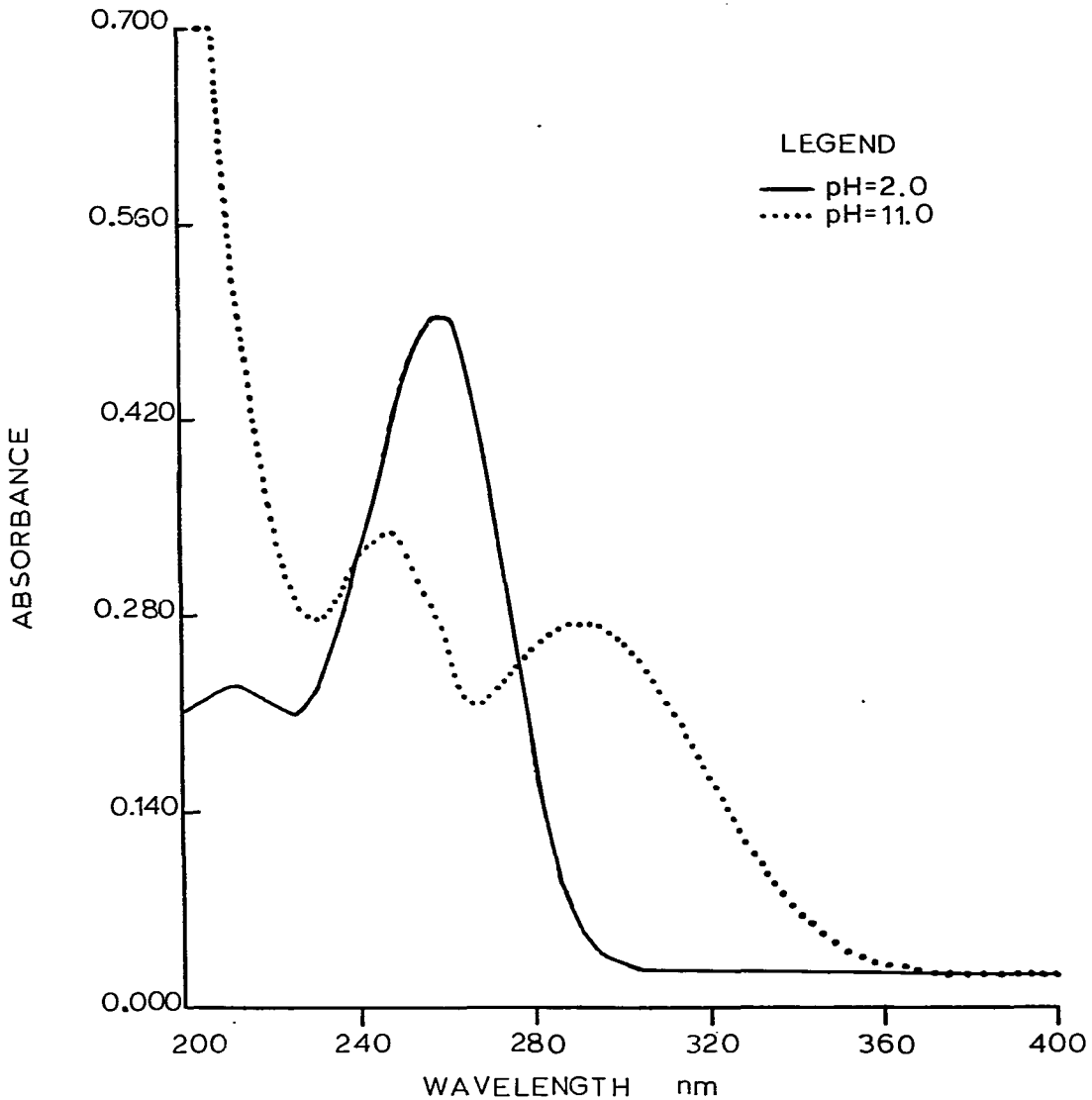
0.700
0.560
0.420
0.280
0.140
0.000
ABSORBANCE
LEGEND
pH=2.0
pH=11.0
200
240
280
320
360
400
WAVELENGTH nm

the high background from NMFHA in those eluents at pH 8 or greater, a post-column reactor system was used. The zirconium(IV) and hafnium(IV) NMFHA complexes were very strong; there was interference due to NMFHA with most of the standard colorimetric reagents, which ruled out post-column reaction as a means of detection for these metals.

Silica Gel Studies

The first studies were carried out on a silica based C-18 column. Initial chromatograms indicated that NMFHA needed to be present in the eluent. When no NMFHA was present in the eluent, no metal ion peaks were seen; only tailed NMFHA peaks eluted from the column. The presence of 0.01 M NMFHA in the eluent was necessary for most metal ion peaks to be seen. Figures 32-34 show separations of metal complexes at various pH values. No more than two metals could be separated at one time. Iron(III) and aluminum(III) were separated at pH 5 using direct detection in Figure 32. In Figure 33 the nickel peak eluted in the void volume; the nickel could only be seen because the post column reactor detection system was used. Peak shapes of many of the complexes were poor. In Figure 34 zirconium(IV) and hafnium(IV) could not be separated at all at pH 2 and eluted as a broad peak. It is believed that silanol-metal interactions were responsible for the poor peak shape attained in Figure 34. The residual silanol groups competed for the metal ion with the NMFHA as shown in Equation (10). A NMFHA concentration of 0.01 M was required in order for zirconium(IV) and hafnium(IV) peaks to elute.

$$Zr(NMFHA)_n + \text{-Si-O-H} \rightleftharpoons \text{Si-O-}Zr(NMFHA)_{n-1} + H^+ + NMFHA \qquad (10)$$

Other authors have reported silanol interaction with polar compounds (197-200). Silica columns were then abandoned, and the remaining studies focused on separating the complexes using a polymer-based column in order

Figure 32: Separation of Al(III), Fe(III) NMFHA complexes on a C-18 column at pH 5. Detection at 304 nm

[Al] = 8.3×10^{-5} M, [Fe] = 6.6×10^{-5} M

Eluent conditions: 35% CH_3CN, 65% H_2O, 0.05 M HAc, 0.01 M NMFHA

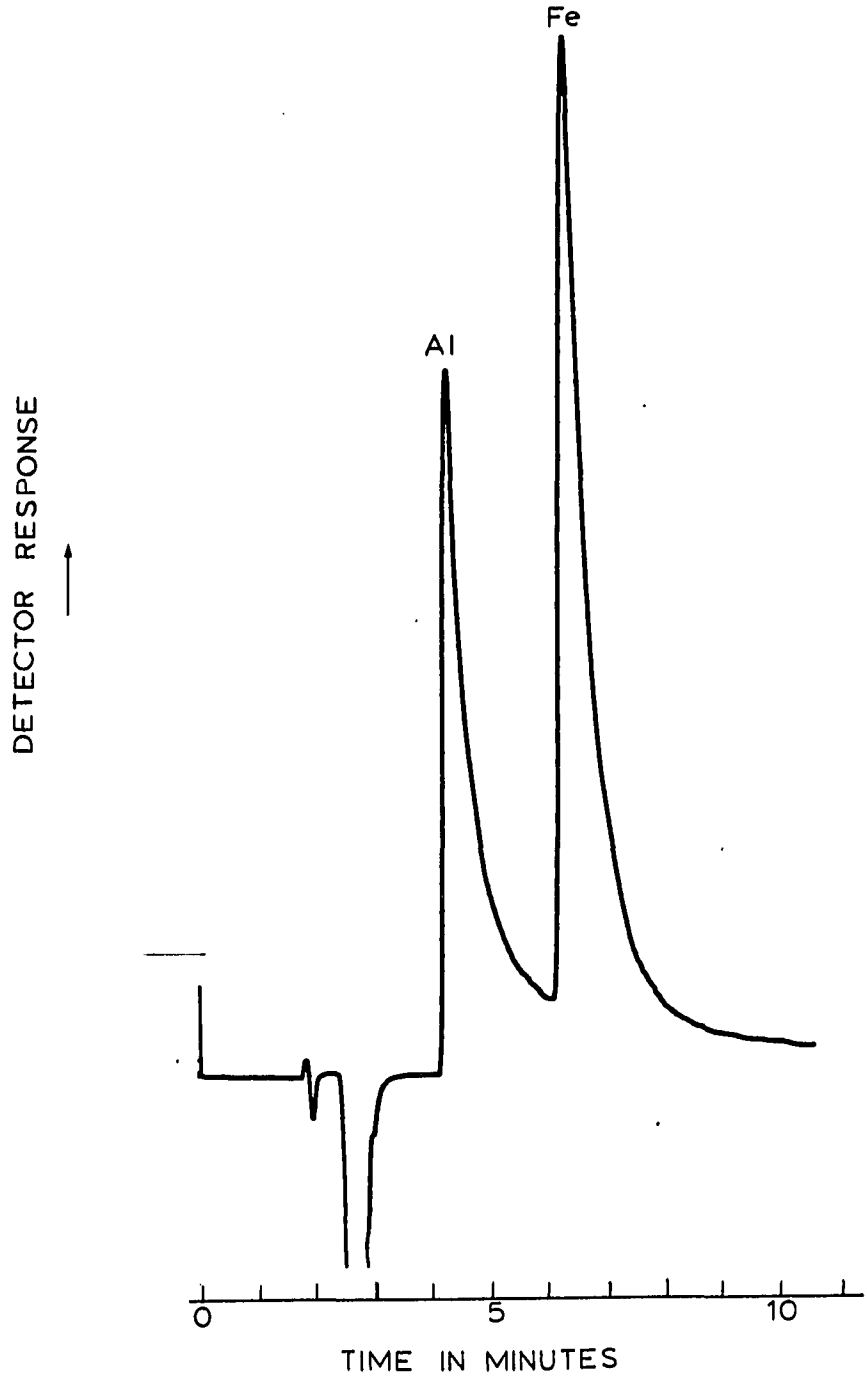
Fe
Al
DETECTOR RESPONSE
0
5
10
TIME IN MINUTES

Figure 33: Separation of Ni(II) and Cu(II) on a C-18 column at pH 8.0.

Detection at 580 nm

[Ni] = 1×10^{-4} M, [Cu] = 1×10^{-4} M

Eluent conditions: 35% CH_3CN, 65% H_2O, 0.01 M NMFHA

Post column reactor conditions: 0.0125% PAR in 2 M NH_4OH, 1 M NH_4HAc, flow rate = 1.0 ml per minute

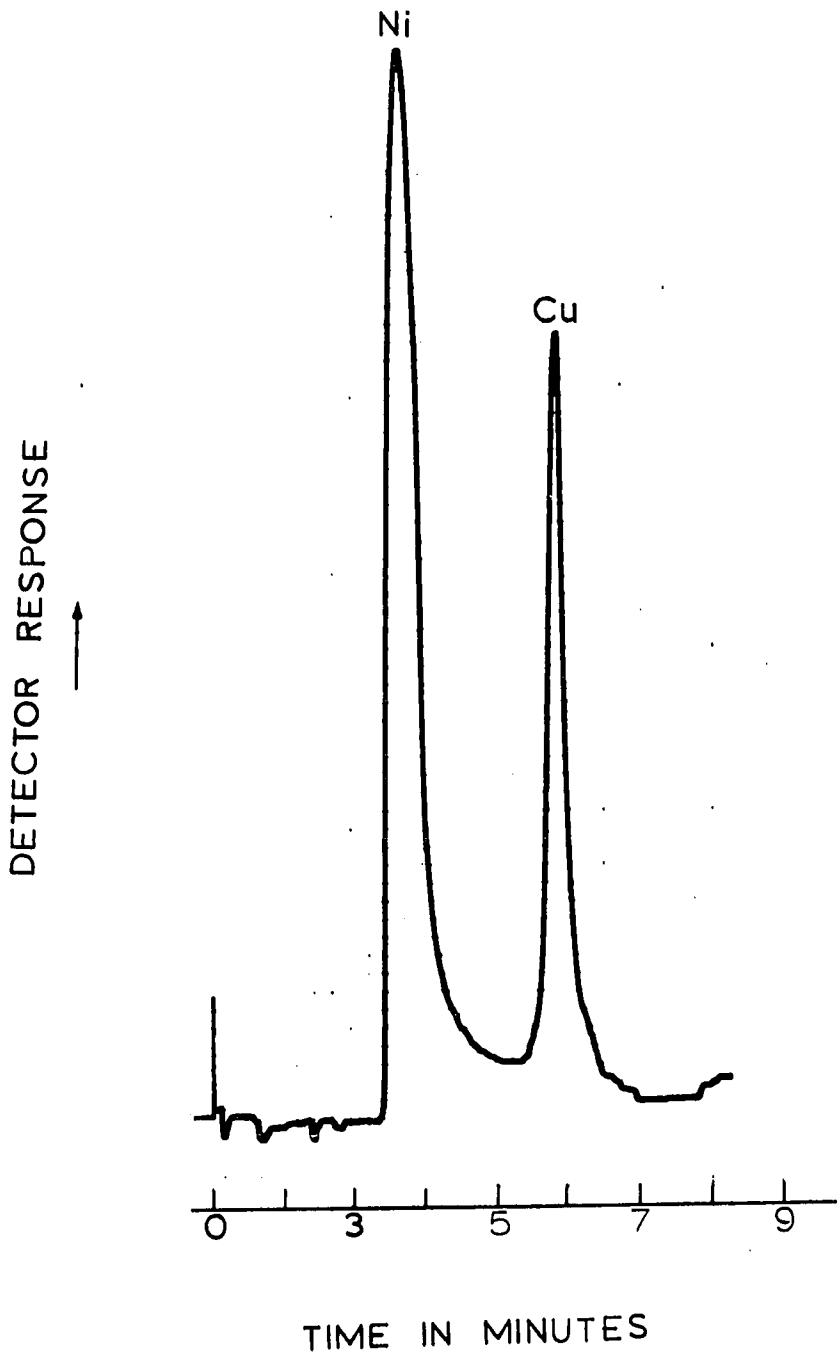
Ni
Cu
DETECTOR RESPONSE
0
3
5
7
9
TIME IN MINUTES

Figure 34: Separation of Zr(IV), Hf(IV), and Fe(III) on a C-18 column at pH 2. Detection at 304 nm
[Fe] = 1.67×10^{-4} M, [Hf] = 1.67×10^{-4} M,
[Zr] = 1.8×10^{-4} M
Eluent conditions: 20% CH_3CN, 80% H_2O, 0.01 M $HClO_4$,
0.01 M NMFHA

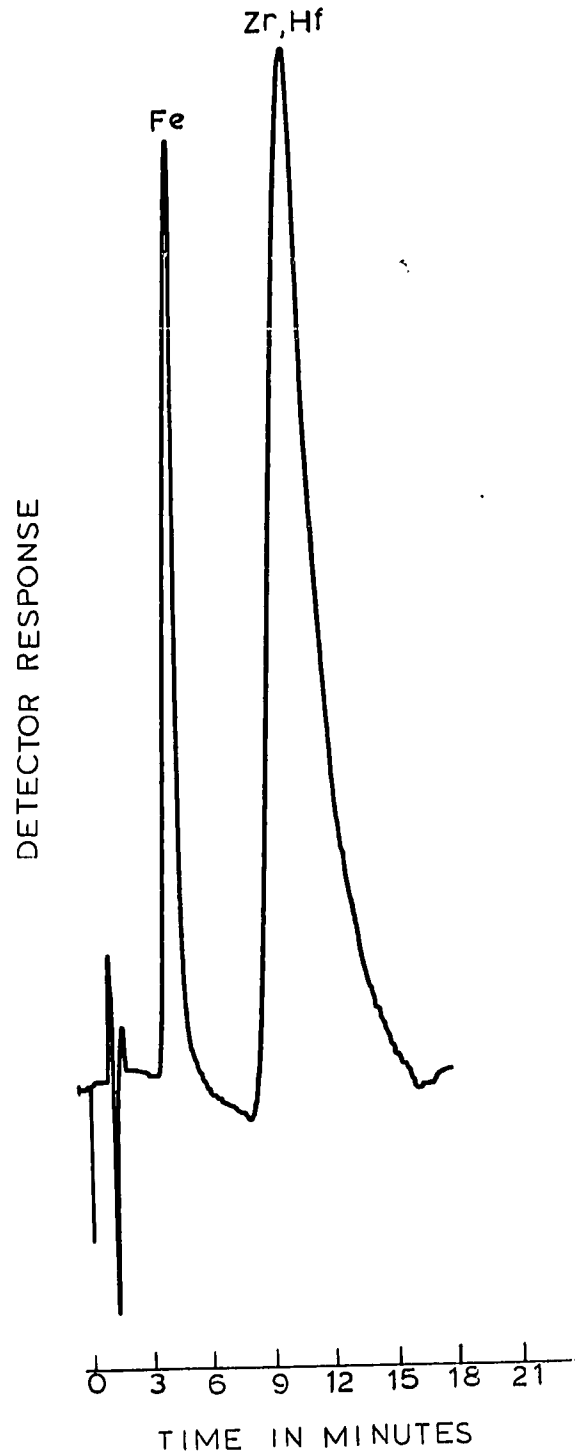
Zr,Hf
Fe
DETECTOR RESPONSE
0
3
6
9
12
15
18
21
TIME IN MINUTES

to minimize the interaction of the stationary phase with the metal ions.

Polymer Column Separations

Unlike silica-based columns, polymeric columns have no reactive sites and are stable over a wide pH range. The PLRP-S column was tested under similar conditions as those used for the iron(III), zirconium(IV), and hafnium(IV) separation in Figure 34. Initial separation studies with no NMFHA in the eluent gave only NMFHA tailed peaks, indicating that the metal ion complex dissociated as it passed though the column. With NMFHA added to the eluent, peaks for iron(III), zirconium(IV), and hafnium(IV) were seen, as shown in Figure 35. The separation achieved on the polymeric column required 10 times less NMFHA in the eluent than that used in the C-18 column eluent. Zirconium(IV) and hafnium(IV) were separated, and the peaks had less tailing and were narrower on the PLRP-S column. These observations supported the theory that the silanol groups on the silica column interacted with the metal ions. The remainder of the studies were carried out using the PLRP-S column.

Eluent Studies

Because NMFHA was required in the eluent for metal complex elution, a study was carried out to determine the effect of the concentration of NMFHA in the eluent on the separation. Table 18 gives retention times of various metals as the NMFHA concentration was varied. The peak shape, peak height, and retention times were dependent on the amount of NMFHA present in the eluent. As the concentration of NMFHA decreased in the eluent, the retention times decreased, peak heights decreased, peak widths increased, and peaks became more tailed for iron(III), zirconium(IV), and hafnium(IV). Because of increased peak width, zirconium(IV) and hafnium(IV) could no longer be resolved at low levels

Figure 35: Separation of Fe(III), Zr(IV) and Hf(III) on a PLRP-S column. Detection at 304 nm

Eluent: 15% CH_3CN, 85% H_2O, 0.01 M $HClO_4$, 0.001 M NMFHA

[Fe] = 1.67×10^{-4} M, [Hf] = 1.67×10^{-4} M,

[Zr] = 1.8×10^{-4} M

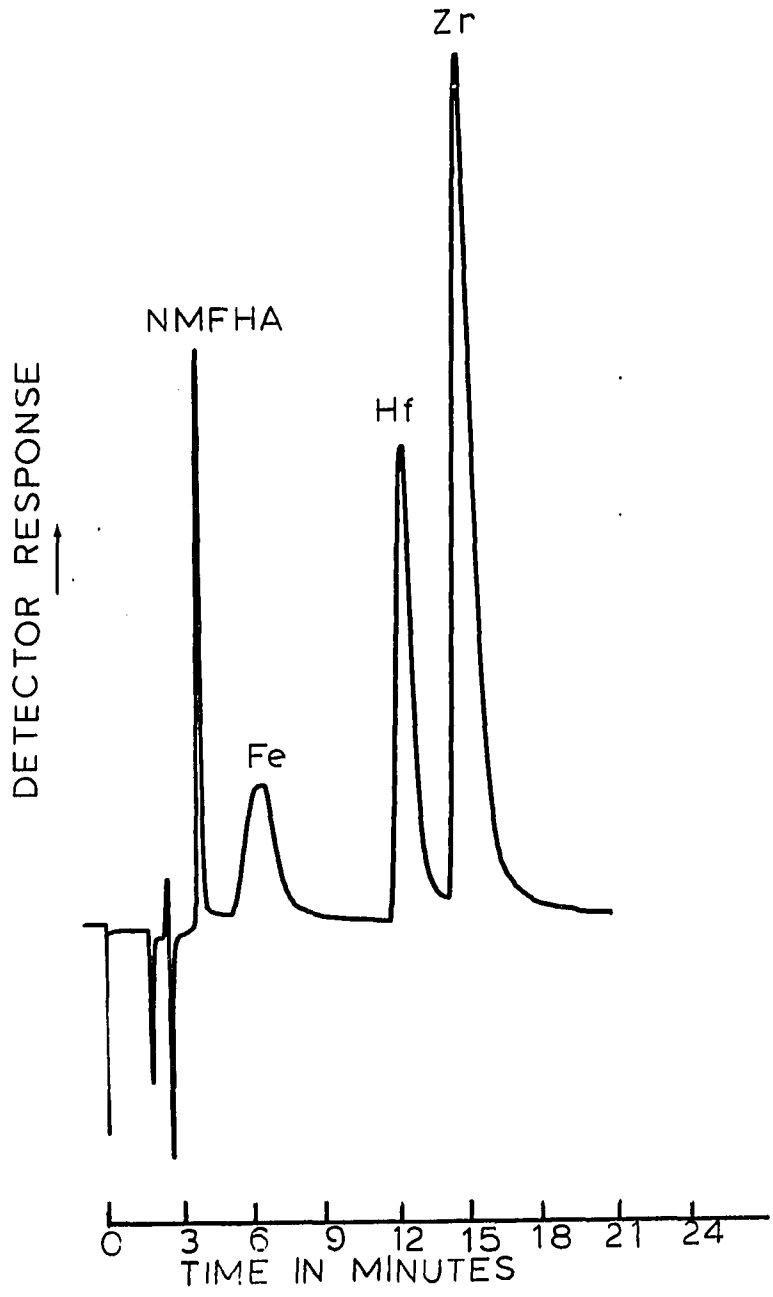
Zr
NMFHA
Hf
Fe
DETECTOR RESPONSE
0
3
6
9
12
15
18
21
24
TIME IN MINUTES

Table 18: Retention times of NMFHA metal complexes with varying NMFHA concentrations in the eluent[a]

[NMFHA]	t_r-Zr	t_r-Hf	t_r-Fe	t_r-Nb
0.0050	13.8	12.6	11.6	8.6
0.0025	12.3	10.9	8.2	6.6
0.0010	11.4	10.2	5.3	6.1
0.00050	10.8	9.6	4.7	4.5
0.00025	9.2	8.6	4.4	3.8
0.00010	8.6	8.2		3.1

[a]Eluent Conditions: 20% CH_3CN, 80% H_2O, .010 M $HClO_4$, Flow Rate = 1.0 ml/min.

of NMFHA. At the 1 x 10^{-4} M NMFHA level in the eluent, the iron(III) peak eluted as a tailed NMFHA peak. The niobium(V) retention time decreased with decreasing NMFHA concentration, but peak width also decreased under the same conditions. The 0.001 M level of NMFHA in the eluent was used in the eluent studies because peaks on the polymeric column had less tailing and narrower peak widths without using a large amount of complexing agent.

The choice of organic modifier affected the separation characteristics of the complexes. Figure 36 compares chromatograms of separations attained using acetonitrile and methanol as organic modifiers in the eluent. The eluents containing methanol required over twice as much organic modifier (51%) as the eluent containing acetonitrile (20%)

Figure 36: Comparison of using MeOH and CH_3CN as organic modifier on a PLRP-S column. Detection at 304 nm

[Zr] = 8 x 10^{-5} M, [Hf] = 6.9 x 10^{-5} M

(A) Eluent: 20% CH_3CN, 80% H_2O, 0.01 M $HClO_4$, 0.001 M NMFHA

(B) Eluent: 51% MeOH, 49% H_2O, 0.01 M $HClO_4$, 0.001 M NMFHA

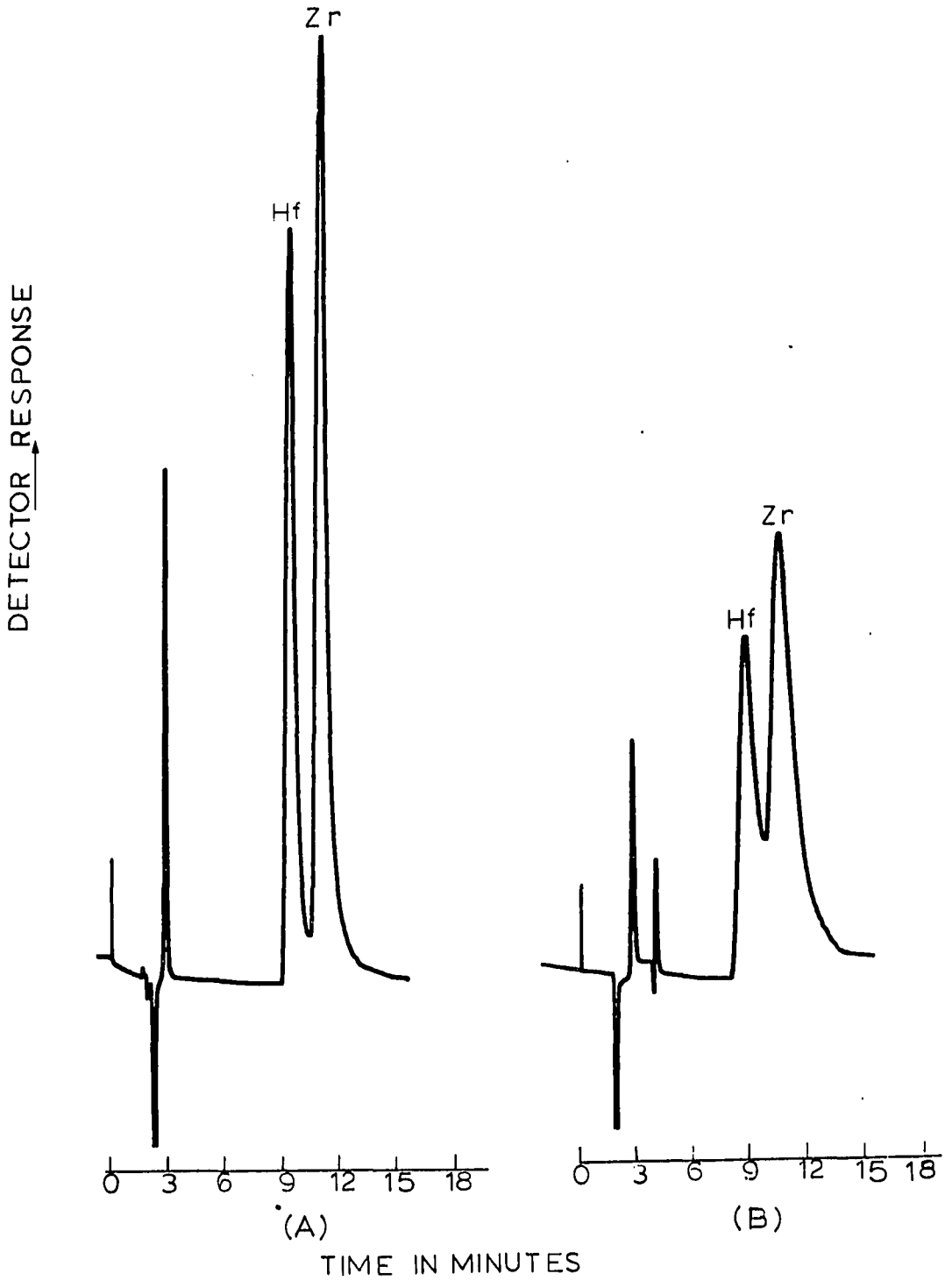
Zr
Hf
DETECTOR RESPONSE
0 3 6 9 12 15 18
(A)
Zr
Hf
0 3 6 9 12 15 18
(B)
TIME IN MINUTES

in order to elute the complexes at approximately the same time. Peaks were broader with the methanol-water eluent, and peak heights also decreased. Because of the broader peaks, resolution of the zirconium(IV) and hafnium(IV) peaks were poorer using methanol: the resolution was 1.1 using acetonitrile and 0.87 using methanol. This poorer elution strength of methanol was due in part to the wetting characteristics of the polystyrene divinylbenzene packing of the column. Other authors have demonstrated that methanol is a poorer wetting agent of the polymeric stationary phase packing than acetonitrile (201). The interaction of the solvent with the complex may also have affected the retention times of the complexes, as was described in Section III for the DMAP separations.

Initially only perchloric acid was added to the eluent to provide an acidic pH. The concentration of the perchlorate anion was varied by adding sodium perchlorate to determine the effect of the concentration of the anion on the separation. Table 19 gives retention times for the metals as a function of the concentration of sodium perchlorate in the eluent. As the perchlorate concentration in the eluent was increased, the retention time increased and reached a plateau at 0.1 M sodium perchlorate. This increase in retention time suggested that an ion-pairing mechanism was occurring.

To confirm that an ion-pairing mechanism was involved in the complex separation, the anion in the eluent was varied by changing the acid used to buffer the eluent. Table 20 gives the retention times for zirconium(IV), hafnium(IV), niobium(V), and iron(III) using different acidic eluents. Retention times of the metals varied depending on the type of acid used and correlated with the ion pairing ability of the anions. Perchlorate is one of the better cationic pairing reagents, and

Table 19: Effect of perchlorate concentration in the eluent on the retention time[a]

$[ClO_4^-]$	t_r-Zr	t_r-Hf	t_r-Nb	t_r-Fe
0.010	11.4	9.8	5.7	5.1
0.025	13.1	11.4	6.8	5.7
0.050	16.6	13.7	7.4	6.5
0.10	17.9	15.8	8.1	7.2
0.20	17.9	15.8	8.1	6.9

[a]Eluent Conditions: 20% CH_3CN, 80% H_2O, 0.01 M $HClO_4$, 0.001 M NMFHA, $NaClO_4$ added to adjust the concentration of ClO_4^-. Flow Rate = 1.0 ml/min. Detection at 304 nm.

the complexes eluted later in perchloric acid than in other acidic eluents. Conversely, metal complexes eluted the earliest in sulfuric acid, reflecting the poor ion pairing ability of sulfate. One exception was seen for the niobium(V) peak; the niobium-NMFHA complex eluted later in sulfuric acid than in the other eluents. Niobium(V) forms stronger complexes with sulfate than with the other anions, and the increased retention of the niobium(V) peak may be due to the formation of a niobium(V), NMFHA, sulfate complex.

pH Study of the Complex

Figure 37 shows the effect of the pH of the eluent on the capacity factor (k') of the complexes. The pH was varied either by changing the concentration of perchloric acid or adding a buffer. Sufficient sodium

Table 20: Effect of eluent anion on the retention time of the NMFHA metal complexes[a]

Anion	t_r-Zr	t_r-Hf	t_r-Nb	t_r-Fe
ClO_4^-	33.3	27.3	15.6	10.8
NO_3^-	14.3	12.3	12.9	6.3
$MeSO_3^-$	11.4	10.5	10.2	5.1
SO_4^{2-}	8.6	7.7	15.9	4.8

[a]Eluent Conditions: 15% CH_3CN, 85% H_2O, 0.001 M NMFHA, 0.01 M anion, 0.01 M acid, adjusted to pH = 2.0. Flow Rate: 1.0 ml/min, Detection at 304 nm.

perchlorate was added to keep the perchlorate concentration at 0.1 M (except at 1 M perchloric acid). Large differences in retention time were seen when the pH was varied. As the pH of the eluent was raised, the retention times increased, indicating that a change in the structure of the complex was occurring as a function of pH. Crossovers of retention were seen for the niobium(V) and iron(III) complexes. Iron(III) changed elution order, from eluting first at pH values less than two, to the last eluting metal at pH 5. At 2 M perchloric acid the iron(III) complex did not form. As the acidity increased, the retention times for niobium decreased at a slower rate than the retention times for zirconium(IV) and hafnium(IV), until at 2 M perchloric acid the niobium(V) peak eluted last. At pH values greater than 4 and for

Figure 37: Effect of pH on k′

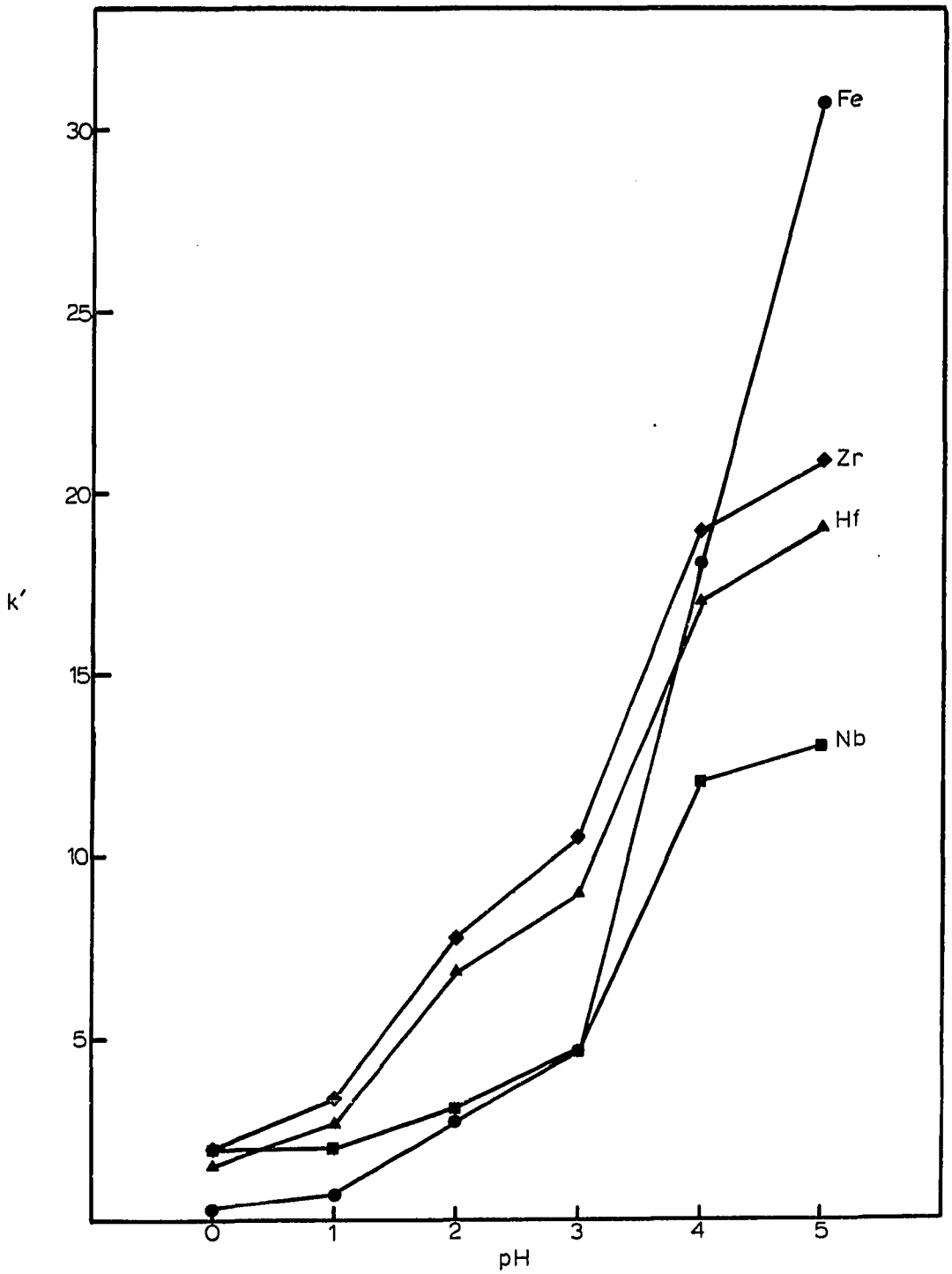
Fe
Zr
Hf
Nb
k'
30
25
20
15
10
5
0
1
2
3
4
5
pH

retention times less than 20 minutes, all separation capability for zirconium(IV), hafnium(IV), and niobium(V) was lost. For the higher eluent pH values, different retention times of the metal were seen, but the peaks were so broad that the three metals could not be resolved.

In addition to changing retention times, peak area and peak shape varied depending upon pH and the metal ion. For iron(III) as the pH increased, the peak height and areas of the iron(III) complex increased, with a large increase occurring between pH 3 and 4. The varying peak areas were mirrored by the change of color of the iron(III) complex described earlier. Peak areas for the niobium(V), zirconium(IV), and hafnium(IV) complexes also increased with pH, although not with as large an increase in absorptivity as seen with the iron(III) complex. For hafnium(IV), zirconium(IV), and niobium(V), peak widths tended to increase as the pH increased, especially between pH 3 and 5.

To determine the variation of the complex structure as a function of pH, Job's plot studies were done at different pH values for the zirconium-NMFHA complex. Table 21 gives the ratio of NMFHA to zirconium(IV) as a function of pH. As the pH increased, the number of NMFHA molecules binding to zirconium(IV) increased. Fouche studied the formation of zirconium-BPHA complexes in acidic solutions and found a similar behavior (258-259). The color changes and increase in retention time of the iron-NMFHA complex as a function of pH, plus the precipitation of the orange iron(III) complex above pH 4, also indicated similar pH effects on the formation of the iron-NMFHA complex were occurring. Other studies carried out on benzohydroxamic acid complexes of iron(III) reflected a similar pH dependency on complex formation (260-261).

Table 21: Effect of pH on complex formation and retention time[a]

pH	NMFHA:Zr	t_r-Zr
0	1.4:1	6.0
1	1.9:1	8.4
2	2.6:1	17.9
3	3.3:1	22.8
4	3.9:1	39.5

[a]Eluent Conditions: 20% CH_3CN, 80% H_2O, 0.001 M NMFHA. The concentration of $HClO_4$ was adjusted to give desired pH. $NaClO_4$ added so that total concentration of ClO_4^- (except at pH = 0) is 0.10. The pH 4 eluent is 0.01 M pyridine and $HClO_4$ adjusted to pH 4.

Chromatography Mechanism

The separation mechanism in chromatography is the equilibrium of the analytes between the stationary and mobile phases. The complexes are differentially retained according to their affinity for the stationary phase relative to their attraction to the mobile phase. Equation (11) shows the solvophobic separation mechanism for the metal (M) NMFHA complex. The greater the attraction of the metal complex to the

$$\text{M-NMFHA}_{(\text{mobile})} \rightleftharpoons \text{M-NMFHA}_{(\text{stationary})} \qquad (11)$$

stationary phase, the longer the retention of the analyte species.

The studies presented on the HPLC separation of the NMFHA complexes under acidic conditions indicated that secondary chemical equilibria (SCE) were occurring in the separation system. In SCE a chemical

equilibrium is present between two or more forms of the analyte species as the analyte travels down the column. The retention of an analyte is now altered because different forms of the analyte will have different retention characteristics (264). The first equilibrium effect changing retention is the ion-pairing effect described earlier. In ion-pairing chromatography, an ion is added to the eluent where it forms neutral complexes with the oppositely charged analytes. The neutral species are then separated by RP-HPLC. In the present case, a negatively charged anion was added to the eluent, reacted with the positively charged metal complex to form a neutral metal-NMFHA complex as shown in Equation (12). The neutral ion paired complexes were then retained and separated on the reversed phase column.

$$M(NMFHA)_n^{r+} + rA^- \rightleftharpoons M(NMFHA)_nA_r \qquad (12)$$

A second equilibrium was taking place between the metal NMFHA complex and free NMFHA in the eluent as shown in Equation (13). Increasing the

$$M(NMFHA)_n + NMFHA \rightleftharpoons M(NMFHA)_{n+1} \qquad (13)$$

NMFHA concentration shifted the equilibrium to the right where the more hydrophobic complex was formed. This shift in equilibrium explained the increase in retention time seen when increased amounts of NMFHA were added to the eluent. The nonintegral values found in the Job's plots also suggested that an equilibrium was present between different forms of the zirconium-NMFHA complex. The niobium(V) complex may have slow exchange properties or poor elution characteristics which would cause the peak broadening seen as the NMFHA concentration was increased. Low NMFHA concentrations in the eluent may favor one complex form, causing the decrease in peak width. The broad peak seen for niobium(V) and iron(III) also suggests that at pH 2, the equilibrium between the various forms of

the metal-NMFHA complexes was rather slow.

Increasing the pH also affected the equilibrium in Equation (12), as indicated by the Job's plot studies and retention times. The Job's plot studies showed that as the pH increased, the ratio of the NMFHA to zirconium(IV) increased. As the eluent pH increased, the equilibrium in Equation (12) shifted to the right, and the complex became more hydrophobic, causing an increase in retention time for the complexes.

The separation of zirconium(IV) and hafnium(IV) has been difficult to achieve because the chemistry of the two metal ions is so similar. In this system, separation of zirconium(IV) and hafnium(IV) NMFHA complexes in acidic solutions probably was seen due to the SCE occurring during the separation. Comparison of zirconium(IV) and hafnium(IV) complex behavior under acidic and neutral conditions sheds some light on the separation mechanism. At pH values greater than 3, no separation of zirconium(IV) and hafnium(IV) was achieved. A greater number of NMFHA molecules were bound to the metal ion at the higher pH values, and the compounds were more neutral than at lower pH values, which lessened the extent of ion pairing. Addition of sodium perchlorate to the eluent had no effect on the retention times of the complexes for eluent pH values greater than 3, indicating that ion-paired complexes were not formed to a great extent. The ratio of NMHFA to zirconium(IV) at pH 4 also indicated that at higher pH values, one form of the complex was predominant in solution; the equilibrium seen in Equation (12) was shifted to one side. Hence at higher pH values, the extent of SCE was less than the SCE seen with the low pH eluents. Because no separation is seen for zirconium(IV) and hafnium(IV) at more neutral pH values, it is reasonable to assume that the separation of the two metal ions in acidic solutions is due to SCE

effects.

Effect of pH on the Formation of Metal-NMFHA Complexes

When the pH was varied, other metal ion complex peaks were seen. At high acidities, the antimony complex peak eluted from the column as shown in Figures 38 and 39. Antimony hydrolyzed and precipitated at acidities less than 0.1 M perchloric acid. No iron(III) peak is seen in Figure 39 because iron(III) does not form a complex with NMFHA in 2 M perchloric acid. A comparison of Figures 38 and 39 shows the inversion of the niobium(V) peak; in 2 M perchloric acid niobium was the last peak to elute, while in 0.1 M perchloric acid zirconium(IV) and hafnium(IV) eluted after niobium(V). A tin(IV) peak was seen at 2 M perchloric acid; the peak only appeared at large concentrations of tin(IV) and eluted just after the dead volume peaks as a broad, tailed peak.

At higher pH values, several other metal-NMFHA complexes were seen. A vanadium(V) peak was seen at pH 3 but gradually disappeared upon subsequent injections. The vanadium(V) complex formed immediately at acidities between 2 M perchloric acid and pH 3.0, but broke apart as the sample aged. Evidence for the breakdown of the complex came from fading of the characteristic purple color of the vanadium-NMFHA complex in the sample. Scandium(III) also eluted at pH 3; the early eluting peak was broad and not very stable. As the acetonitrile content in the eluent decreased, the peak broadened out considerably. At pH values greater than 4, peaks for copper(II) and aluminum(III) eluted from the column. The copper(II) peak was a tailed peak which eluted with the NMFHA peak and which could not be separated from the NMFHA peak. Figure 40 is a chromatogram showing a separation of copper(II), aluminum(III), zirconium(IV), and iron(III) complexes at pH 6.5. Zinc(II) appeared at

Figure 38: Separation of Sb(III), Fe(III), Nb(V), Hf(IV), Zr(IV) on PLRP-S column. Detection at 304 nm

Eluent: 20% CH_3CN, 80% H_2O, 0.1 M $HClO_4$, 0.0025 M NMFHA

[Sb] = 4×10^{-4} M, [Fe] = 4×10^{-4} M, [Hf] = 2×10^{-4} M,

[Zr] = 1×10^{-4} M

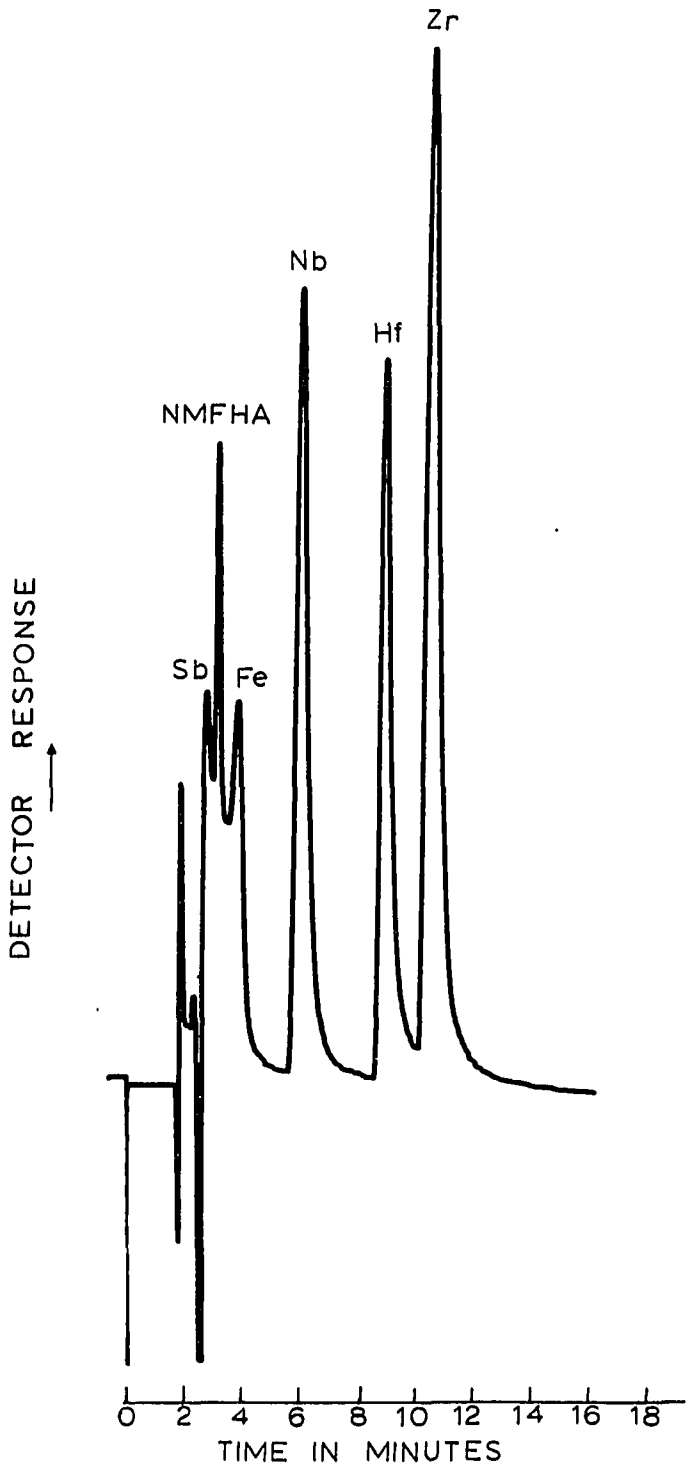
Zr
Nb
Hf
NMFHA
Sb
Fe
DETECTOR RESPONSE
0 2 4 6 8 10 12 14 16 18
TIME IN MINUTES

Figure 39: Separation of Sb(III), Hf(IV), Zr(IV), and Nb(V) on a PLRP-S column in 2 M $HClO_4$. Detection at 304 nm

[Sb] = 4 x 10^{-4} M, [Fe] = 4 x 10^{-4} M, [Hf] = 2 x 10^{-4} M, [Zr] = 1 x 10^{-4} M

Eluent conditions: 12% CH_3CN, 82% H_2O, 2.0 M $HClO_4$, 0.001 M NMFHA

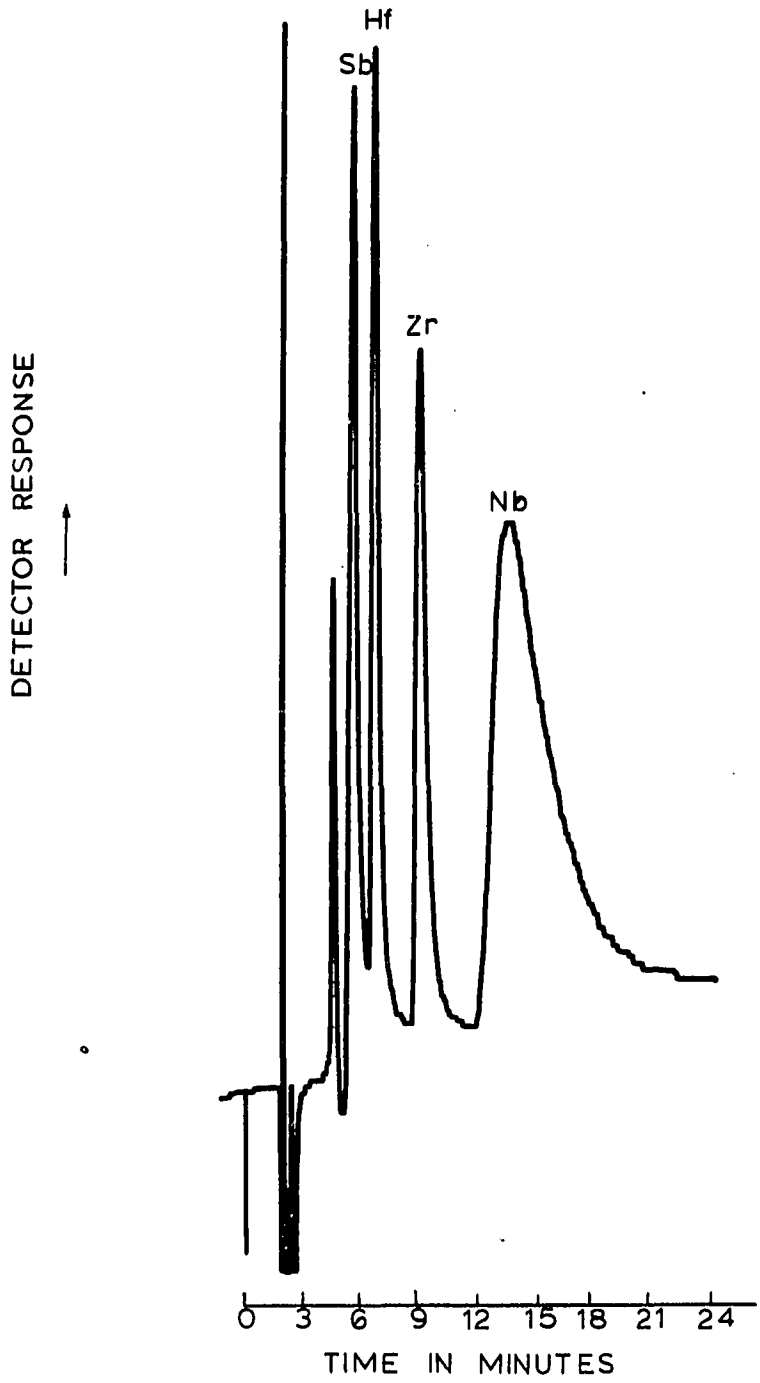
Hf
Sb
Zr
Nb
DETECTOR RESPONSE
0
3
6
9
12
15
18
21
24
TIME IN MINUTES

Figure 40: Separation of Cu(II), Al(III), Zr(IV) and Fe(III) on a PLRP-S column. Detection at 304 nm

Eluent: 28% CH_3CN, 72% H_2O, 0.05 M TEA & $HClO_4$ (pH 6.5), 0.001 M NMFHA

[Cu] = 9.4×10^{-5} M, [Al] = 2×10^{-4} M,

[Zr] = 2×10^{-4} M, [Fe] = 4×10^{-4} M

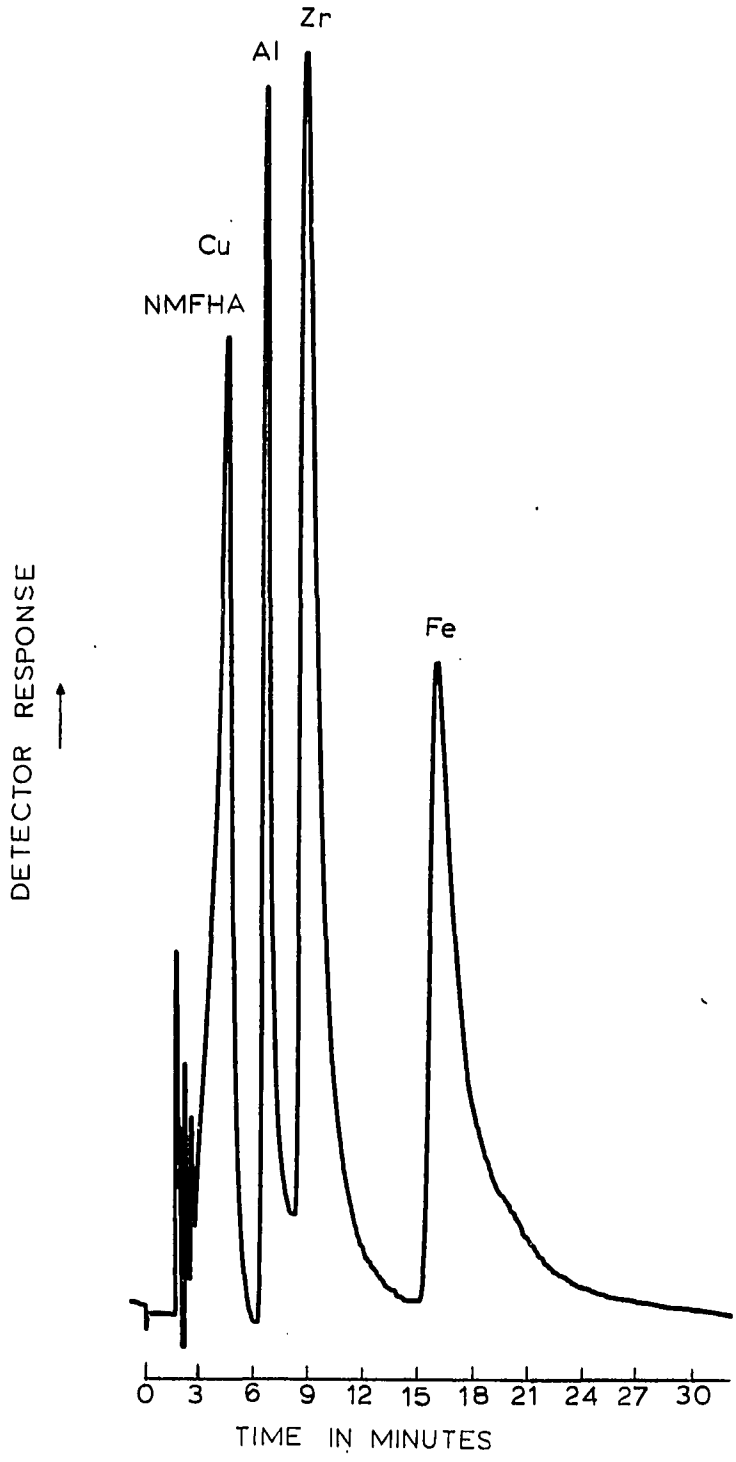
Zr
Al
Cu
NMFHA
Fe
DETECTOR RESPONSE
0 3 6 9 12 15 18 21 24 27 30
TIME IN MINUTES

pH 6 and eluted at or near the NMFHA peak. Hafnium(IV) and niobium(V) coeluted with zirconium(IV) at pH 5 and above. At pH 6 the niobium(V) peak disappeared, due probably to hydrolysis of the niobium(V).

Sample Preparation

Sample preparation affected the peak shapes of the metal complexes in the HPLC separations. Direct injection of the metal ions without pre-derivatization can be done, and Figure 41 compares chromatograms of zirconium(IV) and hafnium(IV) with and without pre-derivatization. Pre-derivatization of the sample gave better peak shapes than direct injection of underivatized sample. In testing with zirconium(IV) and hafnium(IV), larger peak heights were seen with prederivatization which improved detection limits. The broadened peaks seen for the untreated sample was probably due to noninstantaneous formation of the metal complex. Complexed and uncomplexed metal ions would travel at different rates down the column broadening the sample band until all the ions have reacted with NMFHA.

The aluminum(III) peaks were very dependent on sample preparation. As the buffer in the sample was varied, the peak height of the aluminum(III) complex varied. Figure 42 shows chromatograms of the aluminum(III) peak with different buffers used to make up each sample. Aluminum(III) in pyridine gave the greatest response, while aluminum(III) in triethanolamine gave a small broad peak. Using TEA or pyridine as the buffer in the eluent did not seem to greatly affect the aluminum(III) peak shape or response. The effect of the buffers on aluminum(III) peak shape indicated that the formation of the Al-NMFHA complex was prone to interference while being formed, but once formed, the complex was slow to break up.

Figure 41: Effect of prederivatization of tne sample peak shape

[Hf] = 1.67×10^{-4} M, [Zr] = 1.8×10^{-4} M

Eluent conditions: 20% CH_3CN, 80% H_2O, 0.01 M $HClO_4$, 0.001 M NMFHA

Column: PLRP-S, detection at 304 nm

A. No prederivatization

B. Prederivatization

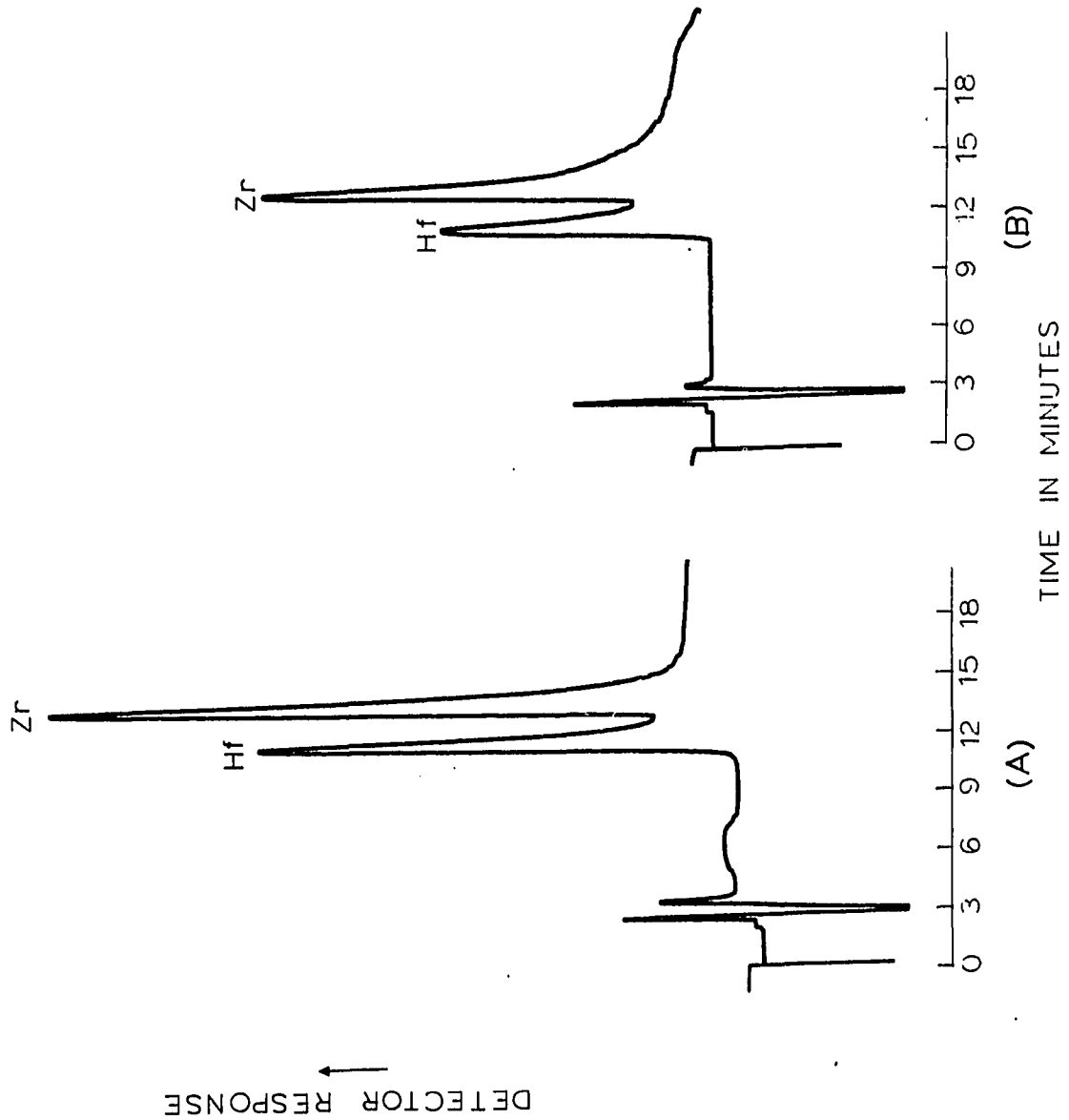
Zr
Hf
Zr
Hf
0 3 6 9 12 15 18
(A)
0 3 6 9 12 15 18
(B)
TIME IN MINUTES
DETECTOR RESPONSE

Figure 42: Effect of sample preparation on Al(III) peak shape.

[Al] = 2×10^{-4} M

Column: PLRP-S, detection at 304 nm

Eluent conditions: 28% CH_3CN, 72% H_2O, 0.01 M TEA,

0.001 M NMFHA

(A) Al-NMFHA in pyridine buffer; pH = 6.5

(B) Al-NMFHA in TEA buffer; pH = 6.5

(C) Al-NMFHA in HAc buffer; pH = 5.0

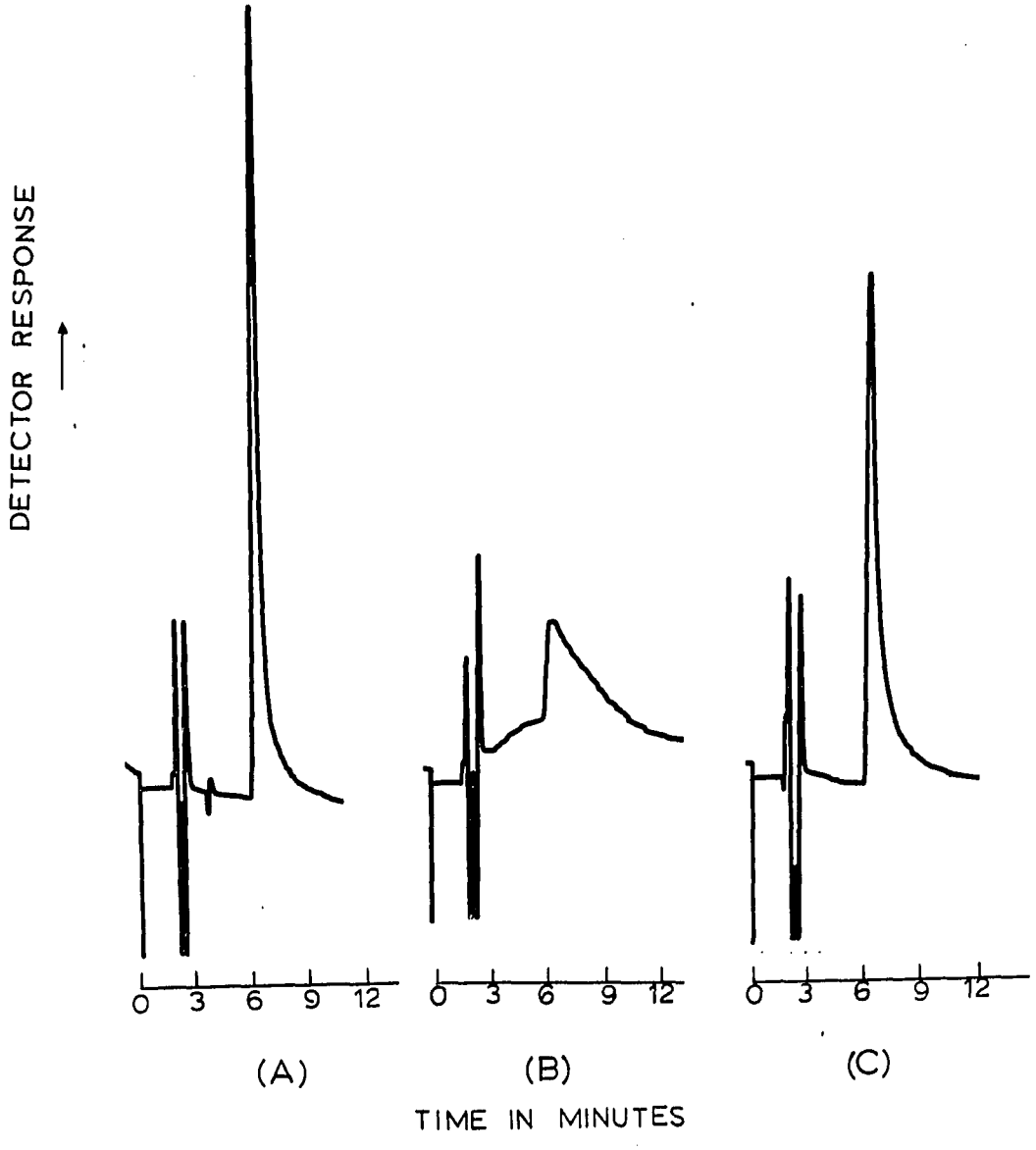
DETECTOR RESPONSE
0 3 6 9 12
0 3 6 9 12
0 3 6 9 12
(A)
(B)
(C)
TIME IN MINUTES

Quantitative and Interference Studies

Optimal separation conditions for zirconium(IV), hafnium(IV), aluminum(III), niobium(V), iron(III), and antimony(III) were determined and are given in Table 22; conditions were chosen such that the complexes eluted from the column under eight minutes. Under these conditions, the peaks were then resolved from the void volume without much overlap from other metal-NMFHA complex peaks. Also included are linear calibration curve ranges and limits of detection. The limit of detection was defined to be the concentration of the metal ion when the peak height is three times the standard deviation of the noise. Figure 43 shows calibration curves for zirconium(IV) and hafnium(IV) at pH 2. For these two ions, linearity was seen for almost three orders of magnitude.

The versatility of the metal ion separations using NMFHA as a complexing agent was tested by adding possible common interferent ions to the sample. The interfering ions were added to a solution containing the analyte ion, and the NMFHA was then added to the solution. Table 23 gives the maximum levels of interferent tolerated for zirconium(IV), iron(III), and aluminum(III). The concentrations shown in Table 23 caused a decrease in peak area of less than 5% for the three metal ions. Most of the interferences from the cations occurred due to overlapping of small, broad peaks of the interferent complex; these interferent peaks often coeluted with NMFHA. All three metals tolerated large concentrations of most of the common anions with the exception of fluoride and phosphate. Zirconium(IV) and aluminum(III) tolerated only extremely low levels of fluoride, which is not surprising since fluoride forms very strong complexes with those two metals. The ions arsenate, arsenite, and tin(IV) were tested for possible interference with

Table 22: Representative elution conditions for analysis of various metals by HPLC using NMFHA as the complexing agent[a]

Metal Ion	Elution Conditions	Linear Calibration Curve Range (M)	Limit of Detection (M)
Zr, Hf	20% CH_3CN 80% H_2O 0.001 M NMFHA 0.01 M $HClO_4$	Zr: 5×10^{-6} - 1×10^{-3} Hf: 4×10^{-6} - 8.5×10^{-4}	Zr: 2×10^{-6} Hf: 2×10^{-6}
Fe	40% CH_3CN 60% H_2O 0.001 M NMFHA 0.05 M HAc/$HClO_4$ pH = 5.9	5×10^{-6} - 1×10^{-3}	3×10^{-6}
Al	28% CH_3CN 72% H_2O 0.001 M NMFHA 0.05 M TEA/$HClO_4$ pH = 6.5	5×10^{-6} - 1×10^{-3}	1×10^{-6}
Nb	20% CH_3CN 80% H_2O 0.001 M NMFHA 0.10 M $HClO_4$	1.5×10^{-6} - 1.4×10^{-4}	5×10^{-7}
Sb	12% CH_3CN 82% H_2O 0.001 M NMFHA 2.0 M $HClO_4$	2×10^{-5} - 2×10^{-3} M	5×10^{-6}

[a]For all eluents: Flowrate = 1.0 ml/min UV-Detection, λ = 304 nm, injection volume = 20 µl.

Figure 43: Calibration Curves for Zr(IV) and Hf(IV) at pH 2.
Elution conditions given in Table 22

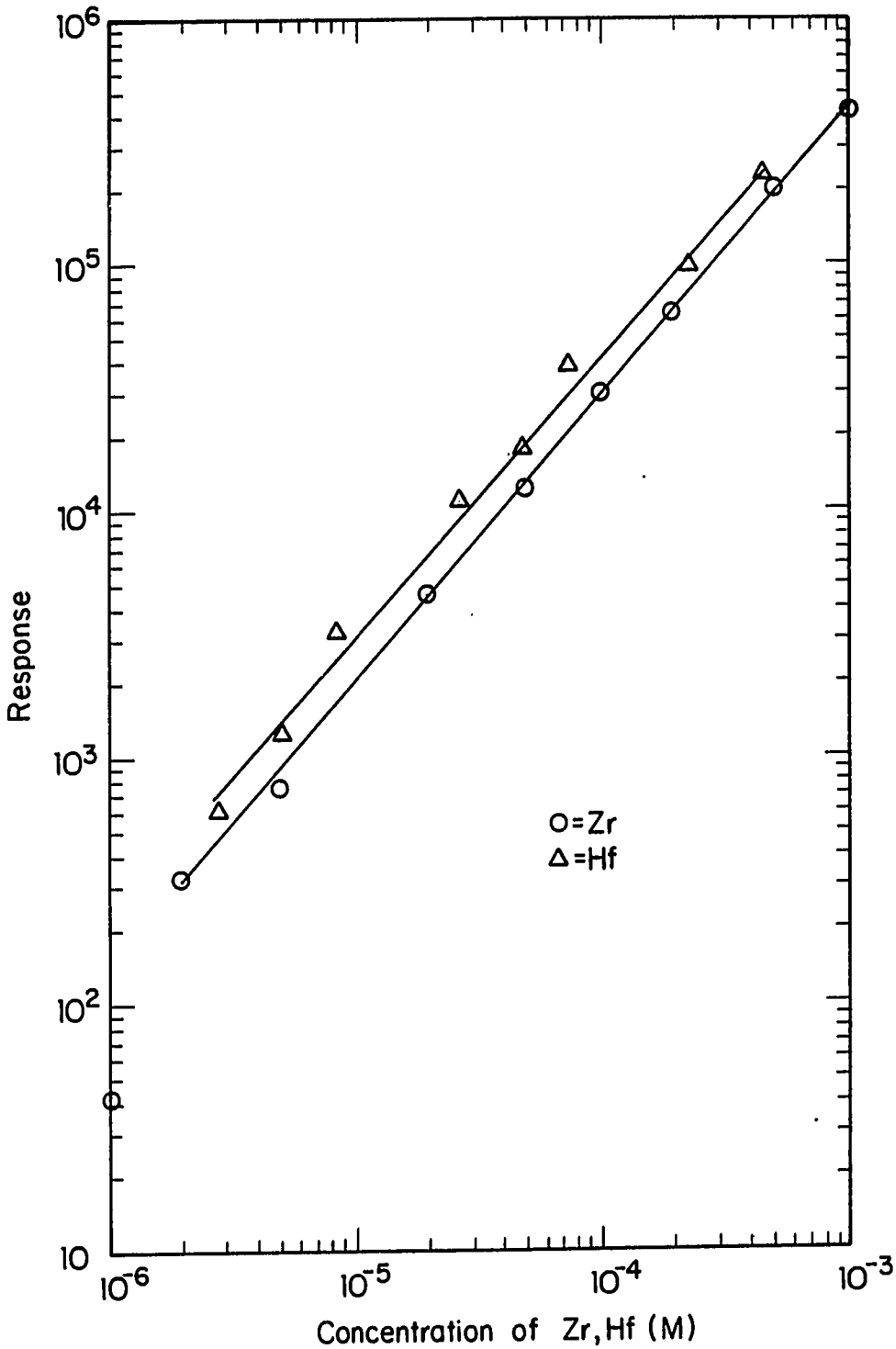
Response
10^6
10^5
10^4
10^3
10^2
10
10^{-6}
10^{-5}
10^{-4}
10^{-3}
Concentration of Zr, Hf (M)
O=Zr
Δ=Hf

Table 23: Concentration level (M) of other ions tolerated in the determination of Zr, Al, and Fe[a]

[ion]	Al	Fe	Zr
Na^+	0.8	1.0*[b]	1.2*
Cl^-	0.5	0.5*	1.2*
F^-	2×10^{-5}		5×10^{-4}
NO_3^-	0.8	1.0*	0.6
ClO_4^-	0.8	1.0*	1.2*
lactate	0.001		
Cu^{2+}		6.3×10^{-4}	1.3*
Ca^{2+}	0.4	0.5*	
Pb^{2+}		0.25*	
Mg^{2+}	0.05		
Mn^{2+}		0.25*	0.25*
Ni^{2+}	0.004	0.05	0.5*
UO_2^{2+}			0.3
Zn^{2+}	0.002	0.05	
$Cr_2O_7^{2-}$		0.02	
HPO_4^{2-}	0.001	0.0002	2×10^{-5}
SO_4^{2-}	0.18*	0.18*	0.18*
Al^{3+}			0.50*
Eu^{3+}			0.48*
Gd^{3+}	0.0017	0.44*	
Ti^{4+}			0.002

[a]Eluent conditions given in Table V. Concentrations of metal ions: [Zr] = 2.0×10^{-4} M, [Fe] = 2.0×10^{-4} M, [Al] = 2.2×10^{-4} M

[b]Asterisk (*) indicates greatest concentration of interferent ion tested.

antimony(III); Table 24 gives the maximum level of these ions which do not interfere with the determination of antimony(III).

Table 24: Concentration level (M) of other ions tolerated in the determination of antimony[a]

Metal ion	Concentration Level (M)
Sn^{4+}	0.01
Arsenite	0.1
Arsenate	0.1

[a]The elements did not interfere if less than a 4% difference in peak area was seen.

Analysis of an Antiperspirant Sample

To test whether the chromatography method could be used for real life samples, an analysis of a commercial solid antiperspirant for zirconium(IV) was done. Sample preparation was extensive in order to break down the sample into an aqueous solution. Silica was present in the sample as cyclomethicone, so the sample was fumed with hydrofluoric acid to volatilize the silica liberated. When this step was not carried out, silica precipitated out of solution, and zirconium(IV) and aluminum(III) were carried out with the precipitate. After the addition of hydrofluoric acid to the samples, the samples were fumed to near dryness several times with perchloric acid not only to digest organic matter, but to fume off hydrofluoric acid which would interfere with the

chromatographic analysis. Figure 44 is a chromatogram showing the presence of zirconium(IV) and aluminum(III) in the sample.

The chromatographic determination of zirconium was carried out using the eluent conditions described in the Experimental Section. Under these conditions, there was no chromatographic interference from aluminum(III). The average zirconium content determined by HPLC for the four samples was 3.59%; the same samples were also analyzed by ICP-MS and the average zirconium content was 3.70%. Considering the extensive sample procedure and the relative standard deviations of up to 5% by chromatographic and ICP-MS analyses, the agreement between the two analyses was considered satisfactory.

The antiperspirant sample was also analyzed for aluminum by HPLC using the conditions described in Figure 44. The average aluminum content for the samples was 3.6%, while the average aluminum content was determined by atomic absorption to be 4.3%. The difference in the two determinations was 0.7% which gave a relative error in the two analyses of 15%. There may have been enough residual fluoride present to interfere with the aluminum determination. In the interference studies, aluminum(III) was more sensitive to the presence of fluoride than zirconium(IV);and any fluoride in the sample would have a greater effect on the aluminum determination.

A spectroscopic standard of zirconyl oxide containing 0.99% hafnyl oxide was dissolved and analyzed for hafnium(IV) by HPLC. The amount of hafnium(IV) in the sample was determined to be 0.91%, a difference of approximately 0.08% from the known content. Figure 45 shows the chromatogram of the separation of zirconium(IV) and hafnium(IV). Given the large zirconium(IV) signal and the overlap of the two peaks, the

Figure 44: Antiperspirant analysis

Column: PLRP-S column, detection at 304 nm

Eluent conditions: 28% CH_3CN, 72% H_2O, 0.01 M TEA,

0.001 M NMFHA, pH = 6.5

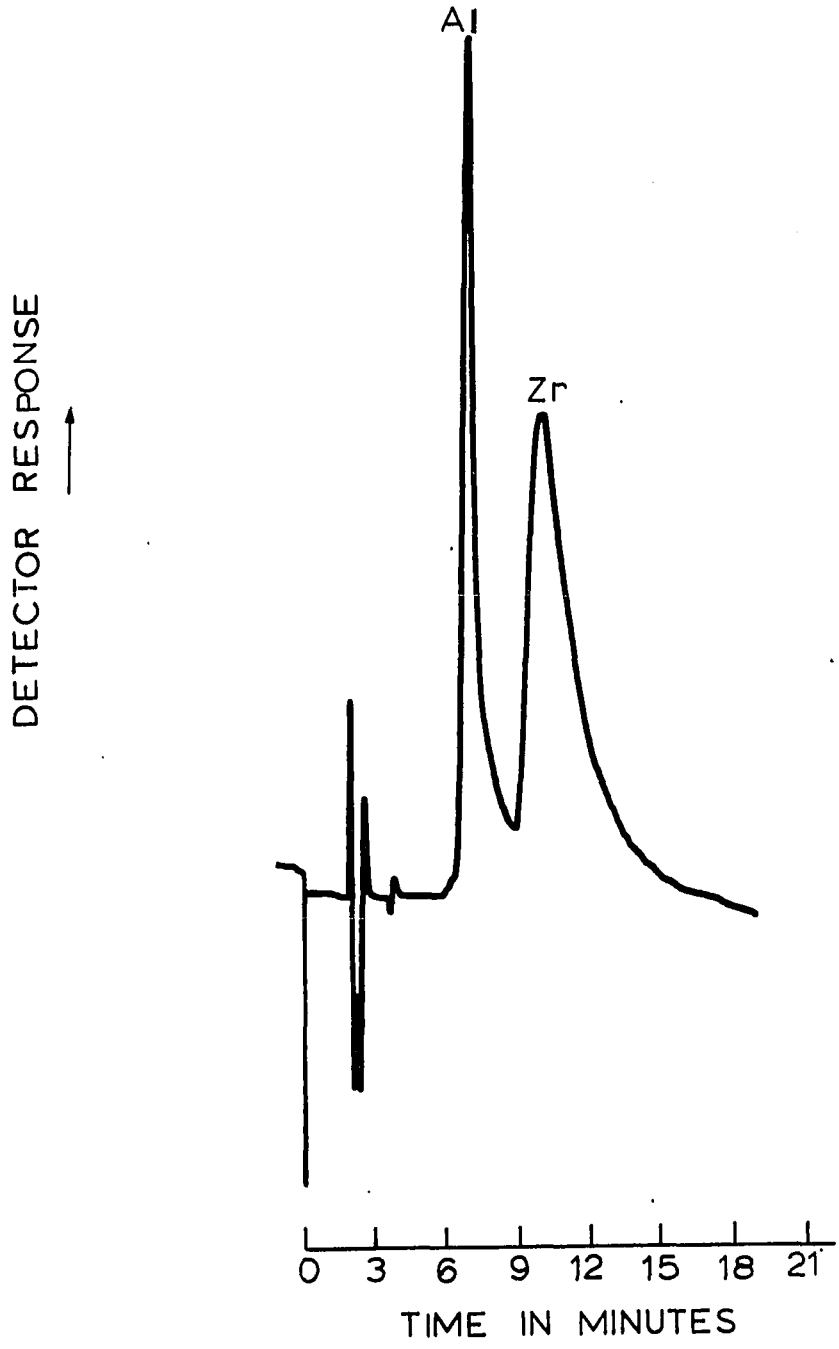
Al
Zr
DETECTOR RESPONSE
0 3 6 9 12 15 18 21
TIME IN MINUTES

Figure 45: 0.99% HfO_2 in ZrO_2

Column: PLRP-S, detection at 304 nm flow rate = 0.53 ml per minute

Eluent conditions: 20% CH_3CN, 80% H_2O, 0.1 M $HClO_4$, 0.001 M NMFHA

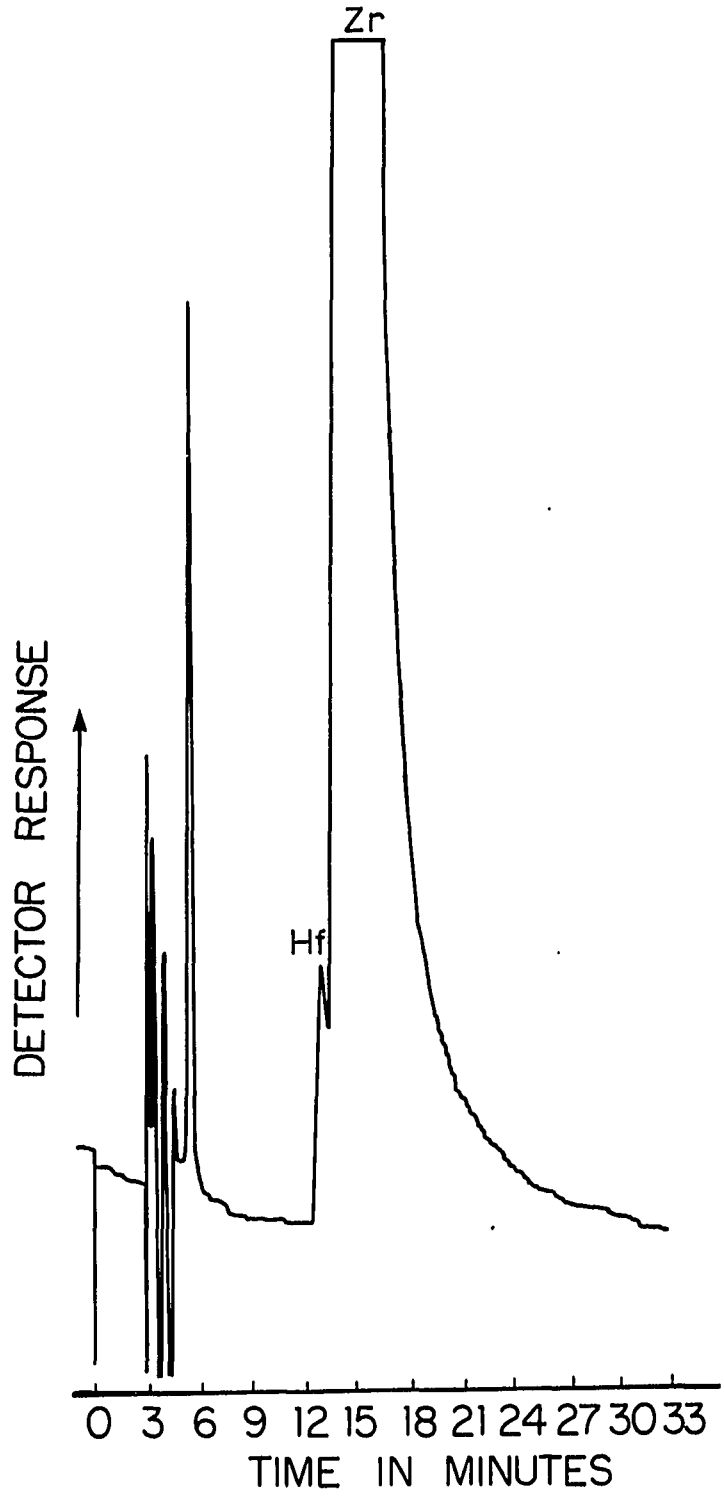
Zr
Hf
DETECTOR RESPONSE
0 3 6 9 12 15 18 21 24 27 30 33
TIME IN MINUTES

percentage error is not unreasonable.

Determination of Rare Earths in Uranium Solutions

As described in Section I, large amounts of uranium can cause ionization suppression when carrying out ICP-MS analyses. The Sciex instrument displayed ionization suppression when relatively low levels of uranium (10-100 mgL^{-1}) were present in solution. As an alternative to using solvent extraction for removing uranium from a solution, sorption of a uranium complex onto a hydrophobic resin was tested. Between pH 5 and 8, uranium formed a complex with NMFHA. NMFHA was added to a uranium solution, the pH was set between 5 and 8, and the solution was passed though a small gravity column. A yellow band of uranium-NMFHA complex formed at the top of the column, indicating the retention of the complex. Due to precipitation of the uranium-NMFHA complex in aqueous solutions, the concentration of uranium was limited to under 400 mgL^{-1}. Initial concentration studies showed some retention of the rare earths on the XAD column; EDTA, which forms strong complexes with rare earth ions was then added as a masking agent. Percentage recoveries of 1 mgL^{-1} lanthanum(III), europium(III), terbium(III), thulium(III), and lutetium(III) ions in 100 mgL^{-1} were 101.3%, 99.9%, 101.5%, and 101.2% respectively. Between runs the column was washed with methanol to elute the uranium.

Terbium recovery from a 100 mgL^{-1} uranium solution was tested using an on-line separation system. A polymeric LC column was coupled to the Sciex ICP-MS, and the solutions were injected directly onto the ICP-MS system. NMFHA was required in the eluent to hold the uranium complex together, thereby preventing uranium(VI) bleed from the column. After injection of the uranium-NMFHA complex onto the system, the count rate at

m/z = 238 was indistinguishable from the background, indicating that the sorption of the uranium complex onto the column was complete. The terbium signal was measured at m/z = 159, and solutions contained varying amounts of terbium in 100 mgL^{-1} uranium were injected onto the system. Terbium(II) recoveries were essentially quantitative: Figure 46 shows the peaks of solutions containing 0.10, 0.50, 1.0, 5.0, and 10.0 mgL^{-1} terbium in 100 mgL^{-1} uranium(VI). Without any separation of the uranium from the solution, a 40% reduction in terbium signal would have been seen due to the ionization suppression by uranium. The calibration curve calculated from the peak heights was linear with a correlation coefficient of 0.9998. The upper limit of analysis of terbium was 1 mgL^{-1}; at this concentration the signal no longer increasdd linearly with increasing concentration.

Figure 46: Analysis of Tb(III) in 100 ppm U(VI). Separation on Hamilton PRP column, ICP-MS detection. at m/e = 163

Eluent Conditions: 1% MeOH, 99% H_2O, 0.001 M NMFHA, flow rate = 1.0 ml per minute

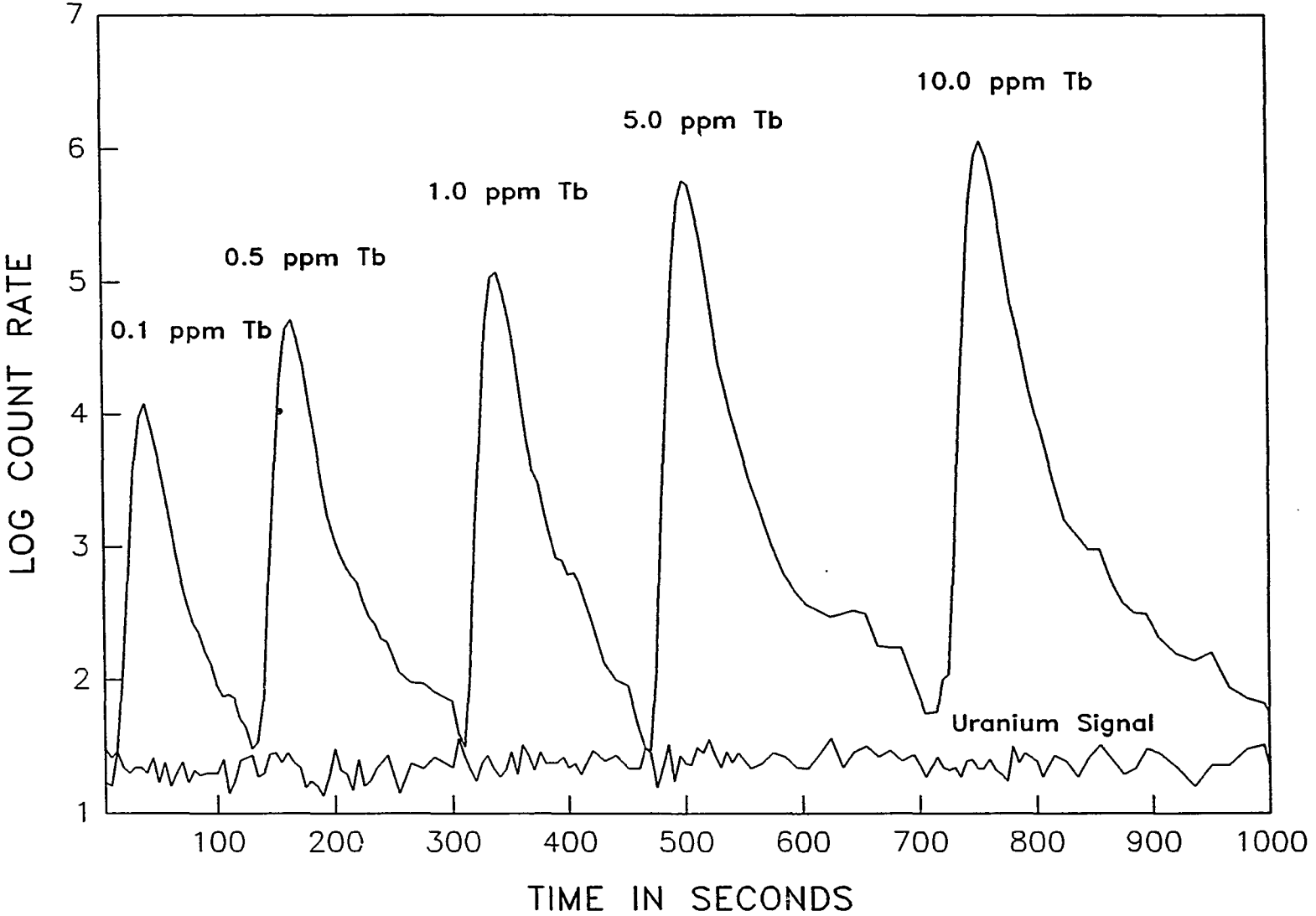
LOG COUNT RATE
7
6
5
4
3
2
1
0.1 ppm Tb
0.5 ppm Tb
1.0 ppm Tb
5.0 ppm Tb
10.0 ppm Tb
Uranium Signal
100
200
300
400
500
600
700
800
900
1000
TIME IN SECONDS

CONCLUSION

Applications of NMFHA could be extended to include other elements. Other groups have reported that hydroxamic acids are stable to radiolytic decay, and that hydroxamic acids form complexes with quadrivalent actinides under fairly acidic conditions (266). Separations of plutonium(IV) and neptunium(IV) from uranium(VI) should be possible between pH values of 0 and 3 by sorbing the transplutonium NMFHA complexes onto a hydrophobic resin. HPLC of the actinide elements under acidic conditions may also be tested. Transition and rare earth element separations could also be carried out at higher pH values using an inert polymeric column. Some of the preliminary work using the C-18 column indicated that transition metal separations may be feasible. A post column reactor would have to be used for the detection of these elements.

The work presented here has shown that the separation of hydroxamic acid metal ion complexes could be achieved using RP-HPLC. Other hydroxamic acids could be tested for use as possible reagents in metal chelate separation by HPLC. BPHA would be a logical first choice because its complexation characteristics with metal ions has been extensively studied. Both normal and reversed phase chromatography systems could be tested. Because of the insolubility of the metal chelates, high concentrations of organic modifier and less hydrophobic columns would be preferable when performing RP-HPLC. Normal phase separations may be more desirable than reversed phase because hydrolysis would be avoided, but silanol interactions from the silica-based columns may interact with the complexes.

GENERAL CONCLUSIONS

This dissertation describes applications of four organic complexing reagents in the determination of several trace metal ions. Organic chelating reagents play an important role in analytical chemistry. Various separation techniques can be applied to metal-organic complexes in order to separate metal analytes from potential interferents. Organic complexing agents can be used in such classical analytical separation methods as solvent extraction and gravimetry and also in newer procedures involving solid phase extraction and liquid chromatography. The formation of metal-organic complexes also can also be used to enhance the detection of metal ions; the increased UV and visible absorbance of the metal-organic complexes forms the basis of most of the spectrophotometric procedures developed for determining metal ions. In order to solve new problems, the synthesis and analytical applications of new organic chelating agents will continue to be of interest to analytical chemists.

REFERENCES

1. Brown, T. L.; LeMay H. E. "Chemistry the Central Science"; Prentice Hall: Englewood Cliffs, 1977; 607-613.

2. Pepper, C. E. USAEC Report NLCO-999, 1967.

3. Scribner, B. F.; Mullin, H. R. J. Res. Nat. Bur. Std. 1946, 37, 379.

4. Franklin, R.; Woodman, F. J. UKAEA Report SCS-R-67, 1949.

5. Birks, F. T. Anal. Chem. 1951, 23, 793.

6. Schoenfeld, I. April 1964 Israel AEC Report IA-925.

7. Harrison, G. R.; Kent III, R. USAEC Report MDDC-1581, 1946.

8. Walsh, A. Spectrochim. Acta 1950, 4, 47.

9. Bangia, T. R.; May, J.; Ranan, V. A.; Joshi, B. D. India AEC BARC-950, 1978.

10. Zmbova, B.; Tripkovic, M.; Secerov, O. Talanta 1971, 18(11), 1117.

11. Kim, N. S.; Lee, B. K. Punsok Hwahak 1970, 8(2), 10.

12. Wing, N. S. AEC Accession No. 26746, Report ISO-SA-13, 1966.

13. Atwell, M. G.; Pepper, C. E.; Slukenbroeker, G. L. USAEC TID-7568 (pt 1), 1958, 243-521.

14. Leclainche, C. Method Phys. Anal. 1971, 7(2), 115.

15. Maney, J. P.; Luciano, V.; Ward, A. F. Jarrell-Ash Plasma Newsl. 1979, 2, 11.

16. Walker, C. R.; Vita, O. A. Anal. Chim. Acta 1968, 43(1). 27.

17. Jursik, M. L. AEC Accession No. 1249, Report NLCO-987,1967.

18. Almagro, V. An. Real. Soc. Espan. Fis. Quim. Ser. B 1966, 62(11),1129.

19. Ishii, D.; Takeuchi, T. Bunseki Kagaku 1961, 10, 272.

20. Ishii, D.; Takeuchi, T. Bunseki Kagaku 1961, 10, 267.

21. Ishii, D.; Takeuchi, T. Bunseki Kagaku 1961, 10, 1125.

22. Chitambar, S. A.; Mathews, C. K. Z. Anal. Chem. 1975, 274(1), 9.

23. Serin, P. A.; Franklin, R. U.K. At. Energy Authority, SCS-R-77, 1959.

24. Quill, L. L.; Rodden, C. J. Natl Nuclear Energy Ser. Div. VIII Anal. Chem. Manhattan Project, 1950, 494-508.

25. Abdel Rassoul, A. A.; Wahba, S. S.; Abdel-Aziz, A. Talanta 1966, 13(3), 1966.

26. Heres, A. Report 1973 CEA-R-4433.

27. Lagendyk, A.; Russell, B. G.; Steel, J. W. Nat. Inst. Met. Repub. S. Afr. Res. Rep. NIM-440, 1968.

28. "Procedures for Handling and Analysis of Uranium Hexafluoride", Volume 2, USAEC, ORO-671-2, April 1972.

29. Jones, R. J. USAEC TID-7029, 1963, 383.

30. Floyd, R. A.; Morrow, R. W.; Farrar, R. B. Spectrochim. Acta, Part B, 1983, 38, 303.

31. Halouma, A. A.; Farrar, R. B.; Hester, E. A.; Morrow, R. W. Anal. Chem. Spectrosc. Symp. Ser. 1984, 19, 201.

32. Coleman, C. J. Anal. Chem. Spectrosc. Symp. Ser. 1984, 19, 195.

33. Short, B. W.; Spring, H. S.; Grant, R. L. CAT-T-3184, 1983.

34. Seshagiri, J. K.; Babu, Y.; Jayanth Kumar, M. L.; Dalvi, A. G. I.; Sastry, M. D.; Joshi, B.D. Talanta 1984, 31, 773.

35. De Moraes S.; Cipriani, M.; Abraio, A. Report IEA-367, 1974.

36. Miller, A. G. Report ARH-SA-160, 1973.

37. Kurohi, T; Tsukahara, T.; Shibuya, S. Bunseki Kagaku 1971, 20(9), 1137.

38. Ishii, D.; Takeuchi, T. Bunseki Kagaku 1961, 10, 1391.

39. Ishii, D.; Takeuchi, T. Bunseki Kagaku 1961, 10, 1394.

40. Muzik, R. J.; Vita, O. A. Anal. Chim. Acta 1971, 57(2), 331.

41. Birnett, H. M.; Pena, J. V.; Martell, C. J.; Phelps, R. T. USAEC LA-3985, 1968.

42. Federgruen, L.; Abrao, A. Inst. Energ. At. Rep., IE8-65, 1968.

43. Walker, C. R.; Vita, O. A.; Sparks, R. W. Anal. Chim. Acta 1969, 47(1), 1.

44. Bear, B. R.; Edelson, M. C.; Gopalan, B.; Fassel, V. A. Anal. Chem. Spectrosc. Symp. Ser. 1984, 19, 187.

45. Saranathan, T. R.; D'Silva, A. P. India At. Energy Comm. AEET-Anal 23, 1963.

46. Ishii, D.; Takeuchi, T. Bunseki Kagaku 1961, 10, 1129.

47. Drago, R. S.; Meek, D. W.; Joeston, M. D. Inorg. Chem. 1963, 2, 18.

48. Bright, J. H.; Drago, R. S., Hart; D. M.; Madan, S.K. Inorg. Chem. 1965, 4, 18.

49. Siddall III, T. H. USAEC Report No. DP-541, 1961.

50. Gasparini, G. M.; Grossi, G. Sep. Sci. Tech. 1980, 15, 825.

51. Feder, H. M. USAEC Report No. ANL-4675, 1951.

52. Siddall III, T. H. J. Phys. Chem. 1960, 64, 1963.

53. Brown, K.B.; Blake, C. A.; Schmitt, J. M. USAEC Chem. Technol. Div. Ann. Prog. Rept. ORNL-3452, 1963, 178.

54. Brown, K. B.; Blake, C. A.; Schmitt, J. M. USAEC Chem. Technol. Div. Chem. Develop. Sect. C. Prog. Rept. Separations Chem. and Separations Process Res. ORNL-3496, 1963, 70.

55. Baldwin, W. H.; Higgens, C. E.; Schmitt, J. M. USAEC Chem. Div. Prog. Rept. ORNL-3679, 1964.

56. USAEC Chem. Div. Prog. Rept. ORNL-3627, 1964, 184.

57. Fritz, J. S.; Orf, G. Anal. Chem. 1975, 47, 2043.

58. Winge, R. K.; Fassel, V. A.; Peterson, V. J.; Floyd, M. A. "Inductively Coupled Plasma Atomic Emission Spectometry: An Atlas of Spectral Information"; Elsevier: New York, 1985.

59. Houk, R. S.; Fassel, V. A.; Flesch, G. D.; Svec, H. J.; Gray, A. L.; Taylor, C. E. Anal. Chem. 1980, 52, 2283.

60. Houk. R. S. Anal. Chem. 1986, 58, 97A.

61. Date, A. R.; Gray, A. L. Analyst (London) 1983, 108, 1033.

62. Douglas, D. J.; Houk, R. S. Prog. Anal. At. Spectrosc. 1985, 8, 1.

63. Snell, F. D. "Photometric and Fluorometric Methods of Analysis"; Wiley-Interscience: New York, 1978.

64. Fritz, J. S.; Johnson-Richard, M. Anal. Chim. Acta 1959, 20, 164.

65. ASTM, "1974 Annual Book of ASTM Standards", Volume 26; ASTM: Philadelphia, 1974; 543.

66. Phillips, R. J. Ph.D. Dissertation, Iowa State University, Ames, IA 1980.

67. Olivares, J. A.; Houk, R. S. Anal. Chem. 1985, 57, 2674.

68. Horlick, G.; Tan, S. H.; Vaughn, M. A.; Rose, C. A. Spectrochim. Acta Part B, 1985, 40, 1555.

69. Palmieri, M. D.; Thompson, J. J.; Fritz, J. S.; Houk, R. S. Anal. Chim. Acta 1986, 184, 187.

70. Bergamin, F. H.; Medeiros, J. X.; Reis, B. F.; Zagatto, E. A. Anal. Chim. Acta 1978, 101, 9.

71. Pederson, B. S.; Scheibye, S.; Nilsson, N. H.; Lawesson, S. O. Bull. Soc. Chim. Belg. 1978, 87, 229.

72. Fritz. H.; Hugo, P.; Lawesson, S. O.; Logeman, E.; Pederson, B. S.; Sauter, H.; Scheibye, S.; Winkler, T. Bull. Soc. Chim. Belg. 1978, 87, 525.

73. Douglas, D. J. Short Course on Inductively Coupled Plasma Mass Spectrometry, Winter Conference on Plasma Spectrochemistry, Kona HI 1986.

74. Houk, R. S.; Department of Chemistry, Iowa State University, Ames IA, 1987, personal communication.

75. Olivares, J. A.; Houk, R. S. Anal. Chem. 1986, 58, 20.

76. Nord, L. Anal. Chim. Acta 1980, 118, 285.

77. Fossey, L.; Cantwell, F. F. Anal. Chem. 1983, 55, 1882.

78. Backstrom, K.; Danielson, L. G.; Nord, L. Anal. Chim. Acta 1985, 169, 43.

79. Wendt, H.; Keller, C. Ed. "Gmelin Handbook of Inorganic Chemistry" Uranium Supplement, Volume A7; Springer Verlag: Berlin, 1982.

80. Fritz, J. S.; Schenk, G. H. "Quantitative Analytical Chemistry", 3rd ed.; Allyn and Bacon: Boston, 1979.

81. Olsen, E. U. "Modern Optical Methods of Analysis"; McGraw-Hill: New York, 1975.

82. Skoog, D. A.; West, D. M. "Principles of Instrumental Analysis", Saunders College: Philadelphia, 1980.

83. Snell, F. D. "Photometric and Fluorometric Methods of Analysis" Volume 2; Wiley-Interscience: New York, 1978; 1351-1416.

84. Shibatu, S. L.; Matsumai, T. Bull. Chem. Soc. Japan. 1958, 31, 3778.

85. Savvin, S. B. Talanta 1961, 8, 673.

86. Savvin, S. B. Talanta 1964, 11, 1.

87. Korkish, J.; Hubner, H. Talanta 1976, 23, 283.

88. Yoe, J. H.; Will, F.; Black R. A. Anal. Chem. 1953, 25, 1200.

89. Francois, C. A. Anal. Chem. 1958, 30, 50.

90. Rodden, C. J. "Analytical Chemistry of the Manhattan Project"; McGraw-Hill: New York, 1950; 82-99.

91. Eberle, A. R.; Lerner, M. W. Anal. Chem. 1957, 29, 1134.

92. Vernon, F.; Kyffin, T. W.; Nyo, K. M. Anal. Chim. Acta 1976, 87, 491.

93. Florence, T. M.; Johnson, D. A. Anal. Chim. Acta 1971, 53, 73.

94. Florence, T. M.; Johnson, D. A. Talanta 1975, 22, 253.

95. Florence, T. M.; Johnson D. A.; Farrar, Y. J. Anal. Chem. 1969, 41, 1652.

96. Florence, T. M.; Farrar, Y, J. Anal. Chem. 1970, 42, 271.

97. Baltisburger, R. J. Anal. Chem. 1964, 36, 2369.

98. Gill, H. H.; Rolf, R. F.; Armstrong, G. W. Anal. Chem. 1958, 30, 1788.

99. Sommer, L.; Ivanov, V. M.; Novotne, H. Talanta 1967, 14, 329.

100. Florence, T.M.; Farrar, Y. J. Anal. Chem. 1963, 35, 1613.

101. Ph Moeken, H. H.; Van Neste W. A. Anal. Chim. Acta 1967, 37, 480.

102. Currah, J. E.; Beamish, F. E. Anal. Chem. 1947, 19, 609.

103. Okumura, I.; Shimadu, S.; Higashi, K. Anal. Chem. 1973, 43, 1945.

104. Curry, J.; Robinson, M.; Busch, D. Inorg. Chem. 1967, 8, 1570.

105. Webster, D.; Palenik, G. Inorg. Chem. 1976, 15, 755.

106. Webster, D.; Palenik, G. J. C. S. Chem. Comm. 1975, 74.

107. Paolucci, G. Marangoni, G. Inorg. Chim. Acta 1977, 24, 65.

108. Paolucci, G.; Marangoni, G.; Bandoli, G.; Clemente, D. J. Chem. Soc. Dalton Trans. 1980, 3, 459.

109. Mangia, A.; Pelizzi, C.; Pelizzi, G. Acta Cryst. 1974, B 30, 2146.

110. Nardelli, M.; Pelizzi, C. Pelizzi, G. Trans. Met. Chem. 1977, 2, 35.

111. Pelizzi, C,; Pelizzi, G.; Predieri, G.; Resola, S. J. Chem. Soc. Dalton Trans. 1982, 7, 1349.

112. Pelizzi, C.; Pelizzi, G. J. Chem. Soc. Dalton Trans. 1980, 10, 1970.

113. Paolucci, G.; Marangoni, G. Bandoli, G.; Clemente, D. J. Chem. Soc. Dalton Trans. 1980, 8, 1304.

114. Lorenzini, C.; Pelizzi, C.; Pelizzi, G. J. Chem. Soc. Dalton Trans. 1983, 4, 721.

115. Casoli, A.; Mangia, A.; Predieri, G. Anal. Chem. 1985, 57, 561.

116. Casoli, A.; Mangia, A.; Mori, G.; Predieri, G. Anal. Chim. Acta 1986, 186, 283.

117. Garcia-Vargas, M.; Belizon, M. E.; Milla, M.; Perez-Bustamente, J. A. Analyst (London), 1985, 110, 51.

118. Garcia, D. V.; Ramirez, A. A.; Ceba, M. R. Talanta 1979, 26, 215.

119. Steinbruch, B. J. of Liq. Chrom. 1987, 10, 1.

120. O'Laughlin, J. J. of Liq. Chrom. 1984, 7(S-1), 127.

121. Willeford, B.; Veening, H. J. Chromatog. 1982, 251, 61.

122. Veening, H; Willeford, B. Adv. Chromatogr. 1983, 22, 117.

123. Nickless, G. J. Chromatog. 1985, 313, 129.

124. MacDonald, J. C. in "Chemical Analysis", Volume 78; MacDonald J. C. Ed.; Wiley: New York, 1985; Chapter 6.

125. Schwedt, G. Chromatographia, 1979, 12, 613.

126. Cassidy, R. M. in "Trace Analysis", Volume 1; Lawrence, J. F. Ed.; Academic Press: New York, 1982; 122-192.

127. Schwedt, G. "Chromatographic Methods in Inorganic Analysis", Dr. A Huthing; Verlag: Heidelberg, 1981.

128. Cheng, K. L.; Ueno, K.; Imamura, T. "CRC Handbook of Organic Analytical Reagents", CRC Press: Boca Raton, 1982; 85-109.

129. Mehrotra, R. C.; Bohra, R.; Gaur, D. "Metal β-Diketonates and Allied Derivatives"; Academic Press: London, 1978.

130. Minczewski, J.; Chwastowska, J.; Dybczynski, R. "Separation and Preconcentration Methods in Inorganic Analysis"; John Wiley & Sons: New York, 1982; 182-193.

131. Wiley, R. H.; Wiley, P. "Pyrazolones, Pyrazolidones, and Derivatives"; Wiley Interscience: New York, 1964; 88-91.

132. Jenson, B. S. Acta Chem. Scand. 1959, 13, 1347-1357.

133. Jenson, B. S. Acta Chem. Scand. 1959, 13, 1668-1670.

134. Jenson, B. S. Acta Chem. Scand. 1959, 13, 1890-1896.

135. Minczewski, J.; Chwastowska, J.; Dybczynski, R. "Separation and Preconcentration Methods in Inorganic Analysis"; John Wiley & Sons: New York, 1982; 193-195.

136. King, J. N. Ph.D. Dissertation, Iowa State University, Ames, Iowa, 1986.

137. Karalova, Z. K.; Pyzhova, Z. I.; Rodionova, L. M. Zh. Anal. Khim. 1970, 25, 909.

138. Skorko-Trybula, Z.; Rozycki, C.; Kosiarska, E. Chem. Anal. (Warsaw) 1977, 22, 311.

139. Myasoedev, B. F.; Molochnikova, N. P. Radiochem. Radioanal. Lett. 1974, 18, 33.

140. Vdovenko, V. M.; Kovalskaya, M. P.; Smirnova, E. A. Sov. Radiochem. 1973, 15, 320; Anal. Abstr. 1974, 27, 3189.

141. Kochetkova, N. E.; Chmutova, M. K.; Myasoedev, B. F. Zh. Anal. Khim. 1972, 27, 678.

142. Myasoedov, B. F. Proc. Moscow Symp. Chem. Transuranium. Elem. 1976, 151.

143. Mathur, J. N.; Khopkar, P.K. Radiochem. Radioanal. Lett. 1983, 57, 259.

144. Chmutova, M. K.; Pribylova, G. A.; Myasoedov, B. F. Zh. Anal. Khim. 1973, 28, 2340.

145. Zolotov, Yu. A.; Lambrev, V. G. Zh. Anal. Khim. 1965, 20, 659.

146. Arora, H. C.; Rao, G. N. Indian. J. Chem. 1973, 11, 488.

147. Subhani, M. S.; Rev. Roum. Chem. 1980, 25, 121.

148. Chmutova, M. K.; Kochetkova, N. E. Zh. Anal. Khim. 1970, 25, 710.

149. Rao, G.; Nageswara, A. Microchem. J. 1976, 21, 1.

150. Zolotov, Yu. A.; Chmutova, M. K.; Palei, P. N.; Kochetkova, N. E. Zh. Anal. Khim. 1969, 24, 711.

151. Mirza, M. Y. Talanta 1978, 25, 685.

152. Tomilova, L. G.; Efimov, I. P.; Peshkova, V. M. Zh. Anal. Khim. 1973, 28, 666.

153. Hala, J.; Prihoda, J. Collect. Czech. Chem. Comm. 1975, 40, 546.

154. Navratil, O.; Smola, J. Collect. Czech. Chem. Comm. 1981, 46, 1901.

155. Navratil, O.; Smola, J. Collect. Czech. Chem. Comm. 1981, 46, 1764.

156. Navratil, O.; Smola, J.; Kolouch, R. Collect. Czech. Chem. Comm. 1979, 44, 3656.

157. Hala, J.; Smola, L. Radiochem. Radioanal. Lett. 1978, 34, 325.

158. Revenko, V. G.; Bagreev, V. V.; Zolotov, Yu. A.; Kopantskaya, L. S. Zh. Anal. Khim. 1972, 27, 1571.

159. Navratil, O.; Malach, A. Collect. Czech. Chem. Comm. 1978, 43, 2890.

160. Savrova, O. D.; Gibalo, I. M.; Spiridonova, S. S.; Labanov, F. I. Zh. Anal. Khim. 1973, 28, 817.

161. Joshi, S. N.; Evanova, E. K.; Peshkova, V. M. Indian. J. Chem. 1973, 11, 78.

162. Zolotov, Yu. A.; Sizonenko, N. T. Zh. Anal. Khim. 1970, 25, 54.

163. Mysoedov, B. F.; Molochnikova, N. P. Zh. Anal. Khim. 1969, 24, 702.

164. Ahmad, S.; Skarnemark, G. J. Radioanal. Nucl. Chem. 1984, 85, 181.

165. Movikov, Y. P.; Ivanova, S. A.; Myasoedov, B. F. Radiochem. Radioanal. Lett. 1982, 52, 155-161.

166. Akama, Y. Nakai, T,; Kawamura, F. Bunseki Kagaku 1976, 25, 496.

167. Zolotov, Yu. A.; Chmutova, M. K.; Palei, P. M. Zh. Anal. Khim. 1966, 21, 1217-1222.

168. Zolotov, Yu. A.; Lambrev, V. G. Radiokhimiya 1966, 8, 627.

169. Myasoedov, B. F.; Molochnikova, N. P.; Palei, P. N. Radiokhimiya, 1970, 12, 829.

170. Karalova, Z. K.; Pyzhova, Z. I. Zh. Anal. Khim. 1968, 23, 1564.

171. Yu, Y. F.; Tang, J. J. Radiochem. Radioanal. Lett. 1982, 51, 103.

172. Sovostina, V. M.; Shpigun, O. A.; Peshkova, V. M. Zh. Anal. Khim. 1971, 26, 2044.

173. Zolotov, Yu. A. Sizonenko, N. T.; Zolotovitskaya, E. S.; Yakovenko, E. I. Anal. Chem. USSR 1969, 24, 15.

174. Chmutova, M. K.; Palei, P. N.; Zolotov, Yu. A. Zh. Anal. Khim. 1968, 23, 1476.

175. Talavera, C. F.; Mareva, S.; Yordanov, N. Talanta 1982, 29, 119.

176. Talavera, C. F.; Mareva, S.; Yordanov, N. Izv. Khim. 1981, 14, 211.

177. Rao, G. N.; Arora, H. C. J. Inorg. Nucl. Chem. 1977, 39, 2057.

178. Akama, Y.; Nakai, T.; Kawamura, F. Analyst (London) 1981, 106, 250.

179. Zolotov, Yu. A.; Gavrlova, L. G. J. Inorg. Nucl. Chem. 1969, 31, 3613.

180. Mirza, M. Y.; Nwabue, F. I.; Okafo, E. N. J. Inorg. Nucl. Chem. 1981, 43, 1365.

181. Huber, J. F. K.; Kraak, J. C.; Veening, H. Anal. Chem. 1972, 44, 1544.

182. Tollinche, C. A.; Risby, T. H. J. Chromatogr. Sci. 1978, 16, 448.

183. Schwedt, G. Z. Anal. Chem. 1981, 309, 359.

184. Uden, P. C.; Bigley, I. E.; Walters, F. H. Anal. Chim. Acta 1978, 100, 555.

185. Yamazaki, M.; Ichinoki, S.; Igarashi, R. Bunseki Kagaku 1983, 32, 605.

186. Cardwell, T. J.; Lorman, T. H.; Zaoh, Z. F. J. Chromatogr. 1986, 358, 187.

187. Bleyker, D.; Arbogast, K.; Sweet, T. Chromatographia, 1983, 17, 449.

188. Saitoh, K. Satoh, M.; Suzuki, N. J. Chromatogr. 1974, 92, 291.

189. Saitoh, K. Suzuki, N. J. Chromatogr. 1975, 109, 333.

190. Suzuki, N.; Saitoh, K.; Shibukawa, M. J. Chromatogr. 1977, 138, 79.

191. Saitoh, K.; Nobuo, S. Bull. Chem. Soc. Japan 1977, 50, 2907.

192. Noda, H.; Saitoh, K.; Suzuki, N. Chromatographia 1981, 14, 189.

193. Willett, J. D.; Knight, M. M. J. Chromatogr. 1982, 237, 99.

194. Gurira, R. C.; Carr, P. W. J. Chromatogr. Sci. 1982, 20, 461.

195. Wenclawiak, M.; Barkley, R.; Williams, E.; Sievers, R. J. Chromatogr. 1985, 349, 469.

196. Morale, R.; Bartholdi, C. J. Chromatogr. submitted 1987.

197. Rivier, J. E. J. Liq. Chrom. 1978, 1, 343.

198. Hearn, M. T.; Grego, B. J. Chromatogr. 1983, 255, 125.

199. Hearn, M. T.; Grego, B. J. Chromatogr. 1983, 266, 75.

200. King, J. N.; Fritz, J. S. Anal. Chem. 1987, 59. 703.

201. Pedigo, S.; Bowers, L.; (University of Minnesota, Minneapolis, MN), Minnesota Chromatography Forum 1986, Abstract 11.

202. Snyder, L.; Kirkland, J. "Introduction to Modern Liquid Chromatography"; John Wiley & Sons: New York, 1979; 260-265.

203. Vlacil, F.; Hamplova, V. Collect. Czech. Chem. Comm. 1985, 50, 2221.

204. Korkisch, J. Sep. Sci. 1966, 1, 159.

205. Cassidy, R. M. Elchuk, S.; Dasgupta, P. K. Anal. Chem. 1987, 59, 85.

206. Mukherji, A. K. "Analytical Chemistry of Zirconium and Hafnium", Pergamon Press: New York, 1970.

207. Mazzo, D. J.; Cheng, Z. B.; Uden, P. C.; Rausch, M. D. J. Chromatogr. 1983, 269, 11.

208. Kehl, H, Ed. "Chemistry and Biology of Hydroxamic Acids", (Proceedings of First International Symposium on Chemistry and Biology of Hydroxamic Acids, Dayton, OH, May 21, 1981); S. Karger: Basel, 1982.

209. Majumdar, A. "N-Benzoylphenylhydroxylamine and its Analogues"; Pergamon Press: Oxford, 1972.

210. Agrawal, Y. K.; Patel, S. A. Rev. Anal. Chem. 1980, 4, 237.

211. Minczewski, J.; Chwastowska, J.; Dybczynski, R. "Separation and Preconcentration Methods in Inorganic Analysis"; John Wiley & Sons: New York, 1982; 202-206.

212. Shendrikar, A. D. Talanta 1969, 16, 51.

213. Cheng, K. L.; Ueno, K.; Imamura, T. "CRC Handbook of Organic Analytical Reagents", CRC Press: Boca Raton, 1982; 109-127.

214. Villarreal, R.; Krsul, J. R.; Baker, S. A. Anal. Chem. 1969, 41, 1420.

215. Pande, R.; Tandon, S. G. Croat. Chem. Acta 1978, 51, 353.

216. Das, B. Shome, S. C. Anal. Chim. Acta 1968, 40, 353.

217. Lyle, S. J.; Shendrikar, A. D. Anal. Chim. Acta 1965, 32, 575.

218. Sinha, S. K.; Shome, S. C. Anal. Chim. Acta 1961, 24, 33.

219. Agrawal, Y. K. Talanta 1973, 20, 1213.

220. Chwastowska, J.; Minczewski, J. Chem. Anal. (Warsaw) 1964, 9, 791.

221. Chwastowska, J.; Minczewski, J. Chem. Anal. (Warsaw) 1963, 8, 157.

222. Sinha, S. K.; Shome, S. C. Anal. Chim. Acta 1959, 21, 459.

223. Fishil, H.; Einaga, H. Japan Analyst 1968, 17, 1296.

224. Das, H. R.; Shome, S. C. Anal. Chim. Acta 1962, 27, 545.

225. Lyle, S. J.; Shendrikar, A. D. Anal. Chim. Acta 1966, 36, 286.

226. Prihoda, J.; Hala, J. J. Radioanal. Chem. 1976, 30, 343.

227. Hala, J. J. Less Common Metals 1972, 26, 117.

228. Hala, J.; Sotularova, L. J. Inorg. Nucl. Chem. 1969, 31, 2247.

229. Hala, J. Inorg. Nucl. Chem. Letters 1968, 4, 67.

230. Hala, J. J. Inorg. Nucl. Chem. 1967, 29, 1777.

231. Hala, J. J. Inorg. Nucl. Chem. 1967, 29, 187.

232. Das, B.; Shome, S. C. Anal. Chim. Acta 1966, 35, 345.

233. Schweitzer, G. K.; Anderson, M. M. J. Inorg. Nucl. Chem. 1968, 30, 1051.

234. Riedel, A. J. Radioanal. Chem. 1970, 6, 75.

235. Das, B.; Shome, S. C. Anal. Chim. Acta 1965, 32, 52.

236. Cardwell, T. J.; Magee, R. J. Mikrochem. J. 1968, 13, 467.

237. Vita, O. A.; Levier, W. A.; Littreral, E. Anal. Chim. Acta 1968, 42, 87.

238. Villareal, R.; Barker, S. A. Anal. Chem. 1969, 41, 611.

239. Erskine, J. S. Sink, M. L.; Varga, L. P. Anal. Chem. 1969, 41, 70.

240. Lyle, S. J.; Shendrikar, A. D. Talanta 1965, 12, 573.

241. Chmutova, M. K.; Petrukhim, O. M.; Zolotov, Yu. A. Zh. Anal. Khim. 1963, 18. 588.

242. Lyle, S. J.; Shendrikar, A. D. Talanta 1966, 13, 140.

243. Majumdar, A. K.; Mukherjee, A. K. Anal. Chim. Acta 1959, 21, 245.

244. Ryan, D.; Lutwick, G. D. Can. J. Chem. 1953, 31, 9.

245. Jordanov, N.; Mareva, St.; Koeva, M. Anal. Chim. Acta 1972, 59, 75.

246. Moshier, R. W.; Schwarberg, J. E. Anal. Chem. 1957, 29, 947.

247. Pyrssen, D. Acta Chem. Scand. 1956, 10, 353.

248. Afghan, B. K.; Marryati, R. G.; Ryan, D. E. Anal. Chim. Acta 1968, 41, 131.

249. Shukla, J. P.; Agrawal, Y. K.; Bhatt, K. Sep. Sci. 1973, 8, 387.

250. Dryssen, D. Acta Chem. Scand. 1956, 10, 353.

251. Priyadarshini, U.; Tandon, S. G. Anal. Chem. 1961, 33, 435.

252. Ryan, D. E. Analyst 1960, 85, 569.

253. Chakrabari, C. L.; Magee, R. J.; Wilson, C. L. Talanta 1963, 10, 1201.

254. Alimarin, I. P.; Chieh, Y. H. Talanta 1962, 9, 9.

255. Villareal, R.; Young, J. O.; Krsul J. P. Anal. Chem. 1970, 42, 1419.

256. Alimarin, I. P.; Chieh, Y. H. Talanta 1961, 8, 317.

257. Fritz, J. S.; Sherma, J. J. Chromatogr. 1966, 25, 153.

258. Fouche, K. F. J. Inorg. Nucl. Chem. 1968, 30, 3057.

259. Fouche, K. F.; le Roux, H. J.; Philips, F. J. Inorg. Nucl. Chem. 1970, 32, 1949.

260. Brandt, W. W. Rec. Chem. Prog. 1960, 21, 159.

261. Chakraburtty, A. A. Proc. Symp. Chem. Coord. Compd. 1959, 1960, 111, 235.

262. Al-biaty, I.; Fritz, J. S. Anal. Chim. Acta 1983, 146, 191.

263. Cassidy, R. M.; Elchuck, S. Anal. Chem. 1979, 51, 85.

264. Sevenich, G.; Fritz, J. S. J. Chromatogr. 1986, 371, 361.

265. Jiang, J.; Palmieri, M. D.; Fritz, J. S.; Houk, R. S. Anal. Chim. Acta accepted 1987.

266. Foley, J. P. Chromatography 1987, 2, 43.

APPENDIX: PRINCIPLES OF SOLVENT EXTRACTION

Numerous sources give detailed information on the theory of solvent extraction. The intent of this appendix is to describe basic extraction theory required for determining the composition of the extracted uranium species.

Solvent extraction involves the partition of species between two immiscible liquids. In the extraction of uranium using DHA, the following equilibrium occurs:

$$UO_2^{2+} + l(NO_3^-) + wH_2O + nDHA \rightleftharpoons UO_2^{2+}(NO_3^-)_l(H_2O)_w(DHA)_n \quad (14)$$

The equilibrium constant (K) is:

$$K = \frac{[UO_2^{2+}(NO_3^-)_l(H_2O)_w(DHA)_n]}{[UO_2^{2+}][NO_3^-]^l[DHA]^n[H_2O]^w} \quad (15)$$

The distribution coefficient (D_c) is defined to be:

$$D_c = \frac{[U]_{\text{organic phase}}}{[U]_{\text{aqueous phase}}} \quad (16)$$

Substituting in for the uranium extraction system, D_c is

$$D_c = \frac{[UO_2^{2+}(NO_3^-)_l(DHA)_n(H_2O)_w]}{[UO_2^{2+}]} \quad (17)$$

Substituting in the equilibrium constant expression, D_c is

$$D_c = K[NO_3^-]^l[DHA]^n[H_2O]^w \qquad (18)$$

Taking the log of both sides and assuming that K and the concentration of water are constant

$$\log(D_c) = l\log[NO_3^-] + n\log[DHA] + \text{constant} \qquad (19)$$

When the nitrate concentration is varied while the DHA concentration is held constant, a plot of $\log(D_c)$ versus $\log[NO_3^-]$ should yield the number of nitrates in the extracted species. Similarly, if the DHA concentration is varied while holding the nitrate concentration constant, a plot of $\log(D_c)$ versus log[DHA] will produce a slope equal to the number of DHA molecules in the extracted complex.

Efficiency of an extraction (E) is calculated using the following formula:

$$\%E = 100 - 100/(D_c + 1)^m \qquad (20)$$

where m equals the number of extractions.

ACKNOWLEDGEMENT

In many ways, completing this dissertation was a group effort; many people have provided the emotional and technical support required for me to carry out the work. Thanks go to Dr. Fritz for patiently supporting my research and allowing me to develop into an independent researcher. The various collaborators Dr. Houk, Jose Olivares, Marissa Bonilla-Alvarez, Joe Thompson, and S. -J. Jiang made much of this research possible, and I thank them. I would also like to thank the past and present members of Dr. Fritz's research group for all the encouragement and assistance provided. They were not only sounding boards for ideas, but also shared in the successes and failures of research. The support from Tina, Jim, Steve, and all my friends are appreciated. They kept me sane during my stay at Iowa State. Finally I thank my parents for their constant and unwavering interest and support. Without them this thesis would never have been written.